Imine- Nanomaterial Composites as Receptors for Potentiometric and Voltammetric Sensing of Ions

A

Thesis submitted in

fulfillment of the requirement for the degree of

Doctor of Philosophy

Submitted by

Sanjeev Kumar

(901309002)

Under the supervision

of

Dr. Susheel Mittal CChem FRSC

Senior Professor

School of Chemistry & Biochemistry

Thapar Institute of Engineering and Technology

Patiala-147004, India

August, 2019

Certificate

Certified that the thesis entitled "**Imine- Nanomaterial Composites as Receptors for Potentiometric and Voltammetric Sensing of Ions**" which is submitted by Mr. Sanjeev Kumar in fulfillment of the requirement for the award of the Degree of Doctor of Philosophy in School of Chemistry and Biochemistry, Thapar Institute of Engineering and Technology, Patiala, is a record of candidate's own independent and original research work carried out by him under my supervision and guidance. The material embodied in this thesis has not been submitted in part or full to any other University or Institute for the award of any degree.

Susheel Mittal 20.8.19

(Supervisor)

Dr. Susheel Mittal CChem FRSC
Senior Professor
School of Chemistry and Biochemistry
Thapar Institute of Engineering and Technology, Patiala-147004

(Head)

Dr. Amjad Ali
Professor
School of Chemistry and Biochemistry
Thapar Institute of Engineering and Technology, Patiala-147004

Candidate's Declaration

I, hereby declare that the work presented in the thesis entitled "**Imine- Nanomaterial Composites as Receptors for Potentiometric and Voltammetric Sensing of Ions**" in fulfillment of the requirement for the award of the Degree of Doctor of Philosophy in School of Chemistry and Biochemistry, Thapar Institute of Engineering and Technology, Patiala, is an authentic record of my own work carried out under the supervision of Dr. Susheel Mittal, Senior Professor, School of Chemistry & Biochemistry, Thapar Institute of Engineering and Technology, Patiala, India. The matter embodied in this thesis has not been submitted in part or full to any other University or Institute for the award of any degree in India or abroad.

Sanjeev Kumar

Place: Patiala

Date: August 19, 2019

Sanjeev Kumar

901309002

Acknowledgements

I have always thought that life is a journey, and the time spent here at Thapar Institute of Engineering and Technology was part of a new and amazing experience that I had the opportunity to enjoy. This thesis has been kept on track and been seen through to completion with the support and encouragement of numerous people. It is a pleasant task to express my thanks to all those who contributed to the success of this study and made it an unforgettable experience for me.

First and foremost, I want to thank my advisor Dr. Susheel Mittal CChem FRSC, Senior Professor; School of Chemistry & Biochemistry, Thapar Institute of Engineering & Technology, Patiala. His insight into the subject has always made me realize and understand the subject in a broader perspective. His constant guidance, cooperation and support has always kept me going ahead. I owe a lot of gratitude to him for always being there for me and I feel privileged to be associated with a person like him during my life. He has been affectionate and ever ready to help me, even in the midst of his busy schedule. I have been extremely lucky to have Dr. Susheel Mittal as my research guide.

I express my gratitude to Director, Thapar Institute of Engineering and Technology, Patiala and Dr. Amjad Ali, Head, School of Chemistry and Biochemistry, for all the facilities which have been immensely helpful for the completion of my work.

I express my deep gratitude to Dr. Navneet Kaur, Panjab University Chandigarh, her students for providing the molecules to carry out the studies and providing guidance from time to time.

I express my regards to Dr. Amjad Ali, Dr. Vijay Luxami and Dr. Shekhar Agnihotri (PhD committee member- Subject expert) for suggestions and taking interest in the progress of work along with laboratory facilities.

I extend my thanks to all the faculty members of School of Chemistry and Biochemistry, Thapar Institute, Patiala for providing necessary guidance during my research work. I am thankful to Mr. Chandar Thakur, Shekhar, Vishwanath, Hemant, Mayank and other non-teaching staff, School of Chemistry and Biochemistry for the constant official help and cooperation.

My acknowledgement will never be complete without the special mention of my lab seniors who have taught me the lab culture and have lived by example to make me understand the hard facts of life. I would like to acknowledge Dr. Jasminder Singh, Dr. Karamjeet Kaur and Dr. Pawan Kumar for all their support and motivation during the initial days of my stay in the lab. During the course of my work, I had the pleasure of working with several project students Baneesh, Yadwinder, Neeraj, Arjun and Bhumika. No words can suffice to acknowledge the friendly and stimulating atmosphere created by my labmates Ms. Manisha Pabbi, Dr. Rashmi Sharma, Ms. Rupinder Kaur, Ms. Madhvi Rana, Ms. Shivali Gupta, Mr. Gurpreet Saggu, Mr. Rahul Shukla, Mr. Sunil Kumar and Mr. Sachin Gupta. I would like to acknowledge my other friends for their moral support and motivation, which drives me to give my best Ms. Sonia Rana, Dr. Anirudh Sharma and Mr. Ashok Kumar.

I gratefully recall the countless splendid memories of my stay in Patiala; which I had with Gurpreet Singh, Sahil Mishra and Vishnu Goel. I also remember with affection the support and help from Atish Verma, my roommate.

Finally, I would like to acknowledge the people who mean world to me, my parents, my brothers and sisters. My hard-working parents have sacrificed their lives for me and provided unconditional love and care. I love them so much, and I would not have made it this far without them. I am thankful to my sisters, who are always with me and sacrificed so much for me. Thank you, mom, dad, sister and brother, for showing faith in me and giving me liberty to choose what I desired. I consider myself the luckiest in the world to have such a supportive family, standing behind me with their love and support.

Sanjeev Kumar

Sanjeev Kumar

List of Contents

Abstract

This doctoral thesis provides an insight into the development, characterization and application of potentiometric and voltammetric sensor based on Schiff base ionophores (E)-3-((2-aminoethylimino)methyl)-4H-chromen-4-one (IFE), (E)-3-(((2-((2 aminoethyl) amino) ethyl) imino) methyl)-4H-chromen-4-one (ICU) and (E)-3-((2-(2-(2-aminoethylamino) ethylamino) ethylimino)methyl)-4H-chromen-4-one (IFE(III)). These prepared sensors provide better selectivity for the target species (heavy metals of environmental importance). The present thesis work can be divided into two main parts. First approach is the development of ion selective electrodes (ISE) based on modification with multiwalled carbon nanotubes (MWCNTs). It consists of incorporation of multiwalled carbon nanotubes in the polymeric membrane in order to provide improved characteristics of the ISEs. Second approach is the development of voltammetric sensors for the detection of cations using cyclic voltammetry and differential pulse voltammetric techniques.

Potentiometric and voltammetric sensor for creating cationic response for Fe(II) based on (E)-3-((2-aminoethylimino)methyl)-4H-chromen-4-one (IFE) is introduced. The influence of variables including amount of ionophore, plasticizers, anion excluder and multiwalled carbon nanotubes (MWCNTs) on the performance of the potentiometric sensor were investigated. The sensor for Fe(II) improvised the dynamic linear range (1×10^{-7} to 1×10^{-1} mol/L) with a slope of 27 mV/decade and a detection limit of 2.5×10^{-8} mol/L. Selectivity of the ion selective electrode improved after modification with MWCNTs. The reduction and oxidation properties of IFE were studied by voltammetric measurements. Differential pulse voltammetry was applied to the optimized electrode and a linear dynamic range from (9.9×10^{-7} to 2.9×10^{-5} mol/L) with a detection limit of 6.13×10^{-8} mol/L was obtained. The composition and morphology of the modified ion selective electrode were characterized with scanning electron microscopy. The modified electrodes have good selectivity for Fe(II) ions over a number of metal ions. It was successfully applied for direct determination of Fe(II) ions in different real life samples. Theoretical calculations also supported the complexation behavior of Fe(II) with IFE.

Electrochemical sensor based on an ionophore (E)-3-(((2-((2 aminoethyl) amino) ethyl) imino) methyl)-4H-chromen-4-one (ICU) has been developed for the detection of Cu (II). The influence of variables including amount of ionophore, plasticizers, anion excluder sodium tetraphenylborate (NaTPB) and multiwalled carbon nanotubes (MWCNT) on performance of the electrode was studied. At optimized conditions, the sensor has a wide linear range of

concentration ($1.0x10^{-7}$ – 1.0×10^{-1} mol/L) and a low detection limit of 1.0×10^{-7} mol/L of Cu (II) ion with a stable response in a working pH range of 4.0–7.0. This electrode was also used as an indicator electrode in potentiometric titration of Cu (II) ion with EDTA. ICU is a promising molecule with a potential of voltammetric sensor for Cu (II) species in DMSO medium in a concentration range 2.5×10^{-6} M to 4.3×10^{-4} M and detection limit of 9.32×10^{-9} M. Scanning electron microscopy combined with energy dispersive X-ray spectra was used to confirm the interaction between Cu (II) ions and ionophore on the surface of the electrode. The proposed ionophore is highly selective for Cu (II) ions from a number of metal ions. It was successfully applied for the determination of Cu (II) ion in different real-life samples from daily use items. Theoretical calculations also support the complexation behaviour of Cu (II) with ICU.

A highly sensitive and selective potentiometric and voltammteric assay for the detection of Fe^{3+} using (E)-3-((2-(2-(2-aminoethylamino) ethylamino) ethylimino)methyl)-4H-chromen-4-one (IFE(III)) ionophore was developed. To demonstrate the ion-to-electron ability of MWCNT, these were incorporated in the ion-selective membrane and response characteristics of Fe^{3+} electrode was compared with those of the traditional ion selective electrode. The electrode showed an improved Nernstian slope, lower detection limit, response time of less than 5 s and working in a pH range of 3.0 to 8.0. Differential pulse voltammetric studies were performed for IFE(III)-Fe^{3+} complex in DMSO solvent medium at glassy carbon (GC) electrode. A linear relationship between the cathodic peak current and concentration of Fe^{3+} was observed in the range of 1.6×10^{-5} to 4.4×10^{-5} mol/L with a detection limit of 5.2×10^{-8} mol/L. The electrode shows remarkable selectivity for Fe^{3+} ions over alkali, alkaline earth, transition and heavy metal ions. The optimized electrode was successfully applied for the determination of Fe^{3+} ion in different real-life samples using potentiometric technique. Theoretical calculations were used to support the complexation behavior of Fe^{3+} with IFE(III).

Further, organic nanoparticles of (E)-3-((2-aminoethylimino)methyl)-4H-chromen-4-one (IFE) were synthesized in aqueous dispersion by reprecipitation method with an average particle size of 50-65 nm. It was characterized by the dynamic light scattering (DLS) and transmission electron microscopy (TEM). Based on voltammetric measurements, organic nanoparticles of IFE exhibit good response towards sensing and selective detection of Cu(II) ions in aqueous medium. Under optimum conditions, the sensor shows excellent response for Cu(II) even in the presence of other alkali, alkaline earth, and transition metal ions. Differential pulse voltammetry was applied to the optimized electrode and a linear dynamic range from

(2.5×10^{-6} to 1.4×10^{-5} mol/L) with a detection limit of 8.22×10^{-8} mol/L was obtained. This system has also been applied as voltammetric sensor for the determination of Cu(II) ion in various real-life samples.

Chapter 1

Introduction

1.1 Sensors

There are devices, which sense the target species present in the system. We have at least five of these i.e., nose, tongue, ear, eye and skin. In a laboratory, one of the best types of sensor is the litmus paper test for acids and alkalies, which gives a qualitative indication, by means of a colour reaction, of the presence or absence of an acid. A more reliable approach for the degree of acidity is pH measurement by the use of special indicator solutions for colour reactions or by simple pH paper. However, the best method of determining acidity is the use of the pH meter, which is an electrochemical device giving an electrical response that can be read by a digital read-out device.

In such methods, the sensor that responds to the degree of acidity is either a chemical, the dye in litmus or a more complex mixture of chemical dyes in pH indicator solutions or the glass membrane electrode in the pH meter. The chemical or the electrical response then has to be converted into a signal that we can observe. In the case of the pH meter, the electrical response (a voltage change) has to be converted i.e., transduced into an observable response-movement of a meter needle or a digital display. The part of the device that transmits this conversion is called a transducer. We can divide sensors into three types, namely:

(a) Physical sensors for measuring distance, mass, temperature, pressure, etc.,

(b) chemical sensors which measure chemical substances by chemical or physical responses, and

(c) biosensors, which measure chemical substances by using a biological sensing element. All of these devices have to be connected to a transducer of some sort so that a visibly observable response occurs.

Chemical sensors and biosensors are generally concerned with sensing and measuring particular chemicals which may (or may not) be biological themselves. Biosensors are really a sub-set of chemical sensors, but are often treated as a topic in their own right. A biosensor can be defined as a device incorporating a biological sensing element connected to a transducer. It consists of biological identification elements e.g., nucleic acids, enzymes, tissues, antibodies and other biologically derived materials that interact

with the analyte under study. The key difference is that the recognition element is biological in nature.[1-3]

1.2 Aspects of Sensors

1.2.1 Recognition Elements

Recognition elements are the key component of any sensor device. They impart the selectivity that enables the sensor to respond selectively to a particular analyte or group of analytes, thus avoiding interferences from other substances. Method of analysis for specific ions has been available for a long-time is ion-selective electrodes, which usually contain a membrane selective for the analyte of choice.

1.2.2 Transducers - The Detector Device

Analytical methods in chemistry mainly based on photometric transducers, as in spectroscopic and colorimetric methods. However, because of the simplicity of construction and cost, most sensors have been actually developed around electrochemical transducers. With electron-driven microprocessors, the directness of an electrical device will tend to have a maximum appeal. In addition, the use of micro-mass-controlled devices, based on piezoelectric crystals, may become competitive in the near future.

Transducers can be subdivided into the following four main types.

A. Electrochemical Transducers

1. Potentiometric: These involve the measurement of the Emf (potential) of a cell at zero current. The Emf is proportional to the logarithm of the concentration of the substance being determined.
2. Conductometric: Most reactions involve a change in the composition of the solution. This will normally result in a change in the electrical conductivity of the solution, which can be measured electrically.
3. Voltammetric: An increasing (decreasing) potential is applied to the cell until oxidation (reduction) of the substance to be analysed occurs and there is a sharp rise (fall) in the current to give a peak current signal. The height of the peak current is directly proportional to the concentration of the electroactive material. If the appropriate oxidation (reduction) potential is known, one may step the potential directly to that value and observe the current. This mode is known as amperometry.
4. FET-based sensors: Miniaturisation can be achieved by constructing one of the above types of electrochemical transducers on a silicon chip-based field-effect transistor.

This has mainly been used with potentiometric sensors, but could also be used with voltammetric or conductometric sensors.

B. Optical Transducers

These have taken a new turn in fibre optics development to make it more highly flexible and more miniaturized. These include different techniques such as absorption spectroscopy, fluorescence spectroscopy, luminescence spectroscopy, internal reflection spectroscopy, surface plasma spectroscopy, and light scattering.[4]

C. Piezo-Electric Devices

These devices involve the generation of electric currents from a vibrating crystal. The frequency of vibration is affected by the mass of material adsorbed on its surface, which could be related to changes in a reaction. Surface acoustic wave (SAW) devices are a related system.[5]

D. Thermal Sensors

All chemical and biochemical processes involve the production or absorption of heat. This can be measured by sensitive thermistors and hence, be related to the amount of substance to be analysed.[6]

Another approach is the multi-walled carbon nanotubes (MWCNTs) as excellent ion-to-electron transducers in ion-selective electrodes. They indeed improve the stability of the potentiometric signal without suffering from external interference such as undesired redox species, sensitivity to light, etc.[7] In addition, these devices could be easily prepared by incorporating multi-walled carbon nanotubes directly in the ion-selective membrane.

1.3 Supra-Molecular Chemistry

To achieve a ligand 'tailored' for a particular metal-ion binding application, the system needs to be designed in such a way that it is able to read the information encoded in the metal ion of interest and differentiate it from the other metals that might also be present.[8, 9] Clearly, nature has learned to do this excellently in a wide range of biochemical systems. In contrast, the performance of synthetic systems has been somewhat modest. This is perhaps surprising in view of the fact that we are now around a century on from Alfred Werner's time. Thus, although metal ion recognition is inherent to many processes in nature, the factors influencing such behaviour are often difficult to elucidate. This is especially the case when mixed donor sets are present and or heavy metal ions are

involved. For a particular polydentate ligand, metal ion recognition may involve contributions from some or all of the following:[10]

(a) The number and type of donor atoms available.

(b) Their relative positions in terms of both their spacing and sequence within the ligand.

(c) The electronic and structural nature of the ligand's backbone.

(d) The formal charge and or the presence or absence of dipoles (both permanent and induced) on the bound ligand.

(e) The number and size of the chelate ring formed on metal binding.

(f) The changes in salvation of the ligand and metal ion on complex formation.

Further, crystal field effects may also help to reduce free energy for complex formation ions for transitional metal ion. In the case of macrocyclic ligand systems, macrocyclic ring size is another factor that will affect complex stability. The ability of a given ligand to recognize a metal in the presence of others will normally reflect a subtle mix of factors on the type just mentioned (although, it is noted that, in some cases, one factor, such as the donor set type, may appear to dominate the process). The situation is further complicated by the fact that several of the factors listed above are not independent of each other. However, in general terms, recognition for a particular metal ion of interest will occur when the properties of the ligand best match the steric and electronic nature of the metal ions, relative to those of the other metal ions present. It needs to be kept in mind that metal ion selectivity depends on achieving a difference in the binding constants for the respective cations. That is the difference in the constants rather than their absolute magnitude, which is usually of prime concern. Of course, it may be beneficial to have high absolute values since, for example, the latter may commonly be linked with enhanced kinetic stabilities. The process of selecting a cyclic or acyclic ligand was a typical metal ion-recognition test which, based on an analogy with known systems, might be likely to show a preference for the ion of interest. An investigation of ligand for its metal coordination chemistry is then carried out. Since the antibiotic nigericin was isolated in 1951 as the first representative, natural ionophores have attracted wide attention and been the subject of numerous investigations. They are known to explicitly transport biological guest species across a bio-membrane. For example, valinomycin transports the K^+ ion with much larger efficiency than the Na^+ ion, whereas monensin selectively transports the Na^+ ion against its concentration gradient. Their molecular structures, cation binding, physiological activities, transport properties, and other

biochemical actions have been widely investigated and their molecular recognition and transport functions are important topics of current chemistry. Several structurally diverse compounds have been found to act as ionophores in many biological membrane systems. Although they have various molecular skeletons, chain lengths, ligand topologies and donor atoms, a distinction is made between the acyclic podands, the macrocyclic crown ethers, and the armed macrocycles.[11-13]

1.3.1 Coordination Chemistry of Some Supramolecules

In the coordination chemistry of synthetic and natural ionophores there are several important differences. In particular, natural ionophores form three-dimensional complexes with cations. Classically, valinomycin is the most famous ionophore specific for the K^+ ion, which has a 32-member ring of the crown ether type. Monensin is a more flexible podand-type natural ionophore, but shows higher stability constants for several metal cations than synthetic crown ethers and podands. Crystallographic studies of the Ag^+ complex clearly show that a stable complexation results in a characteristic pseudo-cyclic conformation. The ends of the chain are linked by intramolecular head-to-tail hydrogen bonds involving the carboxylate anion and suitably placed -OH groups. Thus, the guest cation is located at the center of pseudo-cavity and tightly coordinated by six oxygen atoms. Rapid development in the synthesis of neutral macrocyclic ligands that can be complexed with anions and cations has stimulated research efforts in various fields of chemistry. The pioneering work of Pedersen on macrocyclic polyethers or crown ethers was chiefly concerned with oxygen containing ring systems and produced a series of powerful complexing agents for alkali and alkaline earth cations.[14] Successive investigations led to macrocycles with nitrogen and sulfur atoms as binding sites in addition to oxygen and often as part of a sub heterocyclic structure such as a pyridine, thiophene, and furan ring. More powerful cation complexing ligands, notably polyaza-polyoxa macropolycycles or cryptands were developed by Lehn and his co-workers.[15, 16] Some of these ligands have been designed to form binuclear cation inclusion complexes such as the cylindrical macro tricycles in which two macrocyclic rings are linked by two bridges. Further, Lehn et al. developed the bis-tren macobicyclic ligands, in which two cations are held inside a large intra-molecular cavity. With the proper design, such a binuclear cryptate can be used for activating substrates by inserting them between the two cations. An interesting class of neutral acyclic ligands coined “podands” and developed recently by Vogtle and Weber[17] have properties similar to those of crown

ethers and cryptands and can also form crystalline alkali ion complexes or extract alkali salts from an aqueous into an organic phase. In addition to carriers for group 1A and 2A cations, ionophores for transition metals and for their enantiomeric salts have also been developed.[18] Electrically neutral, lipophilic ion-complexing agents of rather small relative molar mass are known to behave as ionophores or ion carriers, having the capability to selectively extract ions from aqueous solutions into a hydrophobic membrane phase and to transport these ions across such barriers by carrier translocation.

1.3.2 Structural Features

Thousands of different macrocycles that fall under the general description "crown ether and podands" are now known.[19-21] It is, therefore, impossible to define the structural features beyond the presence of a macrocyclic ring (generally, but not always, considered to be 12 members), in which heteroatoms (generally 4) are separated by a carbon-containing unit of two or more atoms. Oxygen is possibly the predominant heteroatom in macrocycles intended to bind alkali metals. Nitrogen is often incorporated into these structures and may predominate when binding to transition metals. In the case of a heteroaromatic component such as furan or pyridine, the sub cyclic unit may contribute a heteroatom to the donor array. A ligand that behaves as an ionophore must meet the following requirements:

1. The carrier molecule should be composed of polar and nonpolar groups.
2. The carrier should be able to assume a stable conformation that provides a cavity, surrounded by the polar groups, appropriate for the uptake of a cation, while the nonpolar groups form a lipophilic shell around the co-ordination sphere. These groups must confirm sufficiently large lipid solubility for ligand and complex.
3. Among the polar groups of the ligand sphere, there should be preferably 5 to 8, but not more than 12, co-ordinating sites such as oxygen atoms.
4. High selectivity is attained by locking the coordinating sites into a rigid arrangement around the cavity. Such rigidity can be enhanced by the presence of bridged structures, e.g. hydrogen bonds. Within one group of the periodic system, the cation that fits into the offered cavity is preferred. Ideally, all cations should be forced into accepting the same given number of coordinating groups.
5. The ligand should be flexible enough to allow a sufficiently fast ion exchange.

1.3.3 Schiff Bases as a Recognition Unit

Present thesis work is related to the preparation of imine-based sensors for the sensing of cations. The Schiff bases system is known to perform as an efficient donor–bridge–acceptor system.[22, 23] Azomethine grouped Schiff base compounds are the most significant ligand in modern coordination chemistry due to their excellent coordinating ability. The Schiff base moiety in the receptor plays a key role in the host-guest chemistry of these ionophores with transition metal ions. The complex Schiff bases have many applications in various electrochemical fields[24], such as highly selective polymer membrane electrodes[25], optical sensors[26], and other biological probes.[27] Schiff base receptors have a strong tendency to bind with metals like Zn, Cd, Ag and Cu due to substituents groups such as hydroxyl, nitro, phenyl, etc. present on benzene ring which acts as binding sites.

1.4 Analytical Techniques

Quantitative measurement of an analyte will depend on a number of factors. Many available techniques possess varying degrees of selectivity, sensitivity, accuracy, and precision, cost and rapidity. Gravimetric analysis usually involves the selective separation of the analyte by precipitation, followed by the very non-selective measurement of mass. In volumetric analysis, the analyte reacts with a measured volume of a reagent of known concentration, in a process called titration. A change in some physical or chemical property signals the completion of the reaction. Gravimetric and volumetric analyses can provide results accurate and precise to a few parts per thousand or better. But they require relatively large quantities of analyte and are well suited for the measurement of major constituents. Instrumental techniques are used for many analyses (Table 1.1) and constitute the discipline of instrumental analysis. They are based on the measurement of a physical property of the sample, for example, an electrical property or the absorption of electromagnetic radiation. Examples are spectrophotometry (ultraviolet, visible, or infrared), fluorimetry, atomic spectroscopy, mass spectrometry, nuclear magnetic resonance spectrometry (NMR), X-ray spectroscopy, electroanalytical chemistry (potentiometric, voltammetric), chromatography (gas, liquid), and radiochemistry. Instrumental techniques are generally more sensitive and selective than the classical techniques but are less precise, on the order of 1 to 5% or so. These techniques are usually much more expensive. But depending on the numbers of analyses, they may be less expensive when the analysis is done in bulk. They are usually more

rapid, may be automated, and may be capable of measuring more than one analyte at a time. Chromatographic techniques are particularly powerful for analysing complex mixtures. They perform the separation and measurement step simultaneously.

Table 1.1: Various analytical techniques with respect to different parameters

Method	**Approx. Range, (M)**	**Approx. Precision, %**	**Selectivity**	**Cost**	**Application**
Gravimetry	10^{-1}-10^{-2}	0.1	Poor-Moderate	Low	Inorganic
Titrimetry	10^{-1}-10^{-4}	0.1-1	Poor-Moderate	Low	Organic, Inorganic
Electrogravimetry	10^{-1}-10^{-4}	0.01-2	Moderate	Moderate	Organic, Inorganic
Kinetic Methods	10^{-2}-10^{-10}	2-10	Good-Moderate	Moderate	Enzymes, Inorganic
Chromatography	10^{-3}-10^{-9}	2-5	Good	Moderate high	Multicomponent, Inorganic
Spectrophotometry	10^{-3}-10^{-6}	2	Good-Moderate	Low-Moderate	Inorganic, Organic
Fluorometry	10^{-6}-10^{-9}	2-5	Moderate	Moderate	Organic
Atomic spectroscopy	10^{-3}-10^{-6}	2-10	Good	Moderate high	Multicomponent, Inorganic
Potentiometry	10^{-1}-10^{-6}	2	Good	Low	Inorganic, Organic
Voltammetry	10^{-3}-10^{-6}	2-5	Good	Moderate	Inorganic, Organic

Constituents are separated as they are washed down a column of appropriate material that interacts with the analytes to varying degrees, and the analytes are sensed with an appropriate detector as they emerge from the column, to give a transient peak signal, in proportion to the amount of analyte.

In direct determinations, the ion-selective electrode (ISE) and a reference electrode are immersed in a stirred sample and the obtained cell potential related to the analyte activity or concentration by means of a calibration graph: the expected accuracy and precision for such a straightforward method should be comparable to those of a pH measurement. The ‘glass electrode’ is the best-behaved of all ion-selective electrodes, yet measurements of pH to better than ± 0.001 pH is equivalent to ±0.6 mV or in terms of hydrogen ion activity, ± 2% is not known. Thus, using other electrodes an uncertainty of ± 2% or even down to ± 0.5% may only be obtained with care; this may be good in

comparison with other techniques at the 10^{-5} M level but is often poor at 10^{-2} M. The accuracy and precision may be improved by resorting to a more elaborate technique involving several potential measurements. Consequently, a balance must be struck between accuracy and convenience in the choice of technique. A corollary of this is that the sensors are more suited to the relatively imprecise analysis of samples containing the determinant in a wide range of activity than to precise analysis of samples containing the determinant in a narrow range.

One of the most attractive features of the electrodes and probes is the speed with which they permit a sample to be analysed, and the ease with which the methods may be made semi-automatic or fully automatic. If samples are measured by a direct method, all that has to be done is to pre-treat the sample by addition of a pre-treatment reagent, stir the sample and put the ISE and reference electrode into it; the equilibrium cell potential may be read usually within about a minute and the answer is obtained. Other advantages of analyses by electrodes are that the methods may be non-destructive and are adaptable to very small sample volumes. Fluoride samples have been analysed with volumes down to 10 μL. Also, analyses may be made without difficulty of highly coloured, viscous samples containing a high concentration of suspended solids. However, problems do arise in the analysis of some non-aqueous and partially non-aqueous samples.

1.4.1 Classification of Electroanalytical Methods

There are four main classes of electrochemical methods of analysis: potentiometry, voltammetry, conductometry and coulometry

(i) Potentiometry: the measurement of a cell potential at zero current.
(ii) Voltammetry: in which an oxidizing (or reducing) potential is applied between the cell electrodes and the cell current is measured.
(iii) Conductometry: where the conductance of the cell is measured by an alternating current bridge method.
(iv) Coulometry: based on the measurement of quantity of electrical charge that passes through a solution during an electrochemical reaction.

1.4.2 General Sensor Design Criteria

A useful electrochemical sensor (based on potentiometry) must obey a number of experimental design criteria, many of which are linked to its potential benefits. Among the most important are:

1. For potentiometric sensors, there is an adequate electrode material, free from interferences.
2. The concentration of electroactive species can be determined with sufficient accuracy and precision.
3. The drift or diminution of sensor response with time owing to electrode degradation or surface fouling is sufficiently small.
4. The measurements are sufficiently reliable and repeatable.
5. The response time of the sensor is sufficiently fast.
6. Calibration is simple and easy to perform.
7. The detection limit is sufficiently low.

The relative importance of these factors depends on the monitoring necessities as well as on the technique employed and the electrode and cell configuration. Recent tendencies in the development of potentiometric sensors for monitoring have been the production of sensors that are more robust, more reliable (i.e., needing less calibration with smaller potential drift) and can be used in a wider range of solutions. Potentiometric sensors include ion-selective electrodes based on hydrophobic plasticized PVC membranes doped with neutral carriers have been extensively developed for many ions.[28-33] For example, Schiff base ionophores can be incorporated into polymer membranes, the recognition coming from the size of the host cavity or through specific metal-ligand interactions.

1.4.3 Ion Selective Electrode

Ion-selective electrodes are generally membrane-based devices, consisting of permselective materials, which separate the sample from the membrane electrode. On the inside of the membrane is a solution containing the ion of interest at a constant activity. The membrane is usually nonporous, water insoluble, and mechanically stable. A potential is developed with the ion of interest due to selective binding processes leaving co-ions behind. Membrane gradients like ionophores possessing different ion-recognition properties, have thus been developed to impart high selectivity. The detailed theory of the processes occurring at the interface of these membranes, which generate the potential, is available in details in literature.[34-36] As per the thermodynamic considerations, the gradient of activity across the membrane (of the analyte ions in the outer and inner solutions) produces a free energy difference is generated:

$$\Delta G = -RT \ln\left(\frac{a_{i,sample}}{a_{i,int.soln}}\right) \quad [1]$$

where R is the universal gas constant (8.134 $JK^{-1}mol^{-1}$) and T is the absolute temperature. The potential produced across the membrane corresponds to this free energy difference:

$$E = -\frac{\Delta G}{nF} = \frac{RT}{nF} \ln\left(\frac{a_{i,sample}}{a_{i,int.soln}}\right) \quad [2]$$

ISEs respond according to the "activity", rather than the concentration of ions. The difference between concentration and activity is due to different types of possible ionic interactions) that may reduce the effective concentration of the primary species. The activity of an ion *i* in solution is related to its concentration, c_i, by

$$a_i = f_i\, c_i \quad [3]$$

where, *fi* is the activity coefficient. The activity coefficient depends on the types of ions present and on the total ionic strength of the solution. The activity coefficient is given by the Debye-Huckel equation:

$$log f_i = \frac{-0.51 z_i^2 \sqrt{\mu}}{1+\sqrt{\mu}} \quad \text{(at 25 ºC)} \quad [4]$$

where, μ is the ionic strength. The departure from unity increases as the charge of the ion increases.

Measurements with ISEs are performed with respect to well-defined reference electrodes through a liquid junction. In an ISE, polymeric membrane containing organic compound separates the aqueous sample solution from the aqueous inner solution. Reference electrode is dipped in each solution to complete the circuit. Potential across the membrane is generated when the sample solution is connected to both electrodes. The primary ion is transferred from the sample to the membrane phase and vice-versa. This dynamic ion-exchange equilibrium leads to the generation of potential difference on both sides. The potentiometric measurement is carried out when no current is present in the system. The transfer of primary ion from solution to membrane phase in this state is equal to the transfer of ions from membrane to solution phase.[37-41] The resulting potential generated of the ion-selective electrode relative to reference electrode is dependent on the concentration of the primary ion present in a sample solution. The electrode potential for ISE is defined by the Nikolsky-Eisenman equation[42] as:

$$E = E° - 2.303\, \frac{RT}{nF} \log\left(a_A + K_{AB}^{Pot}\, a_B\right) \quad [5]$$

Where E is cell potential, *E*° is standard potential of membrane electrode, R is universal gas constant, n is number of electrons, F is Faraday constant, T is absolute temperature,

a_A is activity of species A, a_B is the activity of species B and K_{AB}^{Pot} is selectivity coefficient of species A relative to species B. For example, if an electrode is 50 times more responsive to A than to B, K_{AB}^{Pot} has a value of 0.02. A K_{AB}^{Pot} of 1.0 corresponds to a similar response for both ions. When K_{AB}^{Pot}»1, then the ISE responds better to the interfering ion B than to the target ion A. Usually, K_{AB}^{Pot} is smaller than 1, which means that the ISE responds more selectively to the target ion. The lower the value of K_{AB}^{Pot}, the more selective is the electrode. Selectivity coefficients lower than 10^{-5} have been achieved for several electrodes. For an ideally selective electrode, K_{AB}^{Pot} would equal zero (i.e., no interference). Obviously, the error in the activity a_A due to the interference of B would also depend upon their relative levels. The term a_A/a_B corrects for a possible charge difference between the target and interfering ions.

Components of Ion-Selective Membrane

Ion-selective membrane contains four fundamental elements that have an important effect on the response and ion-selective electrode characteristics, nature and number of each element [43-46]. The following components are:

1. Polymer matrix (provide flexibility to the membrane)
2. Lipophilic salt (Ionic additive)
3. Plasticizer (membrane solvent)
4. Ionophore (membrane-active recognition)
5. Multi-walled carbon nanotubes (Ion-to-electron transducer)

Polymer Matrix

Polymer matrix provides flexibility and mechanical strength to the membrane, so, it is necessary to use a hydrophobic polymer which has a lower glass transition temperature (T_g) as compared to room temperature. The solvent-plasticizer must be capable of dissolving all the components of the membrane and should not contain any functional group that may interfere in the sensing response of the ion-selective electrode. Among the reported matrix, polyacrylic polymers, silicon rubbers, etc. polyvinyl chloride (PVC) is the one which is most commonly used polymers in ion-selective membranes. It is well known that the potentiometric selectivity of PVC membranes correlates with their transport selectivity and very often it also correlates with the extraction selectivity.[47] The PVC membranes differ from liquid ones in their polarity and therefore in the dissociation degree of membrane electrolytes.[48] It is reported that, generally the PVC does not interact with the ionophore in films.[49]

Lipophilic Ion

The prerequisite for a theoretical Nernstian response of the ISE is that no significant amount of primary ions may be co-extracted together with counter ions (ions with opposite charge sign of the measuring ion) from the sample into the membrane phase. This means that the membrane is permeable only for ions with the same charge sign of the measuring ion. This membrane characteristic is called permselectivity or Donnan exclusion. The presence of non-exchangeable lipophilic ions in the membrane phase guarantees the operation of the ISE by keeping the total concentration of measuring ions in the membrane much higher than the co-extracted amount, i.e. constant. Some of the lipophilic additives as cation exchanger are sodium tetraphenylborate (NaTPB), potassium tetrakis(p-chloropheny1)borate (KTPClPB), trioctylmethylammonium chloride (TOMACl) while tetrakis[3,5-bis(trifluoromethyl)phenyl]borate (TFPB) and tridodecylmethylammonium (TDMACl) chloride as anion exchanger.

Lipophilic Salt

The addition of a lipophilic salt without ion-exchanger properties reduces the electrical resistance of the membrane.

Plasticizer

Plasticizers are additives that improve the mechanical and physical features of the membrane being studied. Plasticizer reduces the polymer glass transition temperature to below the ambient temperature in order to convert hard stiff polymer into softer and more elastic elastomer. The amount of plasticizer greatly influences the selectivity behaviour of membrane by changing its dielectric constant, affecting the ligand state and ionic mobility. It affects membrane selectivity through both extraction of ions into organic phase and influencing their complexation with ionophore. This impacts membrane selectivity with ion removal in an organic phase and influences the complexity of target ions with ionophore. On the other hand, difference in polarity and dielectric constant also have a direct influence on the ion-exchanging properties. High dielectric constant plasticizers must be physically sufficient for polymer. Leaching of the plasticizer also has an important consequence on the physio-chemical properties of the ion-selective electrode because it reduces the solubility of the active components therefore, reducing the selectivity and sensitivity of the membrane. The most commonly used plasticizers for the fabrication of membrane are: o-nitrophenyloctyl ether (o-NPOE), dibutyl phthalates

(DBP), didecyl phthalate (DDP), bis(2-ethylhexyl) phthalate (dioctyl phthalate, DOP) and bis(n-octyl)sebacate (DOS).

Ionophore

The most significant component in the matrix of ion-selective membrane is ionophore that plays a special and vital role in the selectivity of membrane. Ionophore can bind with the target analyte through different interactions like weak Vander Waals forces, hydrogen bonds, metal coordination and hydrophilic/lipophilic forces by forming a host-guest cavity. The ionophore must be retained in the membrane composition and bind with the primary ion more strongly than the interfering ion. Thus, ionophore must be synthesized according to the nature and amount of the analyte, as well as their capacity to interact with the target analysts as a host-guest. Additionally, to stop the leaching out of the ionophore from the membrane there should have enough lipophilic sites (lipophilic additives) available.

Multi-Walled Carbon Nanotubes (MWCNTs)

Some nanostructured materials are interfaced with outstanding electrical characteristics, such as elevated charge transfer and amazing electrical capabilities, which are of principal significance when they are used as ion-to-electron transducers in potentiometric sensors. MWCNTs have very exciting physicochemical properties like high aspect ratio, ultralightweight, high mechanical strength, and electrical conductivity, high surface area and thermal conductivity.[50, 51] Due to the three-dimensional spatial arrangement of carbon nanotubes which is favourable for the high loading of electroactive species occurs on the electrode surface, consequently enhancing the sensitivity of the chemically modified electrodes. These characteristics features of MWCNTs make it exceptional materials with the potential towards various applications.[52-54]

Using CNT in ion-selective electrodes not only improves the sensor's electrical conductivity but also enhances the transduction characteristics. The dynamic range, lifetime and response time of the sensor improve with increased conductivity and the potential response of the sensor to Nernstian values.[55, 56]

Response Mechanism

An electrochemical-measuring cell consists of two galvanic half-cells: the ion-selective electrode and the reference electrode. The total potential difference (electromotive force, EMF) measured under zero current conditions between the two electrodes is the sum of

local potential differences, arising at each electrochemical interface. Membranes of ionophore-based ISEs normally consist of a plasticized polymeric phase, typically with polyvinylchloride as a polymeric matrix, lipophilic ion-exchanger sites, and a lipophilic or covalently immobilized ionophore. Such membranes are placed between two aqueous solutions, one being the sample and the other, the so-called inner electrolyte

Various theoretical models for assessing the ion-selective electrode response have been defined.[57-59] Among these, phase boundary potential method is preferred because it describes the potentiometric response under steady-state/equilibrium conditions. The phase-boundary potential model describes the potential emerging at the interface of the aqueous and organic membrane phases by using thermodynamic equilibria and the electroneutrality condition within each phase and by assuming kinetic processes being fast between the two phases. It directly relates the spontaneous equilibrium partitioning of ions across the sample membrane interface to the phase-boundary potential. the response of ISEs can be described by the phase-boundary potential, E_{PB} because all other contributions of the Emf of the potentiometric cell are sufficiently constant:[37, 60, 61]

$$E_{PB} = E° \pm \frac{RT}{nF} \ln \frac{a_1(\text{aq})}{a_1(org)} \qquad [6]$$

with R, T, and F having usual meaning, n being the charge, and;

$$E^o = \frac{\mu^o(\text{aq}) - \mu^o(\text{org})}{nF} \qquad [7]$$

$\mu°$ and a_1 being the standard potentials and the ion activity in the respective phases.

The phase-boundary potential model has been used for many different cases to calculate the activity of the uncomplexed ion, a_1(org), in the membrane based on mass and charge balances and complex formation equilibria. If a_1 (org) does not depend on a_1(aq), the ISE response has a Nernstian slope of 59/x mV/decade. Apparent deviations from this slope can be described by changes of a_1(org) with a_1(aq) or by differences between a_1(aq) at the membrane surface and in bulk of the sample. The influence of an interfering ion was first described with the Nicolskii-Eisenman equation (eq. 1).

1.4.4 Voltammetric Sensors

Voltammetric measurement is based on the principle of current generation during redox reaction at electrode surface. The current-voltage relationship provides a basis for the voltammetric sensor.[37] Voltammetry is an electrochemical method involving

implementation of the potential (E), and measurement of the resulting current (I) present in electrochemical cell over a period of time (T).[1,37] Thus, all voltammetric techniques can be described as function of E, I, and T. Voltammetry systems include quantitative and qualitative analyses of inorganic and organic ions present in different medium, large range of concentrations (10^{-12} to 10^{-1} mol/L), rapid analysis, sensitive and selective detection.

In voltammetry, several well-known laws explain the effects of the applied potential and behaviour of the redox current. The applied potential monitors the redox species concentrations on the electrode surface (C_O^0 and C_R^0) and the rate of the reaction (k^0), as described by the Nernst or Butler–Volmer equations, respectively. When diffusion plays a controlling role, the resulting current from the redox process (known as the faradaic current) is related to the material flux at the electrode-solution interface and is described by Fick's law. The interrelation between these processes results in the characteristics features of the voltammograms observed in the different techniques. For a reversible electrochemical reaction, which can be described by $O + ne^- \leftrightarrow R$, the application of a potential E forces the respective concentrations of O and R at the surface of the electrode (i.e., c_O^0 and c_R^0) to a ratio in compliance with the Nernst equation: (8)

$$E = E° - \frac{RT}{nF}\ln\frac{c_R^o}{c_O^o} \qquad [8]$$

where R is the molar gas constant (8.3144 $J\ mol^{-1}K^{-1}$), T is the absolute temperature (K), n is the number of electrons transferred, F = Faraday constant (96,485 C/equiv), and E^0 is the standard reduction potential for the redox couple. If the potential applied to the electrode is changed, the ratio c_R^o/c_O^o at the surface will also change so as to satisfy Eq. 8. If the potential is made more negative the ratio becomes larger (that is, O is reduced) and, conversely, if the potential is made more positive the ratio becomes smaller (that is, R is oxidized).

For some techniques it is useful to use the relationship that links the variables for current, potential, and concentration, known as the Butler–Volmer equation: (9)

$$\frac{I}{nFA} = k^o\{c_O^o\exp[-\alpha\theta] - c_R^o\exp[(1-\alpha)\theta]\} \qquad [9]$$

where $\theta = nF\,(E - E^0)/RT$, k^0 is the heterogeneous rate constant, α is known as the transfer coefficient, and A is the area of the electrode. The value of I and k^0 obtain from this relationship. Finally, in most cases the current flow also depends directly on the flux of

material to the electrode surface. When new O or R is formed at the surface, the increased concentration provides the force for its diffusion toward the bulk of the solution. Likewise, when O or R is destroyed, the decreased concentration promotes the diffusion of new material from the bulk solution. The resulting concentration gradient and mass transport are described by Fick's law, which states that the flux of matter (F) is directly proportional to the concentration gradient: (10)

$$\phi = -ADo\left(\frac{\partial c_O}{\partial x}\right) \qquad [10]$$

where D_O is the diffusion coefficient of O and x is the distance from the electrode surface. An analogous equation can be written for R. The flux of O or R at the electrode surface controls the rate of reaction, and thus the faradaic current flowing in the cell. In the bulk solution, concentration gradients are generally small and ionic migration carries most of the current. The current is a quantitative measure of how fast a species is being reduced or oxidized at the electrode surface. The current is affected by many additional factors, the concentration of redox species, size, shape, and material of the electrode, solution resistance, cell volume, and the number of electrons transferred.

Modes of Mass transport

In electrochemical reaction, due to the cell potential difference rate of reaction can be changed, however, the rate of exchange of electroactive species to the electrode surface also influences the overall electrical response. The measured current corresponds to the mass transfer and electron flow rate in an electrochemical cell. Three methods of mass transfer are available for neutral and charged species onto the electrode surface in an electrochemical cell; diffusion, migration and convection.[62-64]

(a) Diffusion

Diffusion arises from the local uneven concentration of reagents. It results due to the movement of analyte species from the region of higher concentration to the region of lower concentration, consequently maximize the entropy which is the driving force for the process. The rate of movement of chemical species by diffusion can be predicted mathematically and it is described by the Fick's law as;

$$J_o = -D_o\left(\frac{\partial C_0}{\partial x}\right)$$

Where J_o is the diffusional flux and D_o is the diffusion coefficient and $\frac{\partial C_0}{\partial x}$ is the concentration gradient at point x. The negative sign indicates movement of species from region of high concentration to low.

(b) Migration

It is the movement of charged species under the influence of electrostatic field which arises due to the applied potential across the electrodes. This results in either attraction or repulsion of charged species by the electrostatic field.

(c) Convection

The flux to the electrode is not just affected by the diffusion or migration, but can also be affected by the convection. There are two forms of convection available. First is termed as natural convection arise due to density and thermal gradient present in any solution and cause unpredictable changes in the flux to the electrode. Second is forced convection which occurs due to stirring of the solution, or by the rotation or vibration of the electrode. Forced convection is generally more favourable than natural convection if it is introduced in a well-defined and quantitative manner. This allows control of flux to the electrode and eliminates any random aspects from the measurements.

Electrochemical Set up for Voltammetry

An electrochemical cell consists of the sample dissolved in a solvent, an ionic electrolyte and three electrode cell set-up comprising of a working electrode, reference electrode and an auxiliary electrode. Cell that is sample holder come in variety of sizes, shapes and materials (glass, Teflon, polyethylene) and their requirement depend on the type of reaction, techniques and analytical data to be obtained. In many cases, the reference electrode should be placed near to the working electrode and to avoid contamination it is necessary to place the reference electrode in separate compartment. The three electrodes are connected to the energy source containing a specially constructed circuit which is often referred to as a potentiostat.[65, 66] The detailed information about each of the electrodes is given below:

Working Electrode

Working electrode (WE) is the site in which an electrochemical reaction occurs under controlled potential with respect to the reference electrode using potentiostat. Working electrode is composed of redox-inert material and most important aspect is that electrode surface is extremely cleaned and working surface area is well-defined and its size is few

square mm. the working electrode is a polarised electrode and is able to acquire the applied potential. Examples of working electrodes are gold, glassy carbon, platinum, and mercury electrode. The surface of glassy carbon and platinum electrodes can be regenerated via mechanical polishing. To remove the dust particles and any other adsorbed substance from the working electrode polishing carried out with alumina slurry. Rest alumina particles can then be excluded by putting the electrode in an ultrasonic cleaner for approximately 15 minutes.[67, 68]

Reference Electrode

Reference electrode (RE) has constant potential throughout the experiment. There are some normally used reference electrodes available commercially: Standard hydrogen electrode (SHE), saturated calomel electrode (SCE), and Ag/AgCl electrode. For non-aqueous medium, generally Ag/Ag^+ couple reference electrode is used. The silver wire is dipped in a solution of silver salt, typically containing silver nitrate ($AgNO_3$).[69]

Counter Electrode

Introduction of the counter electrode is to permit the passage of current among the working electrode and counter electrode in the electrochemical cell. Counter electrode completes the circuit in a system and assists as a source of electrons flows. Because of the inert nature of platinum wire it is used as a counter electrode.[70]

Supporting Electrolyte

Supporting electrolyte is an electrolyte solution, whose constituents are not electro active in the range of applied potentials being studied, and whose ionic strength is usually much larger than the concentration of an electroactive substance to be dissolved in it and also it is an inert or inactive electrolyte. It is used to increase the conductivity of the solution, to eliminate the transport of electro active species by ion migration in the electric field and to maintain the constant ionic strength and guarantee a low electrical resistance.[71] Chlorides, sulphates and nitrates of lithium, sodium and potassium and tetraalkyl-ammonium salts of the general formula $NR_4^+X^-$ (R = methyl, ethyl, n-butyl and X^- =Cl^-, Br^-, I^-, $ClO4^-$) are generally used as supporting electrolytes. Acids (HCl, H_2SO_4), bases (LiOH, NaOH, $NR_4^+OH^-$) and buffer solutions also used as the supporting electrolyte.

Electrodes Processes

The reaction taking place between the electrode surface and species within the solution can proceed through a series of steps that cause the conversion of the dissolved oxidised

species (O) to reduced species (R) in solution. The electrode reaction rate is governed by the reaction rates such as:

(i) Mass transfer

(ii) Electron transfer of non-adsorbing species

(iii) The electron transfer in a chemical reaction which could be homogeneous such as protonation or heterogeneous like catalytic decompositions on the electrode surfaces.

(iv) Other surface reactions such as adsorption, desorption, crystallization, etc.

The simplest reaction involves only mass transfer of reactant to the electrode, heterogenous electron transfer involving non-adsorbed species and the mass transfer of the product to the bulk solution. A more complex reaction sequence involving a series of electron transfer, protonation, or modification of the electrode surfaces is quite common.

Voltammetric Techniques

The most commonly used voltammetric techniques are linear sweep voltammetry, cyclic voltammetry, and differential pulse voltammetry. These methods use the three-electrode system which measures the current passed at the working electrode either at fixed or variable applied potential. A brief introduction of these techniques is outlined below.

Linear Sweep Voltammetry

It involves measurement of current while potential is made to vary linearly with time. With the increase of scan rate, the value of faradaic current is found to increase. This is because the electrode surface has improved electroactive flux at a greater scan rate speed.[72]

Cyclic Voltammetry

Cyclic voltammetry provides evidence for a reaction mechanism. It gives information on the position of oxidation/reduction potentials of the electroactive compounds and influence of media on the redox process.[73] During the cyclic voltammetric experiments, potential is swapped linearly from the starting potential to the end potential and then originate back to the starting potential. The peak current magnitude increases where the oxidation or reduction of analyte occurs. Three electrodes comprise the voltammetric cell: a working electrode, reference electrode and an auxiliary electrode (counter). The three electrode systems are essential to avoid the current passing through the reference

electrode, which would otherwise change their potential through modifications in the species' activities.[74] Cyclic voltammetry process could be reversible, irreversible and quasi reversible depending on the analysis.[67, 75]

Reversible System

A system is said to be electrochemically reversible when kinetics at the electrode surface is faster than the rate of diffusion. An electrochemical reversible system obeys Nernst equation where oxidation and reduction of species occur in the same current strength and maintain the equilibrium condition.[64] The Nernst equation[67] for the reversible system is

$$E=E^{o}-\frac{RT}{nF}\ln\frac{C^{0}}{C^{R}}$$

Where E is potential of an electrode, E^{o} is formal potential, R, T and F have their usual meaning, C^{o} and C^{R} are concentrations of oxidised and reduced species. The equation for a reversible system is given by the Randels Sevcik equation[76] (at 25 °C):

$$i_p = (2.69 \times 10^5)\, n^{3/2}\, A\, D^{1/2}\, C\, \nu^{1/2}$$

Where A is an area of the electrode, D is the diffusion coefficient in cm^2s^{-1}, C is concentration in mol cm^{-3}, and ν refers to scan rate in Vs^{-1} and i_p is the peak current in amperes.

The separation of peak potentials for a reversible system is given by [77]

$$\Delta E_p = E_{pa} - E_{pc} = 59\,\frac{mV}{n}$$

Where E_{pa} and E_{pc} are the cathodic and anodic peak potentials. The numerical value of the peak potential at 25 °C is 59 mV for one-electron transfer. Another important parameter is the ratio of peak current i_{pa} (anodic peak current) and i_{pc} (cathodic peak current) is equal to one for a reversible system.

Irreversible System

The scheme is said to be irreversible if the response rate on the electrode surface is lower than the diffusion rate. Scan rate depends on the maximum peak potential separation and maximum current separation. With the scan rate for a completely irreversible system, the peak potential change. The equation for a peak current for an irreversible system is given by [76]

$$i_p = (2.99 \times 10^5)\alpha^{1/2}\, AD^{1/2}\, C\nu^{1/2}$$

Where, α is transfer coefficient (rate of electron transfer).

Quasi-Reversible System

Quasi-reversible system lies between the reversible and irreversible system in which the reaction is measured by the charge transfer as well as mass transfer. As compared to the reversible system, the peak potential separation in the quasi-reversible system is very large. The current for a quasi-reversible system is given by:[76]

$$i= FAD^{1/2}Cf^{1/2}\ \nu^{1/2}\psi(E)$$

Where $f = \frac{F}{RT}$, and $\psi(E)$ is funa ction of quasi-reversible system.

Differential Pulse Voltammetry

Differential pulse voltammetry applied for the measurements of trace amount of electroactive species in inorganic and organic samples. In this technique, potential is scanned with a number of periodic pulses superimposed on the linear potential ramp. The current is recorded at first point where the pulse starts and second point is where the pulse end. The difference of current among these two points is measured and plotted against the base applied potential.[77]

1.5 Research Proposal

As trace elements, some heavy metals are important for sustaining the metabolism of the human body.[78-80] However, long-term exposure to heavy metals can cause deleterious health effects in humans. Industrial wastes comprising metal ions such as aluminium, copper, nickel, zinc and lead are common due to their large-scale uses in many industrial processes like electroplating, battery manufacture, mining, metal finishing, brewing, pharmaceutical manufacture, etc.[81] Consequently, there is an urgent requirement to develop a appropriate method for the detection of trace metal ions in chemical, biological and environmental samples.

Sophisticated methods for metal ion detection include inductively coupled plasma (ICP), spectrophotometry, atomic absorption spectrometry (AAS), and liquid-phase chromatography. Although these methods provide accurate results, they have some practical limitations such as nonportability, being expensive and time-consuming and require sample pre-treatment. To overcome these limitations electrochemical methods (voltammetry and potentiometry) have proven to be very promising analytical techniques due to their ability to provide high selectivity, sensitivity and lower detection limit, low cost and does not require complicated sample pre-treatment.

Recently, nanomaterials played an important role in modifying electroactive ionophores which improved their performance as electrode materials for chemical sensing. It is widely accepted that performance of electrochemical sensing platforms has improved amazingly with incorporation of nanostructure material like multiwalled carbon nanotubes (MWCNTs) and nanoparticles.

It is proposed to study a series of imine based ionophores with a varying number of amine groups. MWCNTs in optimized amounts shall be added to the ionophores with a potential of trace level detection of heavy metal ions. It will be interesting to compare performance of the projected group of molecules with those incorporated with CNTs. Performance of the chemical sensors was found as improved and can be applied for various applications in biomedical, environmental and routine chemical sensing of heavy metal ions using potentiometric and voltammetric techniques.

References

1. B. R. Eggins, *Chemical Sensors and Biosensors*, John Wiley & Sons, 2008.
2. F.-G. Banica, *Chemical Sensors and Biosensors: Fundamentals and Applications*, John Wiley & Sons, 2012.
3. C. Steinem and A. Janshoff, *Piezoelectric Sensors*, Springer Science & Business Media, 2007.
4. M. Leclerc, *Advanced Materials*, 1999, 11, 1491-1498.
5. H. Jaffe and D. Berlincourt, *Proceedings of the IEEE*, 1965, 53, 1372-1386.
6. J. Lai, T. Perazzo, Z. Shi and A. Majumdar, *Sensors and Actuators A: Physical*, 1997, 58, 113-119.
7. E. J. Parra, G. A. Crespo, J. Riu, A. Ruiz and F. X. Rius, *Analyst*, 2009, 134, 1905-1910.
8. R. M. Izatt, K. Pawlak, J. S. Bradshaw and R. L. Bruening, *Chemical Reviews*, 1991, 91, 1721-2085.
9. L. F. Lindoy, *The chemistry of macrocyclic ligand complexes*, Cambridge University Press, 1990.
10. B. Wang and M. R. Wasielewski, *Journal of the American Chemical Society*, 1997, 119, 12-21.
11. J. W. Steed and J. L. Atwood, *Supramolecular Chemistry*, John Wiley & Sons, 2013.
12. D. J. Cram, *Angewandte Chemie International Edition in English*, 1988, 27, 1009-1020.
13. H. J. Schneider, *Angewandte Chemie International Edition*, 2009, 48, 3924-3977.
14. C. J. Pedersen, *Journal of the American Chemical Society*, 1967, 89, 7017-7036.
15. J.-M. Lehn, *Science*, 1993, 260, 1762-1764.
16. J. M. Lehn, *Angewandte Chemie International Edition in English*, 1990, 29, 1304-1319.
17. F. Vögtle and E. Blasius, *Host Guest Complex Chemistry*, Springer-Verlag, 1981.
18. A. Ajayaghosh, E. Arunkumar and J. Daub, *Angewandte Chemie International Edition*, 2002, 41, 1766-1769.
19. F. Vogtle, J. P. Dix and D. Jaworek, Google Patents, 1983.
20. S.-K. Chang and I. Cho, *Journal of the Chemical Society, Perkin Transactions 1*, 1986, 211-214.
21. Y. Inoue and T. Hakushi, *Journal of the Chemical Society, Perkin Transactions 2*, 1985, 935-946.
22. V. K. Gupta, A. K. Singh and L. K. Kumawat, *Sensors and Actuators B: Chemical*, 2014, 204, 507-514.

23. Y. Zhang, G.-M. Zeng, L. Tang, C.-G. Niu, Y. Pang, L.-J. Chen, C.-L. Feng and G.-H. Huang, *Talanta*, 2010, 83, 210-215.

24. I. Yilmaz, H. Temel and H. Alp, *Polyhedron*, 2008, 27, 125-132.

25. W. Al Zoubi and N. Al Mohanna, *Spectrochimica Acta Part A: Molecular and Biomolecular Spectroscopy*, 2014, 132, 854-870.

26. A. A. A. Aziz, *Journal of luminescence*, 2013, 143, 663-669.

27. N. M. Hosny, M. A. Hussien, F. M. Radwan and N. Nawar, *Spectrochimica Acta Part A: Molecular and Biomolecular Spectroscopy*, 2014, 132, 121-129.

28. P. Kumar and S. K. Mittal, *Journal of Chemical Sciences*, 2014, 126, 33-40.

29. N. Rani Gupta, S. K. Mittal and S. Kumar Sonkar, *Advanced Science, Engineering and Medicine*, 2013, 5, 656-661.

30. J. Buffle, F. L. Greter and W. Haerdi, *Analytical Chemistry*, 1977, 49, 216-222.

31. A. Abbaspour, A. Esmaeilbeig, A. Jarrahpour, B. Khajeh and R. Kia, *Talanta*, 2002, 58, 397-403.

32. S. K. Mittal, P. Kumar, S. Kumar and L. F. Lindoy, *International Journal of Electrochemical Science*, 2010, 5, 1984-1995.

33. H. A. Zamani, M. R. Ganjali and M. Adib, *Sensors and Actuators B: Chemical*, 2007, 120, 545-550.

34. R. P. Buck and S. Ciani, 1975.

35. D. Ammann, W. Morf, P. Anker, P. Meier, E. Pretsch and W. Simon, in *Ion-Selective Electrode Reviews*, Elsevier, 1983, vol. 5, pp. 3-92.

36. A. K. Covington, *Ion Selective Electrode Method: Volume 1*, CRC press, 2018.

37. E. Bakker, P. Bühlmann and E. Pretsch, *Chemical Reviews*, 1997, 97, 3083-3132.

38. P. Bühlmann, E. Pretsch and E. Bakker, *Chemical Reviews*, 1998, 98, 1593-1688.

39. H. Freiser, *Ion-Selective Slectrodes in Analytical Chemistry*, Springer Science & Business Media, 2012.

40. R. De Marco, G. Clarke and B. Pejcic, *Electroanalysis: An International Journal Devoted to Fundamental and Practical Aspects of Electroanalysis*, 2007, 19, 1987-2001.

41. U. Oesch, D. Ammann and W. Simon, *Clinical Chemistry*, 1986, 32, 1448-1459.

42. M. M. Walczak, D. A. Dryer, D. D. Jacobson, M. G. Foss and N. T. Flynn, *Journal of Chemical Education*, 1997, 74, 1195.

43. M. A. Arnold and M. E. Meyerhoff, *Analytical Chemistry*, 1984, 56, 20-48.

44. E. Pungor, *Analytical Sciences*, 1998, 14, 249-256.

45. A. Hodinar and A. Jyo, *Analytical Chemistry*, 1989, 61, 1169-1171.

46. N. Lakshminarayanaiah, *Membrane Electrodes*, Elsevier, 2012.

47. W. Morf, *Kiado, Budapest*, 1981, 430.

48. R. Armstrong and M. Todd, *Journal of Electroanalytical Chemistry and Interfacial Electrochemistry*, 1987, 237, 181-185.

49. K. Mikhelson, *Sensors and Actuators B: Chemical*, 1994, 18, 31-37.

50. B. Pérez-López and A. Merkoçi, *Microchimica Acta*, 2012, 179, 1-16.

51. Y.-P. Sun, K. Fu, Y. Lin and W. Huang, *Accounts of Chemical Research*, 2002, 35, 1096-1104.

52. P. Ajayan, *Chemical Reviews*, 1999, 99, 1787-1800.

53. A. Bianco, K. Kostarelos and M. Prato, *Current Opinion in Chemical Biology*, 2005, 9, 674-679.

54. L. Lacerda, A. Bianco, M. Prato and K. Kostarelos, *Advanced Drug Delivery Reviews*, 2006, 58, 1460-1470.

55. G. A. Crespo, S. Macho and F. X. Rius, *Analytical Chemistry*, 2008, 80, 1316-1322.

56. Z. Mousavi, J. Bobacka, A. Lewenstam and A. Ivaska, *Journal of Electroanalytical Chemistry*, 2009, 633, 246-252.

57. M. Rothmaier, U. Schaller, W. E. Morf and E. Pretsch, *Analytica Chimica Acta*, 1996, 327, 17-28.

58. S. S. Koseoglu, C. Z. Lai, C. Ferguson and P. Bühlmann, *Electroanalysis: An International Journal Devoted to Fundamental and Practical Aspects of Electroanalysis*, 2008, 20, 331-339.

59. A. Thoma, A. Viviani-Nauer, S. Arvanitis, W. Morf and W. Simon, *Analytical Chemistry*, 1977, 49, 1567-1572.

60. W. E. Morf, *The Principles of Ion-Selective Electrodes and of Membrane Transport*, Elsevier, 2012.

61. U. Schaller, E. Bakker and E. Pretsch, *Analytical Chemistry*, 1995, 67, 3123-3132.

62. N. V. Rees, J. A. Alden, R. A. Dryfe, B. A. Coles and R. G. Compton, *The Journal of Physical Chemistry*, 1995, 99, 14813-14818.

63. R. Compton, J. Eklund, S. Page, T. Mason and D. Walton, *Journal of Applied Electrochemistry*, 1996, 26, 775-784.

64. G. A. Mabbott, *Journal of Chemical Education*, 1983, 60, 697.

65. D. A. Gough, Google Patents, 1987.

66. B. H. Kim, H. Park, H. Kim, G. Kim, I. Chang, J. Lee and N. Phung, *Applied Microbiology and Biotechnology*, 2004, 63, 672-681.

67. P. T. Kissinger and W. R. Heineman, *Journal of Chemical Education*, 1983, 60, 702.

68. F. Winquist, P. Wide and I. Lundström, *Analytica Chimica Acta*, 1997, 357, 21-31.

69. R. C. Larson, R. T. Iwamoto and R. N. Adams, *Analytica Chimica Acta*, 1961, 25, 371-374.

70. N. Elgrishi, K. J. Rountree, B. D. McCarthy, E. S. Rountree, T. T. Eisenhart and J. L. Dempsey, *Journal of Chemical Education*, 2017, 95, 197-206.

71. J. J. Van Benschoten, J. Y. Lewis, W. R. Heineman, D. A. Roston and P. T. Kissinger, *Journal of Chemical Education*, 1983, 60, 772.

72. L. Nadjo and J. Savéant, *Journal of Electroanalytical Chemistry and Interfacial Electrochemistry*, 1973, 48, 113-145.

73. C. Andrieux, C. Blocman, J. Dumas-Bouchiat, F. M'halla and J. Saveant, *Journal of Electroanalytical Chemistry and Interfacial Electrochemistry*, 1980, 113, 19-40.

74. R. S. Nicholson, *Analytical Chemistry*, 1965, 37, 1351-1355.

75. J. Heinze, *Angewandte Chemie International Edition in English*, 1984, 23, 831-847.

76. A. J. Bard and L. R. Faulkner, *Electrochemical Methods*, 2001, 2, 482.

77. A. P. Brown and F. C. Anson, *Analytical Chemistry*, 1977, 49, 1589-1595.

78. C. V. Mohod and J. Dhote, *International Journal of Innovative Research in Science, Engineering and Technology*, 2013, 2, 2992-2996.

79. R. Singh, N. Gautam, A. Mishra and R. Gupta, *Indian Journal of Pharmacology*, 2011, 43, 246.

80. R. A. Wuana and F. E. Okieimen, *Isrn Ecology*, 2011, 2011.

81. K. Kadirvelu, K. Thamaraiselvi and C. Namasivayam, *Bioresource Technology*, 2001, 76, 63-65.

Chapter 2

Review of Literature

A class of compounds, which coordinate with metal ions, are a significant class arising from amino and carbonyl groups having azomethine group (-C=N-).[1-3] In azomethine derivatives, because of the existent of lone pair of electrons on nitrogen atom and its electron-donating capability, Schiff base possesses basic properties which are responsible for the formation of a complex with metals.[4,5] Schiff base coordination with metal ion depends on the nature of donor atoms, their tuneable electronic and steric properties, size of cavity formed and conformational flexibility of the ligand.[6-11] Because of these diverse structural features, large number of synthesis of Schiff base complexes have been carried out and these are successfully used in developing electrochemical sensors.

2.1 Schiff Base Ionophores for Chemical Sensing Using Potentiometry

Carrier-based ion-selective electrodes are well-known analytical methods, generally used for the measurement of diverse ions present in different biological and environmental samples.[12,13] A fused carrier that defines selectivity of electrodes via selective complex formation with target species is the main component of such a plasticized PVC membrane. Nitrogen-containing compounds have been extensively studied for cation sensing.[14] A few reports on imine-based structures are also reported in the literature.[15,16] As nitrogen is present in sp^2 hybridization in imine-based receptors which enables strong binding, thus it works as good receptors.[17,18] Due to electrical neutrality, potential electroactive material and ability to bind metal ions selectively, these compounds have attracted the attention of analytical scientists. Advantage of an ion-selective electrode as a potentiometric sensor for the identification of analytes in real-time analysis provides simplicity, low cost, easy preparation of samples, fast response time, lower detection limit and broad linear range. The literature survey discussing the response mechanisms, selectivity, detection limit, response time, measurement range and lifetime of the potentiometric sensor for cation recognitions based on the Schiff base ionophore and the important observation are given below:

Kaur *et al.* (2019)[19] synthesized Schiff base N,N′-bis(1-hydroxynaphthalene-2-carbaldehyde)-o-phenylenediamine for the potentiometric determination of Zn(II) ion. The electrode showed stable potential response when placed in contact with zinc solution

due to rapid exchange kinetics of the resulting ligand-metal ion complex. The sensor showed characteristics response in a wide concentration range of 10^{-7} to10^{-1} mol/L with a limit of detection of 0.18 nM. Analytical applicability was also checked by using it as an indicator electrode and for the Zn(II) recognition in pharmaceutical samples. **Kardas *et al.* (2019)[20]** synthesized and characterized Schiff base derivative containing azomethine group as PVC membrane sensor for copper(II) ion detection. The prepared sensor has quick response time, Nernstian response and wide concentration range of 1.0×10^{-5} - 1.0×10^{-1} mol/L. This probe was effectively utilized for the detection of Cu(II) in daily life samples. **Aglan *et al.* (2019)[21]** described the detection of Cd(II) with an electrode using lanthanum tungstate as a sensing material. Among the various plasticizers, o-NPOE was the best solvent mediator for the potentiometric determination of Cd(II) ions in aqueous samples. Proposed sensor had a well-defined detection limit of 0.8 nM with Nernstian response of 29.4 ± 0.12 and decent linear range with fast response time.

Hasani *et al.* (2018)[22] used Schiff bases (L^{I}, L^{II} and L^{III}) for solvent extraction of Cu(II) ions from the mixture of Co(II) and Ni(II). Due to the same electronic environment of the L^{I} and L^{II},selectivity was observed on the basis of plasticizer used for fabrication. The study reveals the selectivity of Schiff bases for copper ions and were utilized as copper ion-selective electrodes. The optimized electrode showed a wider concentration range and lower detection limit. **Abbas *et al.* (2018)[23]** reported Schiff base ionophore which was covalently linked to polyacrylamide ionophores and prepared polymeric membrane electrodes that were precoated with poly (3,4-ethylenedioxy-thiophen) conducting polymer onto the gold electrode. Author described the reactivity of 3-carbonyl group for Ca^{2+} over 2-carbonyl group. 2-carbonyl group has amide character due to the adjacent position of nitrogen atom, the lone pair of which readily delocalised on the 2-carbonyl group thereby reducing the electrophilic character. The sensor exhibited a very less detection limit of 2×10^{-10} mol/L, good Nernstian response of 28.5 mV/decade.

Sahani *et al.* (2017)[24] described zinc ion-selective electrode on the basis of a Schiff base. Outcomes of different plasticizers and anion excluder on the potentiometric response of the electrode was examined and this optimized electrode was checked for the performance characteristics of the sensor like detection limit of 8 nM, Nernstian slope of 29.6 ± 0.2 mV/decade and works in acidic pH range with fast response time of 10 s.

Ali *et al.* (2017)[25] used four Schiff base ionophores for the fabrication of plasticized carbon paste electrodes. The potentiometric response was evaluated towards the sensitive and selective detection of Co(II) and gave higher response characteristics like Nernstian response, low detection limit and wide working pH range. **Chandra *et al.* (2016)[26]** explored neutral carrier for the construction of PVC membrane electrode on the basis of copper complex of Schiff base p-hydroxyacetophenone semicarbazone towards selective identification of copper ions. The sensor response was found to be good with low detection limit, Nernstian response and applicable pH range with fast response time. Author also reported that this sensor works well in partially aqueous medium of up to 75% of distilled water used for the experiment. The proposed sensor permits direct detection of copper ions in various daily-life samples. **Demir *et al.* (2015)[27]** reported cation recognition sensor based on Schiff base (H_2IF). Spectrophotometrically, upon deprotonation the ligand form a complex with Cu(II) by red shifting. It has been probed as potentiometric sensor for the sensitive and selective determination of Cu(II) ions. The PVC membrane electrode, under optimized conditions provided Nernstian response over broad concentration range (1.0×10^{-7} to 1.0×10^{-1} mol/L), lower detection limit of 0.44 nM. It was also implemented to detect copper ions in daily life samples as an indicator electrode.

Dena *et al.* (2014)[28] reviewed some Schiff base ionophores as sensing materials in electrochemical analysis. Synthesis of Schiff base, preparation of polymeric membrane sensors for the assembly of ion-selective electrodes were explored. The discussed research papers embrace potentiometric detection of transition metal ions and lanthanides. Author also reported the Schiff base ionophore for the construction of biosensor for different enzymes. The selective capability of Schiff base containing pyridine moiety as ionophore component in the PVC membrane electrode was explored by **Demir *et al.* (2014)[29].** The reported ionophore was utilized for copper(II) ions detection in the coexistence of some cations. The obtained results were also compared with the theoretical calculations using DFT/B3LYP method. Interference observed from the other cations also confirmed by the theoretical calculations. **Bandi *et al.* (2014)[30]** explored two novel Schiff bases for the selective detection of copper ions using PVC membrane electrode and coated graphite electrode. From comparison of the PME and CGE, results showed that CGE showed better detection with lower limit of detection 1.2×10^{-8} M and good Nernstian response, wide working concentration range with fast

response time and long shelf life of 90 days. The proposed ionophore is also capable of determining copper in various real-life samples. **Kumar *et al.* (2014)[31]** presented Cr(III) selective sensor based on N_2O_2 donor ligand. Under optimized conditions, the sensor showed Nernstian slope (20.1±0.2 mV/decade) in broad concentration range of 1.2×10^{-7}-1.0×10^{-1} mol/L under acidic condition (pH 3.8-4.5). Most metal ions have no impact in the identification of chromium and this sensor can be utilized for the daily-life sample analysis. On the basis of Schiff base ionophore, ion selective electrode was examined as sensor for determining Al(III) ions, as reported by **Yao *et al.* (2014)[32]**. Stable coordination compound was obtained by the aluminium which had empty orbital and Schiff base ionophore which also had lone pair of electrons available on the nitrogen and oxygen. The proposed electrode revealed good Nernstian response over a broad concentration range of 1.2×10^{-5}-1.0×10^{-1} mol/L. It detects Al(III) ions up to 5.1×10^{-6} mol/L and was successfully applied for the real-life sample analysis.

Tomar *et al.* (2013)[33] recognized Ni(II) selective potentiometric sensor based on 3-aminoacetophenonesemicarbazone which had nitrogen and oxygen donor atoms. The proposed sensor revealed wide concentration range of 1.0×10^{-7} to 1.0×10^{-2} mol/L with limit of detection 5.1×10^{-8} mol/L. **Bandi *et al.* (2013)[34]** developed a PVC membrane electrode for the recognition of Nd^{3+} using novel multidentate Schiff base. Recognition came from the study of conductometric experiments. On addition of Nd^{3+} sharp decrease in conductance was observed, indicating the lower mobility of the complexed cations as compared to the free ones. The polymeric membrane electrodes (PME) and coated graphite electrode (CGE) used the same composition with 4% ionophore and other constituents for the assembly of ion-selective electrode. CGE showed a detection limit of 1.1×10^{-8} mol L^{-1}, long shelf life, response time (10 s) and detection toward Nd^{3+} ion. **Arvand *et al.* (2013)[16]** reported optical sensing film based on Schiff base ionophore for the identification of copper(II). The prepared membrane electrode works on the principle of cation exchange with a fast response time of 3 s. The prepared optode membrane was effectively implemented for the detection of copper in real time analysis.

Mizani *et al.* (2012)[35] developed potentiometric sensor based on Schiff base substituents with hydroxyl and methoxy group and utilized for the determination of zinc ions. Due to the arrangement of different parts of ligand containing three soft N atoms around the determined metal ion a semi cavity is formed. This results in a low detection limit of 1.1×10^{-8}. It can also be utilized for the identification of Zn(II) by potentiometric titration

with EDTA. **Lee *et al.* (2012)[36]** synthesized diphenol Schiff base and explored it as an ionophore in potentiometric membrane electrode. Schiff base ionophore has high affinity for the silvers ions as demonstrated by the potentiometric response. The concentration range was obtained as 1.0×10^{-7} to 1.0×10^{-2} and a detection limit as 3.4×10^{-7} mol/L. **Saadeh *et al.* (2012)[37]** prepared lead complex with Schiff bases, synthesized by the reaction of lead acetate with reported ligands (1:2) in methanol. These compounds are soluble in DMF and DMSO. Octahedral geometry of Pb(II) complexes was obtained, in which ligand is attached to Pb(II) via benzoyl oxygen, azomethine nitrogen and thiophene sulfur or furan oxygen atom by deprotonation. One of the prepared complexes was utilized as an carrier in the PVC membrane electrode and its performance characteristics were evaluated. The detection limit was observed with two plasticizers, Doph and DOS as 3.9×10^{-7} M, 7.9×10^{-7} M. **Ghaedi *et al.* (2012)[38]** developed carbon paste electrode in which Schiff base ligand was incorporated in graphite powder matrix. This electrode was selective for Cu(II) ion and forms stable square planar four dentate complex through N_2O_2 donor atoms . The electrode was optimized with the amount of graphite, NaTPB, ionophore and nujol. Under optimized conditions, the sensor responds in a broad linear concentration range of 5.0×10^{-8} to 1.0×10^{-1} with a Nernstian slope Cu^{2+} ion activity. **Zamani *et al.* (2012)[39]** reported Gd(III) complex as electroactive species in the fabrication of ISE based on Schiff base ionophore. The preparation of electrode was carried out using acetophenon (AP) as plasticizer and sodium tetraphenyl borate (NaTPB) as an anion excluder. The fabricated sensor displayed a Nernstian behaviour in a varied concentration range of 1.0×10^{-6} to 1.0×10^{-2} mol/L and detection limit of 5.0×10^{-7} mol/L with a quick response time of 10 s.

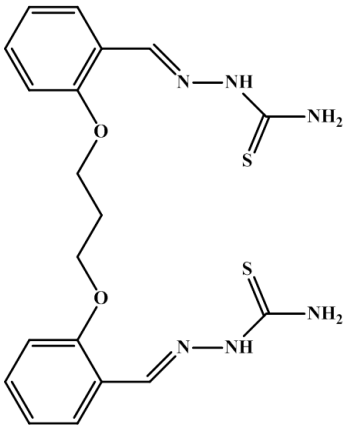

(L2) (24)

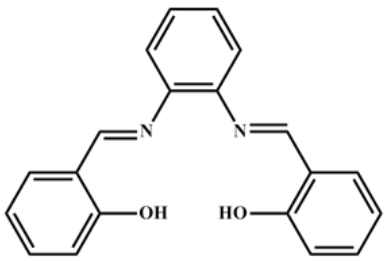

(Bis salicylaldehyde)-o-phenylenediamine) (25)

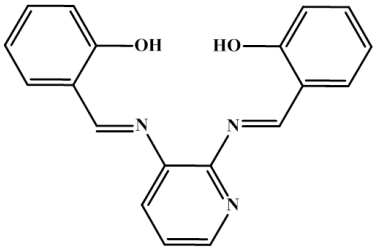

H_2IF (27)

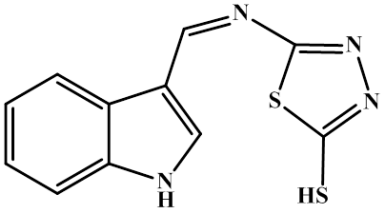

S2 (30)

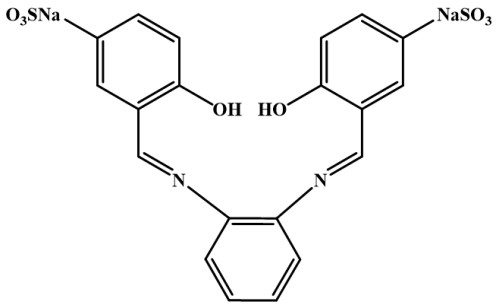

SSDA (32)

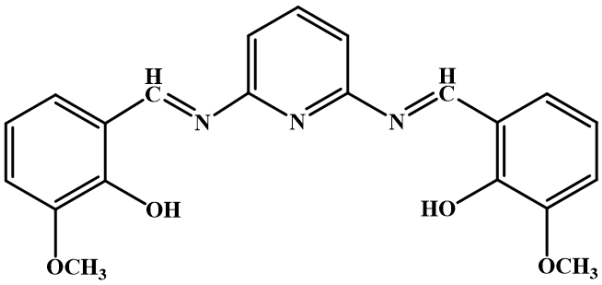

Schiff base (35)

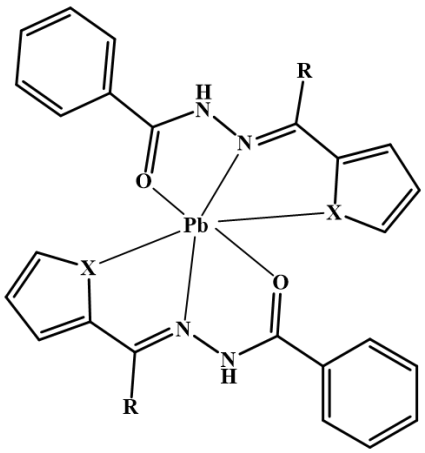

Pb(II) complex (X = S, O and R = H, CH_3) (36)

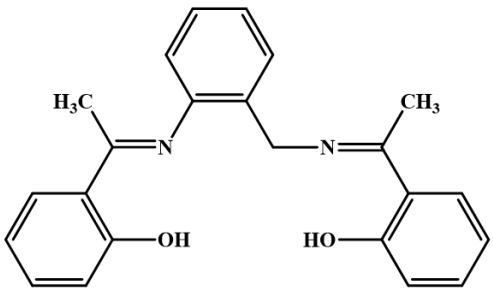

(39)

2.2 CNT Modified Ion Selective Electrodes

Carbon nanotubes (CNTs) have been studied due to its exceptional properties and attracted in the field of research because of their application in different fields of nanotechnology. They are in the range of nanometers. The electronic properties of CNT can be effectively tuned by modifying the surface of the CNT, which plays a vital role in the process of electrochemical sensing. Carbon nanotubes (CNTs) can be effectively used for the construction of an ion selective electrode.[40,41] Introduction of CNTs in the polymer matrix enhances the dispersion and interfacial adhesion, consequently strengthening the mechanical properties of the nanocomposite.[41,42] Due to these unique properties, CNTs can be embedded in polymer matrix to provide a much faster and reproducible way to develop electrode in one step. In this section of literature survey various CNT based sensors and their principle of sensing are discussed.

Ertürün *et al.* (2017)[43] discussed first perchlorate-selective ion-selective electrodes modified with carbon nanomaterials based on a calix[4]arene derivative. Different electrodes with different substituted MWCNTs such as MWCNT-COOH, MWCNT-OH and MWCNT were used and their performance characteristics were evaluated. MWCNT-COOH showed best performance like selectivity and Nernstian slope. The electrode responded to perchlorate ion in the existence of other tested anions. **Alizadeh *et al.* (2017)[44]** reported Cr(III) selective electrochemical sensor based on CPE transformed with ion-imprinted polymer (IIP) and MWCNTs. The optimized electrode composition was (w/w) 76.7% graphite, 14.3% binder, 5% IIP, and 4% CNT. The prepared electrode exhibited high selectivity, stability, long shelf life and wide working range. This sensor was also used for the Cr(III) detection in different real-life samples.

Wardak et al. (2015)[45] reported ion-to-electron transducer for cadmium ion-selective electrode based on multi-walled carbon nanotubes (MWCNTs). The widespread linearity in concentration range of 1×10^{-2}-1×10^{-7}mol/L with the Nernstian slope 30 mV/decade was identified. **Tashkhourian *et al.* (2015)[46]** developed nickel selective electrode modified with carbon nanotubes based on bis(2-hydroxyac-etophenone)-1,2-propandiimine (BHAPN) as ionophore. Modification of polymer matrix with MWCNTs improved the sensitivity, selectivity and linear range of the electrode with the detection limit of 3.2×10^{-7} M.

Anirudhan *et al.* (2014)[47] studied ion-selective electrode based molecularly imprinted polymer transformed with MWCNTs such as MWCNT-NIPIM and MWCNT-IPIM. Due to nonspecific binding of analyte to the MWCNT-NIPIM unstable potential occurs whereas stable potential values obtained from the specific site selective binding in the case of MWCNT-IPIM. The sensor had a nanomolar detection of 1.2×10^{-9} mol/L. **Agrahari et al. (2014)[48]** developed a uranyl ion sensor based on composite of carbon nanostructured materials such as multiwalled carbon nanotube and polyvinyl chloride (PVC) with benzo-15-crown-5 (B15C5) as ionophore. The sensor displayed a linear response over the widespread concentration range of 1×10^{-7} to 1×10^{-1} mol/L with lower detection limit.

As a modification on the graphite matrices **Ghaedi *et al.* (2013)[49]** published a report on copper selective carbon paste electrode based on multiwall carbon nanotubes. The surface of MWCNT was modified by performing a reaction with trimethoxysilylpropyl ethilendiamine and 2-hydroxybenzaldehyde and this modified material was further utilized for the preparation of electrode. Carbon paste electrode based on modification of MWCNT surface due to improvement in charge transfer and the number of surface reactive atom and surface area lead to enhancement in electrochemical response. The prepared electrode gave superior response with wide working range and lower detection limit of 2.5×10^{-7} mol/L. **Parra *et al.* (2013)[50]** reported synthesis of pyrene based benzo-18-crown-6 ether by non-covalent interaction of multi-walled carbon nanotubes. The proposed sensor was used to recognize potassium effectively. The selectivity for particular analyte was not affected after the modification. **Jaworska *et al.* (2013)[51]** reported disposable ion selective electrodes based carbon nanostructured material such as graphene or multiwalled nanotubes. The performance characteristics of the electrodes were compared with that of conventional ion-selective electrodes and found to be better as compared with the other disposable sensors.

Parra *et al.* (2011)[52] synthesized another carrier, i.e., benzo-18-crown-6 covalently attached to MWCNTs. This new insight led to potentiometric sensors with enormously high selectivity. The ionophore benzo-18-crown-6 was localised at the open ends of MWCNTs. Therefore, due to the side wall defect of the CNTs, formation of sandwich complex occurred between the two ionophore molecules and the lead ions, which provided an increased affinity. The sensor responded towards Pb^{2+} ion with linear response in a range 1.5×10^{-6} and 1×10^{-3} mol/L of Pb^{2+}. The obtained detection limit was

1.6×10^{-6} mol/L for Pb^{2+} for the MWCNT-B18C6 system. **Mousavi *et al.* (2011)[53]** compared carbon nanostructured material such as MWCNTs with POT as transducer in potentiometric electrode with valinomycin. Results obtained from electrochemical measurements revealed that the MWCNT-based electrodes have a greater reproducible response than that of POT based electrodes, however, similar sensitivity was observed for the target analyte.

Although a huge number of publications on conventional ionophore based potentiometric chemical sensor could be seen in the recent past, however very limited literature is available on the nanostructured or nanomaterial incorporated ionophores.

2.3 Schiff Base Ionophores for Chemical Sensing Using Voltammetry

Several analytical techniques have been utilized towards sensing of target analytes. Traditional techniques such as spectrophotometry[54], FAAS (Flame atomic absorption spectroscopy)[55] and ICP-AES (inductively coupled plasma-atomic emission spectrometry)[56] have been utilized for most of the metal ion detection. These techniques are expensive, complex and not practical for quick online monitoring of metal ions. Among the various sensing applications, voltammetry is employed for the direct quantification of trace analysis of ions. A brief literature survey on Schiff base receptors as voltammetric sensors for metals ions is reported here:

Maleki *et al.* (2019)[57] reported highly sensitive electrochemical sensor based on magnetic nanoparticles (Fe_3O_4@G2-PAD) for the identification of Pb(II) and Cd(II) ions. Due to the high surface-to-volume ratio and high adsorption ability of the Fe_3O_4@G2-PAD nanocomposite, the modified electrode shows excellent electrochemical properties. The sensor was optimized using supporting electrolyte, pH, modifier amount, deposition time and potential. Under optimum conditions, the proposed sensor had a detection limit of 8.21×10^{-10} mol/L, 1.8×10^{-9} for Pb(II) and Cd(II) ions. **Baghayeri *et al.* (2019)[58]** reported another magnetic graphene oxide (GO-Fe_3O_4-PAMAM) functionalized with poly(amidoamine) dendrimer based voltammetric sensor for recognition of Cd(II) and Pb(II) ions in environmental waters. Low detection limits of 6.2×10^{-10} for respective ions were observed. **Hashemi *et al.* (2019)[59]** reported a new carbon paste electrode modified using Schiff base modified for the detection of mercury using voltammetry techniques. This device was utilized for real-life sample analysis like tobacco and water. **Aqlana *et al.* (2019)[60]** reported tetradentate Schiff base ligand (TDL) for the fabrication of Pb(II)

ion sensor using TDL/binder/GCE electrode. This prepared sensor is very effective to detect Pb(II) ion in real environmental samples.

Rahman *et al.* (2018)[61] synthesized new Schiff base (NDNA) for the determination of Sb(III) based on NDNA/nafion/GCE electrode. This device has a sensing limit of 7.5×10^{-11} mol/L and can be utilized for the recognition of Sb(III) in heavy metal cations in environmental and healthcare fields. **Bharathi *et al.* (2018)[62]** developed quantification method for paracetamol based on chromium (III) Schiff base complexes using GCE electrode. The redox properties of the complex were carried out by cyclic voltammetric studies. **Selvan *et al.* (2018)[63]** discussed nanomolar sensor based on modified graphite electrode with CNT/tetradentate Schiff base ligand and used it as electroanalytical sensor for the detection of lead and mercury by voltammetric technique. Lower detection limit was observed as 1.1×10^{-11} M and 3.6×10^{-12} M for Pb and Hg ions, respectively. **Mehrjardi *et al.* (2018)[64]** studied the electrochemical behaviour of Dopamine and Ascorbic acid with modified CPE/molybdenum Schiff base. From the CV and DPV results, the modified electrode is very useful for the recognition of Dopamine (DA) and Ascorbic acid (AA).

Chowdhury *et al.* (2017)[65] prepared a hydrazine based novel NBPBIH chemoreceptor for the selective detection of fluoride ion. Voltammetric studies were carried out in DMSO medium for the reason that of enhanced fluorescence responses and the detection limit was obtained as 1.42×10^{-5} mol/L. **Shamsipur *et al.* (2017)[66]** reported complex of manganese Schiff base as a electrocatalyst for the investigation of progesterone in milk by hydrodynamic amperometry and cyclic voltammetry. **Li *et al.* (2017)[67]** developed modified CPE/Schiff base/carbon nanospheres and utilized as a sensor for cadmium ion by voltammetric techniques. **Ourari *et al.* (2017)[68]** reported nanomolar detection of bromated and nitrite based on Cu (II)-Schiff base modified electrode using differential pulse voltammetry and amperometry. **Sonkar *et al.* (2017)[69]** proposed MWCNT coupled manganese salen nanostructure as a sensor for riboflavin (B_2) and pyridoxine (B_6) recognition by differential pulse voltammetry. **Rana *et al.* (2017)[70]** developed screen-printed electrode transformed with Schiff base for electrochemical identification of the Fe(II) ions. Cathodic peaks can be attributed to the reduction of imine group while anodic peak arise because of the hydroxyl group in the ionophore. A linear response was observed in concentration range of 6×10^{-7} to 4×10^{-6} M with a sensing limit of 5.4×10^{-7} M. **Gutierrez *et al.* (2017)[71]** reported the advantage of electrochemical sensor based on

a glassy carbon electrode modification with cysteine-functional SWCNTs. Application of the proposed sensor was described by using it as a sensor for quantification of cadmium in daily life samples. Another sensor is reported on the detection of dopamine (DA) and ascorbic acid (AA) based on cobalt Schiff base complex as described by **Hassanzadeh *et al.* (2017)[72].** At pH 4.0 the modified CPE is capable of distinguished separate voltammetric peaks for DA and AA.

Gorczyński *et al.* (2016)[73] designed manganese complex based on subunits of Schiff base which has high affinity for gold substrate. Voltammetric sensor selectively detected dopamine in the existence of uric and ascorbic acid coexisting in the mixture. **Gorczyński *et al.* (2016)[74]** reported another gold/Schiff-base iron(III) complex composite which was stable than previously reported manganese complex. This sensor was effectively utilized for the epinephrine (EP) detection with a high sensing limit of 7.4×10^{-9} mol/L. **Kumar *et al.* (2016)[75]** developed GCE modified with Poly(chromium Schiff base complex) and evaluated redox properties of the complex voltametrically. The sensor responded to the paracetamol and 4-aminophenol, simultaneously. The obtained detection limits are in the nanomolar range. **Ribeiro *et al.* (2016)[76]** performed voltammetric experiments based on modification of screen-printed electrode with uranyl Schiff base for identification of the cocaine. Results revealed a fast and accurate analysis of cocaine in the presence of morphine and 3,4-methylenedioxymethanphetamine. **Nourifard *et al.* (2016)[77]** reported a suitable, accurate and precise technique for the recognition of cadmium and mercury based on modified CPE by voltammetric methods. The prepared sensor responded to Cd and Hg without the interference of other tested ions with low detection limit and utilised as a sensor for identification of the selected metal ions in water samples. **Afkhami *et al.* (2016)[78]** fabricated the chemically modified electrode based on SiO_2 nanoparticles coated with Schiff base. The sensor had a fast response, reproducible stability and used for the quantification of Cu (II) and Cd (II) in real time analysis. **Pazalja *et al.* (2016)[79]** reported electrochemical sensors developed by modifying glassy carbon and screen-printed electrode with Ru (III) Schiff base complex, nafion and MWCNTs. Outcomes showed that the voltammetric response was improved upon modification with MWCNTs. The prepared modified electrodes were utilised for the detection of L-cysteine through voltammetric techniques and flow injection analysis in Britton-Robinson buffer. **Keypour *et al.* (2016)[80]** reported another modification of GC electrode with carbon nanoparticles and Schiff base functionalized magnetic Fe_3O_4

nanoparticle. The sensor response was optimized using working pH range and scan rates. This device analysed anti-depressant drug namely citalopram in aqueous medium without any interference of oxalic acid, glucose, lactose and citric acid.

Ouari *et al.* (2015)[81] synthesized and characterized zinc(II)-Schiff base complex by different spectroscopic techniques. The structural analysis confirmed the stability of complex through strong C-H….π interactions and forms square planar coordination geometry at the metal center. The electrochemical behaviour was analysed using cyclic voltammetry on GCE and Pt electrode in DMF medium at a scan rate of 100 mV/s. **Ouari *et al.* (2015)[82]** reported another synthesis of unsymmetrical tetradentate copper (II) Schiff base complex. The structural confirmation was done using the reported spectroscopic techniques. The electrochemical investigation was carried out in DMF using cyclic voltammetry on GC, indium tin oxide and fluorine tin oxide.

Izadkhah *et al.* (2015)[83] reported the voltammetric behaviour of a modified MWCNTs paste sensor based on Schiff base for the recognition of copper. The prepared electrode had a well-defined linear range and lower detection limits and could be utilized as copper recognition in real-life samples. **Nourifard *et al.* (2015)[84]** developed voltammetric sensor for the copper, mercury and cadmium based on bis-Schiff base ligand. The sensing limit of this probe is relatively low and has wide working range and effectively used for the selected metal ions in different Merck and water samples. **Taei *et al.* (2015)[85]** developed MWCNT/CPE using ferrocenyl Schiff base. Measurements were carried out using cyclic voltammetry for the identification of glutathione (GSH). It was found that the modification with MWCNTs led to improved performance of the electrode. The peak current was linear in the GSH concentration range of 0.3-3.3×10^{-5} mol/L with detection limit of 8.0×10^{-8} mol/L. **Parsaei *et al.* (2015)[86]** modified carbon paste electrode with magnetite nanospheres and cobalt (II)-Schiff base complex for the recognition of nitrite by using voltammetric technique. The proposed method is very sensitive towards the detection of nitrite ions as compared to the unmodified electrode with lower detection limit. Analytical applicability was studied by testing nitrite in real-life water samples.

Afkhami *et al.* (2014)[87] constructed nanocomposite carbon paste electrode using MWCNTs, ionic liquid and macrocyclic Schiff base ligand. The sensitivity and selectivity of the modified electrode were improved for identification of Cd(II) ions with detection limit of 7.14×10^{-10} mol/L. In a different study **Afkhami *et al.* (2014)[88]**

described nanomolar detection of Hg(II) ions based on modification of CPE with MWCNT, ionic liquid and Schiff base. The sensing limit was found to be 0.05 nM. Simultaneously **Afkhami *et al.* (2014)[89]** reported multi-ion detection by incorporation of magnetite nanoparticles with Schiff base onto carbon paste electrode. Advantage of above-mentioned modifier led to enhanced performance of the sensor with good selectivity of Cd(II), Cu(II) and Hg(II). Another report available on the simultaneous quantification of Cd(II), Cu(II) and Hg(II) based on modified CPE as defined by **Afkhami *et al.* (2013).[90]** Limit of detections 1.4×10^{-8}, 1.7×10^{-9} and 5.0×10^{-9} for Copper, cadmium and mercury were obtained.

Ghoreishi *et al.* (2012)[91] investigated detection of uranyl ion by using voltammetric method based on Schiff base/CNT/CPE modified electrode. All the measurements were done in 0.1 mol/L phosphate buffer and sensing limit was observed as 0.206 nM. **Nadiki *et al.* (2012)[92]** also reported modified CPE with CNT and Schiff base for the identification of silver ions. Effect of supporting solution was also confirmed by the voltammetric response and in the presence of HCl as a medium sharp peak were observed. Analytical applicability of the proposed sensor was checked by using it for the detection of Ag(I) in X-ray photographic films and water samples. **Afkhami *et al.* (2012)[93]** determined trace amount of mercury and lead based on Schiff base/CNT/CPE modified electrode using stripping voltammetry. Different parameters were optimized such as pH, deposition potential and time for trace detection of the analytes and make it appropriate probe for the detection of mercury and lead in different daily life samples. **Hasanzadeh *et al.* (2012)[94]** reported voltammetric sensor for the recognition of mefenamic acid and indomethacin based on Fe(III)-Schiff base complex. All the voltammetric measurements were done in phosphate buffer at pH 3.5. This device had high stability, linear dynamic range, lower detection limit and high sensitivity which made it appropriate biosensor transducer for practical applications. **Deng *et al.* (2011)[95]** developed acetylene black paste electrode modified with chitosan via drop coating method for the identification of tryptophan. Under optimized condition the sensor has nanomolar detection of 2.0×10^{-9} for tryptophan in linear range of 6.0×10^{-8} to 1.0×10^{-4}.

It is a well-known fact that the basic site in Schiff base, -C=N- forms stable complexes with different metal ions. Keeping this fact in view, the author in the present thesis work tried to demonstrate the complexing ability of newly prepared Schiff bases towards industrially important metal ions through potentiometric and voltammetric studies.

References

(1) Prakash, A.; Adhikari, D. *International Journal of Chem Tech Research* **2011**, *3*, 1891-1896.

(2) Witkop, B.; Beiler, T. W. *Journal of the American Chemical Society* **1954**, *76*, 5589-5597.

(3) Di Bernardo, P.; Zanonato, P.; Tamburini, S.; Tomasin, P.; Vigato, P. *Dalton Transactions* **2006**, 4711-4721.

(4) Qin, W.; Long, S.; Panunzio, M.; Biondi, S. *Molecules* **2013**, *18*, 12264-12289.

(5) Awad, M.; Issa, R.; Atlam, F. *Materials and Corrosion* **2009**, *60*, 813-819.

(6) De Clercq, B.; Verpoort, F. *Journal of Molecular Catalysis A: Chemical* **2002**, *180*, 67-76.

(7) Lopez, J.; Liang, S.; Bu, X. R. *Tetrahedron letters* **1998**, *39*, 4199-4202.

(8) Nakajima, K.; Kojima, K.; Kojima, M.; Fujita, J. *Bulletin of the Chemical Society of Japan* **1990**, *63*, 2620-2630.

(9) Das, P.; Linert, W. *Coordination Chemistry Reviews* **2016**, *311*, 1-23.

(10) Kianfar, A.; Mohebbi, S. *Journal of the Iranian Chemical Society* **2007**, *4*, 215-220.

(11) Akitsu, T.; Einaga, Y. *Polyhedron* **2005**, *24*, 1869-1877.

(12) Schaller, U.; Bakker, E.; Spichiger, U. E.; Pretsch, E. *Analytical Chemistry* **1994**, *66*, 391-398.

(13) Oesch, U.; Simon, W. *Analytical Chemistry* **1980**, *52*, 692-700.

(14) Shamsipur, M.; Mohammadi, M.; Taherpour, A. A.; Lippolis, V.; Montis, R. *Sensors and Actuators B: Chemical* **2014**, *192*, 378-385.

(15) Dadkhah, A.; Rofouei, M. K.; Mashhadizadeh, M. H. *Sensors and Actuators B: Chemical* **2014**, *202*, 410-416.

(16) Arvand, M.; Lashkari, Z. *Spectrochimica Acta Part A: Molecular and Biomolecular Spectroscopy* **2013**, *107*, 280-288.

(17) Bolm, C.; Hildebrand, J. P.; Rudolph, J. *Synthesis* **2000**, *2000*, 911-913.

(18) Raban, M. *Journal of the Chemical Society D: Chemical Communications* **1970**, 1415-1416.

(19) Kaur, K.; Aulakh, J. S.; Malik, A. K. *Journal of Analytical Chemistry* **2019**, *74*, 134-142.

(20) Kardaş, F. *Analytical Letters* **2019**, *52*, 1418-1431.

(21) Aglan, R. F.; Hamed, M. M.; Saleh, H. M. *Journal of Analytical Science and Technology* **2019**, *10*, 7.

(22) Hasani, B.; Zamani, A.; Moftakhar, M. K.; Mostafavi, M.; Yaftian, M. R.; Ghorbanloo, M. *Journal of Analytical Chemistry* **2018**, *73*, 82-90.

(23) Abbas, M. N.; Magar, H. S. *Journal of Solid State Electrochemistry* **2018**, *22*, 181-192.

(24) Sahani, M. K.; Singh, A.; Jain, A. *Journal of The Electrochemical Society* **2017**, *164*, H657-H666.

(25) Ali, T. A.; Mohamed, G. G.; Omar, M.; Hanafy, N. M. *Journal of Industrial and Engineering Chemistry* **2017**, *47*, 102-111.

(26) Chandra, S.; Tomar, P. K.; Kumar, A.; Malik, A.; Singh, A. *Journal of Saudi Chemical Society* **2016**, *20*, S293-S299.

(27) Demir, S.; Yılmaz, H.; Dilimulati, M.; Andac, M. *Spectrochimica Acta Part A: Molecular and Biomolecular Spectroscopy* **2015**, *150*, 523-532.

(28) Dena, A. S. A. *Russian Journal of Applied Chemistry* **2014**, *87*, 383-396.

(29) Demir, S.; Yilmaz, H.; Dilimulati, M.; Andaç, M. *Journal of Molecular Modeling* **2014**, *20*, 2258.

(30) Bandi, K. R.; Singh, A. K.; Upadhyay, A. *Materials Science and Engineering: C* **2014**, *34*, 149-157.

(31) Kumar, P.; Kumar, S.; Jain, S.; Lamba, B. Y.; Joshi, G.; Arora, S. *Electroanalysis* **2014**, *26*, 2161-2167.

(32) Yao, H.; Wang, S.; Ma, X.; Ren, L.; Yan, F. *International Journal of Electrochemical Science* **2014**, *9*, 2158-2170.

(33) Tomar, P. K.; Chandra, S.; Malik, A.; Kumar, A. *Materials Science and Engineering: C* **2013**, *33*, 4978-4984.

(34) Bandi, K. R.; Singh, A. K.; Upadhyay, A. *Electrochimica Acta* **2013**, *105*, 654-664.

(35) Mizani, F.; Ziaeiha, M. *International Journal of Electrochemical Science* **2012**, *7*, 7770-7783.

(36) Lee, E.; Jeong, E.; Jeon, S. *Journal of Solid State Electrochemistry* **2012**, *16*, 2591-2596.

(37) Saadeh, S. M.; Shawish, H. M. A.; Dalloul, H. M.; El-Halabi, N. M.; Daher, B. K. *Materials Science and Engineering: C* **2012**, *32*, 619-624.

(38) Ghaedi, M.; Khajehsharifi, H.; Montazerozohori, M.; Tavallali, H.; Tahmasebi, K.; Khodadoust, S. *Materials Science and Engineering: C* **2012**, *32*, 674-679.

(39) Zamani, H. A.; Mohammadhosseini, M.; Haji-Mohammadrezazadeh, S.; Faridbod, F.; Ganjali, M. R.; Meghdadi, S.; Davoodnia, A. *Materials Science and Engineering: C* **2012**, *32*, 712-717.

(40) Crespo, G. A.; Macho, S.; Rius, F. X. *Analytical Chemistry* **2008**, *80*, 1316-1322.

(41) Crespo, G. n. A.; Macho, S.; Bobacka, J.; Rius, F. X. *Analytical Chemistry* **2008**, *81*, 676-681.

(42) Ghiazza, M.; Vietti, G.; Fenoglio, I. In *Health and Environmental Safety of Nanomaterials*; Elsevier, 2014, pp 147-174.

(43) Ertürün, H. E. K.; Özel, A. D.; Ayanoğlu, M. N.; Şahin, Ö.; Yılmaz, M. *Ionics* **2017**, *23*, 917-927.

(44) Alizadeh, T.; Mirzaee, S.; Rafiei, F. *International Journal of Environmental Analytical Chemistry* **2017**, *97*, 1283-1297.

(45) Wardak, C. *Sensors and Actuators B: Chemical* **2015**, *209*, 131-137.

(46) Tashkhourian, J.; Ghaderizadeh, S.; Montazerozohori, M. *Russian Journal of Electrochemistry* **2015**, *51*, 209-217.

(47) Anirudhan, T. S.; Alexander, S. *Biosensors and Bioelectronics* **2015**, *64*, 586-593.

(48) Agrahari, S.; Kumar, S.; Srivastava, A. *Journal of Analytical Chemistry* **2014**, *69*, 36-44.

(49) Ghaedi, M.; Naderi, S.; Montazerozohori, M.; Taghizadeh, F.; Asghari, A. *Arabian Journal of Chemistry* **2017**, *10*, S2934-S2943.

(50) Parra, E. J.; Rius, F. X.; Blondeau, P. *Analyst* **2013**, *138*, 2698-2703.

(51) Jaworska, E.; Lewandowski, W.; Mieczkowski, J.; Maksymiuk, K.; Michalska, A. *Analyst* **2013**, *138*, 2363-2371.

(52) Parra, E. J.; Blondeau, P.; Crespo, G. A.; Rius, F. X. *Chemical Communications* **2011**, *47*, 2438-2440.

(53) Mousavi, Z.; Teter, A.; Lewenstam, A.; Maj-Zurawska, M.; Ivaska, A.; Bobacka, J. *Electroanalysis* **2011**, *23*, 1352-1358.

(54) Olsen, S.; Pessenda, L. C.; Růžička, J.; Hansen, E. H. *Analyst* **1983**, *108*, 905-917.

(55) Ghaedi, M.; Ahmadi, F.; Shokrollahi, A. *Journal of Hazardous Materials* **2007**, *142*, 272-278.

(56) Liang, P.; Liu, Y.; Guo, L.; Zeng, J.; Lu, H. *Journal of Analytical Atomic Spectrometry* **2004**, *19*, 1489-1492.

(57) Maleki, B.; Baghayeri, M.; Ghanei-Motlagh, M.; Zonoz, F. M.; Amiri, A.; Hajizadeh, F.; Hosseinifar, A.; Esmaeilnezhad, E. *Measurement* **2019**, *140*, 81-88.

(58) Baghayeri, M.; Alinezhad, H.; Fayazi, M.; Tarahomi, M.; Ghanei-Motlagh, R.; Maleki, B. *Electrochimica Acta* **2019**, *312*, 80-88.

(59) Hashemi, S. E.; Payehghadr, M.; Es' haghi, Z.; Kargar, H. *International Journal of Environmental Analytical Chemistry* **2019**, 1-16.

(60) Aqlan, F. M.; Alam, M.; Asiri, A. M.; Zayed, M. E.; Al-Eryani, D. A.; Al-Zahrani, F. A.; El-Shishtawy, R. M.; Uddin, J.; Rahman, M. M. *Journal of Molecular Liquids* **2019**, *281*, 401-406.

(61) Rahman, M. M.; Sheikh, T. A.; El-Shishtawy, R. M.; Arshad, M. N.; Al-Zahrani, F. A.; Asiri, A. M. *RSC Advances* **2018**, *8*, 19754-19764.

(62) Bharathi, K.; Kumar, S. P.; Prasad, P. S.; Narayanan, V. *Materials Today: Proceedings* **2018**, *5*, 8961-8967.

(63) Selvan, K. S.; Narayanan, S. S. *Journal of Electroanalytical Chemistry* **2018**, *810*, 176-184.

(64) Zare-Mehrjardi, H. R. *Bioanalytical Electrochemistry* **2018**, *10*, 52-63.

(65) Chowdhury, A. R.; Roy, B. G.; Jana, S.; Weyhermuller, T.; Banerjee, P. *Sensors and Actuators B: Chemical* **2017**, *241*, 706-715.

(66) Shamsipur, M.; Pashabadi, A.; Taherpour, A. A.; Bahrami, K.; Sharghi, H. *Electrochimica Acta* **2017**, *225*, 292-302.

(67) Li, N.; Zhang, X.; Guo, H. *International Journal of Electrochemical Science* **2017**, *12*, 11571-11579.

(68) Ourari, A.; Ketfi, B.; Malha, S. I. R.; Amine, A. *Journal of Electroanalytical Chemistry* **2017**, *797*, 31-36.

(69) Sonkar, P. K.; Ganesan, V.; Gupta, S. K. S.; Yadav, D. K.; Gupta, R.; Yadav, M. *Journal of Electroanalytical Chemistry* **2017**, *807*, 235-243.

(70) Rana, S.; Mittal, S. K.; Kaur, N.; Banks, C. E. *Sensors and Actuators B: Chemical* **2017**, *249*, 467-477.

(71) Gutierrez, F. A.; Gonzalez-Dominguez, J. M.; Ansón-Casaos, A.; Hernández-Ferrer, J.; Rubianes, M. D.; Martínez, M. T.; Rivas, G. *Sensors and Actuators B: Chemical* **2017**, *249*, 506-514.

(72) Hassanzadeh, N.; Zare-Mehrjardi, H. R. *International Journal of Electrochemical Science* **2017**, *12*, 3950-3964.

(73) Gorczyński, A.; Pakulski, D.; Szymańska, M.; Kubicki, M.; Bułat, K.; Łuczak, T.; Patroniak, V. *Talanta* **2016**, *149*, 347-355.

(74) Gorczyński, A.; Kubicki, M.; Szymkowiak, K.; Łuczak, T.; Patroniak, V. *RSC Advances* **2016**, *6*, 101888-101899.

(75) Kumar, S. P.; Giribabu, K.; Manigandan, R.; Munusamy, S.; Muthamizh, S.; Padmanaban, A.; Dhanasekaran, T.; Suresh, R.; Narayanan, V. *Electrochimica Acta* **2016**, *194*, 116-126.

(76) Muzetti Ribeiro, M. F.; da Cruz Júnior, J. W.; Dockal, E. R.; McCord, B. R.; de Oliveira, M. F. *Electroanalysis* **2016**, *28*, 320-326.

(77) Nourifard, F.; Payehghadr, M. *International Journal of Environmental Analytical Chemistry* **2016**, *96*, 552-567.

(78) Afkhami, A.; Soltani-Shahrivar, M.; Ghaedi, H.; Madrakian, T. *Electroanalysis* **2016**, *28*, 296-303.

(79) Pazalja, M.; Kahrović, E.; Zahirović, A.; Turkušić, E. *International Journal of Electrochemical Science* **2016**, *11*, 10939-10952.

(80) Keypour, H.; Saremi, S. G.; Veisi, H.; Noroozi, M. *Journal of Electroanalytical Chemistry* **2016**, *780*, 160-168.

(81) Ouari, K.; Bendia, S.; Weiss, J.; Bailly, C. *Spectrochimica Acta Part A: Molecular and Biomolecular Spectroscopy* **2015**, *135*, 624-631.

(82) Ourari, A.; Derafa, W.; Aggoun, D. *RSC Advances* **2015**, *5*, 82894-82905.

(83) Izadkhah, V.; Farmany, A.; Mortazavi, S. *Journal of Industrial and Engineering Chemistry* **2015**, *21*, 994-996.

(84) Nourifard, F.; Payehghadr, M.; Kalhor, M.; Nejadali, A. *Electroanalysis* **2015**, *27*, 2479-2485.

(85) Taei, M.; Hadadzadeh, H.; Hasanpour, F.; Zahedi, G.; Dehbanipour, Z. *IEEE Sensors Journal* **2015**, *15*, 4472-4479.

(86) Parsaei, M.; Asadi, Z.; Khodadoust, S. *Sensors and Actuators B: Chemical* **2015**, *220*, 1131-1138.

(87) Afkhami, A.; Khoshsafar, H.; Bagheri, H.; Madrakian, T. *Materials Science and Engineering: C* **2014**, *35*, 8-14.

(88) Afkhami, A.; Khoshsafar, H.; Keypour, H.; Zeynali, H.; Madrakian, T. *Food Analytical Methods* **2014**, *7*, 1204-1212.

(89) Afkhami, A.; Moosavi, R.; Madrakian, T.; Keypour, H.; Ramezani-Aktij, A.; Mirzaei-Monsef, M. *Electroanalysis* **2014**, *26*, 786-795.

(90) Afkhami, A.; Soltani-Felehgari, F.; Madrakian, T.; Ghaedi, H.; Rezaeivala, M. *Analytica Chimica Acta* **2013**, *771*, 21-30.

(91) Ghoreishi, S.; Behpour, M.; Mazaheri, S.; Naeimi, H. *Journal of Radioanalytical and Nuclear Chemistry* **2012**, *293*, 201-210.

(92) Nadiki, H. H.; Taher, M. A.; Ashkenani, H.; Sheikhshoai, I. *Analyst* **2012**, *137*, 2431-2436.

(93) Afkhami, A.; Bagheri, H.; Khoshsafar, H.; Saber-Tehrani, M.; Tabatabaee, M.; Shirzadmehr, A. *Analytica Chimica Acta* **2012**, *746*, 98-106.

(94) Hasanzadeh, M.; Shadjou, N.; Saghatforoush, L.; Dolatabadi, J. E. N. *Colloids and Surfaces B: Biointerfaces* **2012**, *92*, 91-97.

(95) Deng, P.; Fei, J.; Feng, Y. *Analyst* **2011**, *136*, 5211-5217.

Chapter 3

Materials and Instrumentation

This chapter provides a brief description of materials and instruments used for the ion recognition behaviour of imine-based receptors. Methodology was carried out by using spectroscopic, potentiometric and voltammetric techniques. Theoretical studies further supported the mode of interaction of cation with the receptor molecule. Experimental details of the methods and techniques are mentioned in this chapter in detail.

3.1 Chemicals

All chemicals used were of analytical reagent grade. Multi-walled carbon nanotubes-COOH (MWCNT-COOH) with 10-30 nm diameter, 1-10 μm length and >95% purity were obtained from Nanoshel (USA) and used as received. Polyvinyl chloride (PVC), tetrahydrofuran (THF), sodium tetraphenylborate (NaTPB), various plasticizers such as o-nitrophenyl octyl ether (*o*-NPOE), dibutyl amine (DBA), dioctyl phthalate (DOP) were purchased from Sigma-Aldrich (India) and used as received. Bis (2-ethylhexyl) sebacate (DOS) was purchased from Alpha Aesar (India). dimethyl sulphoxide (DMSO) were obtained from Merck. Electrolyte tetrabutylammonium hexafluorophosphate was obtained from Sigma-Aldrich. Sodium Hydroxide, Hydrogen Peroxide, Hydrazine, Nitric acid, Sulphuric acid and Perchloric acid were obtained from Sd Fine (India). Metal nitrates of concentration 0.1 mol/L were prepared by dissolving in double distilled water. Serial dilutions were carried out in order to obtained different concentrations of solutions.

3.2 Instrumentations

All potentiometric experiments were done with a digital Equip-Tronics potentiometer (EQ-602, accuracy, ± 0.1 mV, Mumbai, India) at ambient temperature of 25.0 ± 0.1 ºC maintained in the laboratory. Simultaneously measurement of the pH was carried out with Equip-Tronics pH meter (EQ-614, Mumbai, India) and conventional glass pH electrode. All electromotive force (EMF) measurements were achieved using the following electrochemical cell assembly.

$$\mathbf{REF} \,\|\, \mathbf{M^{2+}\ test\ solution\ |\ Ionophore\ membrane\ |\ M^{2+}\ (0.1\ mol/L)} \,\|\, \mathbf{REF}$$

All the voltammetric experiments were done with potentiostat (Autolab/PGSTAT12/Eco Chemie/Netherlands) using a three-electrode setup, together with a Glassy Carbon

Working electrode (round disk, diameter 3 mm), Pt electrode as Auxiliary electrode and Ag/Ag^{+} (0.1 mol/L $AgNO_3$ in DMSO) as Reference electrode. The experimental conditions were controlled with NOVA 1.5 software.

Spectrophotometric studies were recorded on Analytic Jena Specord PC 205 spectrophotometer with a quartz cuvette (path length, 1 cm). Surface morphology studies were carried out with JSM-6510LV field emission scanning electron microscope. Elemental analysis of the prepared membrane was carried out with Energy Dispersive X-Ray (EDX) spectroscopy using INCA X-ACT Oxford instrument. All theoretical calculations were done using the GAUSSIAN 03W package. The average particle size and shape of nano-aggregates were determined using dynamic light scattering (DLS) probe and transmission electron microscopy (TEM) analysis.

3.3 Electrochemical Characterization

Potentiometric Measurements

The electrode potential (emf) was recorded using the working electrode and reference electrode. The calibration curves for metal ions were obtained by the successive addition of different concentrations of metal ions.[1,2] From calibration curve, the value of slope was obtained in mV/decade of concentration change and characteristically found around 59 and 29 mV/decade for monovalent and divalent ions, respectively.[3]

Conditioning of the Ion selective Membrane

In order to achieve the lower detection limit of electrode, membranes were kept in a solution of the analyte (10^{-2} mol/L) for about 24 hours. After the conditioning, membranes were cleaned with double distilled water and placed in diluted solution of analyte for 48 hours.[4]

Linear Concentration Range

It is defined as the concentration range obtained from the calibration curve which has a straight-line regression that do not distract from linearity by more than 2 mV. For most of the ISE linear range can be observed from to 10^{-2} to 10^{-7} mol/L.[5]

Limit of Detection

In general, the detection limit values observed from experimental data are in the order of 10^{-7}-10^{-1} mol/L. Therefore, detection limit is described as minimum concentration of

analyte that can be distinguished by the cross-section of two extrapolated linear portions (two straight lines) of the calibration curve, according to the IUPAC recommendation.[5]

Response Time

Response time is one of the most significant characteristic of the ion-selective electrode and is described as the time between the addition of analyte to the solution and the time when a limiting potential has been reached.[5]

Selectivity

The selectivity of an ion selective electrode is a measure of capability of the sensor to accurately examine the concentration of the analyte in the existence of interfering ions which can also affect the determined potential. All possible interferents were analysed towards the response of sensors for the primary ions. This involves knowledge of the composition of the test solution. In this study, selectivity coefficient of the sensor towards different interfering foreign cations was evaluated with the help of fixed interference method (FIM) recommended by IUPAC.[6,7]

Selectivity coefficients of potentiometric sensor can be analysed with three different methods, namely:

1. Separate Solution Method (SSM).
2. Fixed Interference Method (FIM).
3. Matched Potential Method (MPM).

3.4 Cleaning of Glassy Carbon Electrode (GCE)

GCE were cleaned by mechanical polishing with alumina slurry (0.05 μm) on an amry paper followed by ultrasonic cleaning in Millipore water to eliminate all adsorbed substances on the electrode surface. The electrodes were then placed in 0.1 mol/L H_2SO_4 and voltammetric scans were run between 2.0 V to -2.0 V at a scan rate of 100 mV/s vs $Ag/AgNO_3$.

3.5 Calculations of Limit of Detection for Voltammetric Measurement

To measure the detection limit of sensor for a analyte, calculations were carried out using 3 sigma formula based on the standard deviation of blank obtained from calibration curve of the sensor's outcomes and slope of linear graph.[8] Expression for the Limit of detection (LOD) is

$LOD = 3\sigma/m$

Where, σ is the standard deviation and m is the slope of linear portion of calibration graph drawn for the quantification of the analyte.

3.6 Receptors

It is proposed to study a series of imine based ionophores with varying number of amine groups for the potentiometric and voltammetric sensing of metal ions. These compounds were synthesized by our collaborator Dr. Navneet Kaur in Panjab University, Chandigarh. Molecules have been labelled as IFE, ICU and IFE(III).

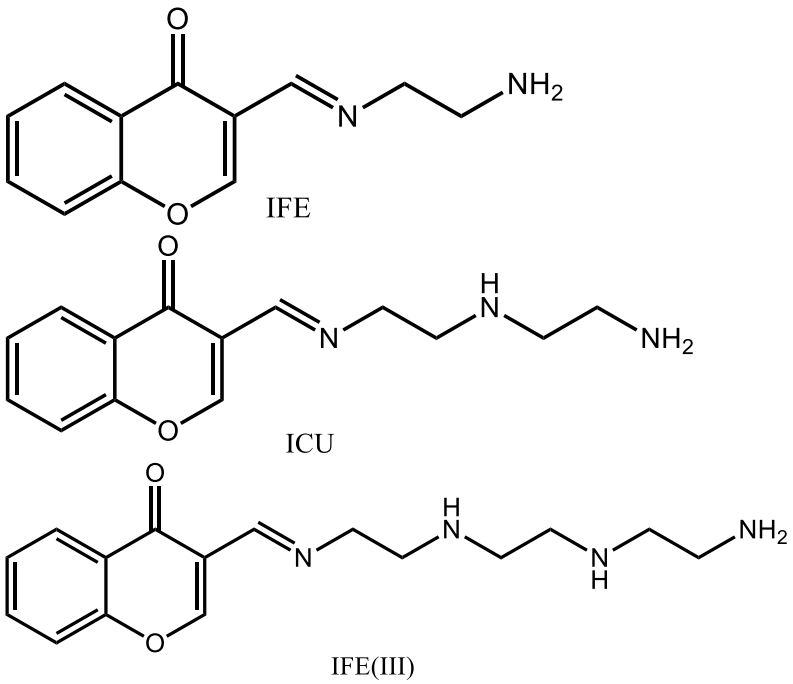

Fig. 3.1: Structure of molecules

References

1 Craggs, A.; Moody, G.; Thomas, J. *Journal of Chemical Education* **1974**, *51*, 541.

2 Morf, W. E. *The Principles of Ion-Selective Electrodes and of Membrane Transport*; Elsevier, 2012; Vol. 2.

3 Eisenman, G. *Analytical Chemistry* **1968**, *40*, 310-320.

4 Bakker, E. *Electroanalysis* **1997**, *9*, 7-12.

5 Buck, R. P.; Lindner, E. *Pure and Applied Chemistry* **1994**, *66*, 2527-2536.

6 Srinivasan, K.; Rechnitz, G. A. *Analytical Chemistry* **1969**, *41*, 1203-1208.

7 Umezawa, Y.; Umezawa, K.; Bühlmann, P.; Hamada, N.; Aoki, H.; Nakanishi, J.; Sato, M.; Xiao, K. P.; Nishimura, Y. *Pure and Applied Chemistry* **2002**, *74*, 923-994.

8 Shrivastava, A.; Gupta, V. B. *Chronicles of Young Scientists* **2011**, *2*, 21.

Chapter 4

Results and Discussion

Studies were conducted on three different ionophores, namely; IFE, ICU and IFE(III). Each of these ionophores has been studied as receptors for suitable guest species by using potentiometry and voltammetry, after their modifications as composite receptors with carbon nanotubes. This chapter has been divided into three sub-sections to present studies on each of these receptors.

4.1 Potentiometric studies on Schiff base compounds as ionophores in liquid membrane electrodes modified with MWCNTs

Abstract

Novel potentiometric sensors based on (E)-3-((2-aminoethylimino)methyl)-4H-chromen-4-one (IFE)[1], (E)-3-(((2-((2 aminoethyl) amino) ethyl) imino) methyl)-4H-chromen-4-one (ICU)[2] and (E)-3-((2-(2-(2-aminoethylamino) ethylamino) ethylimino) methyl)-4H-chromen-4-one (IFE(III))[3] have been established for recognition of Fe(II), Cu(II) and Fe(III), respectively. The effect of different components including the amount of plasticizers, anion excluder sodium tetraphenylborate (NaTPB), ionophore and multiwalled carbon nanotubes (MWCNTs) on the response of potentiometric sensors was studied. Under optimized conditions, the probes have wide linear range of concentrations and improved lower detection limits of 2.5×10^{-8}, 1.0×10^{-7} and 1.6×10^{-7} mol L^{-1} from 1.0×10^{-7}, 5.0×10^{-7} and 1.0×10^{-6} for Fe(II), Cu(II) and Fe(III), respectively, in presence of MWCNTs in the membrane matrix. Ion selective electrodes based on IFE, ICU and IFE(III) were also utilized as indicator electrodes for the potentiometric recognition of Fe(II), Cu(II) and Fe(III) ions.

4.1.1 Introduction

In this section, the application of ion-selective electrodes for assembly of potentiometric sensors for the real-time monitoring of metal ions is presented. For an electrochemical sensor like an ion-selective electrode system, the working electrode generates signals based on sample components.[4] Another critical part is the reference electrode, whose potential remains constant throughout the experiments. Most electro-analytical measurements are done with the reference electrodes separated by salt bridges from samples.[5] Ion selective electrodes (ISEs) have many advantages over traditional methods due to accurate and precise measurements, fast, reproducible, and even selective

recognition of numerous ionic species.[6] Furthermore, ion-selective electrodes used for non-destructive, onsite ions detection in a small quantity of sample without any pre-treatment.[7,8] ISEs characteristically use an ionophore in the PVC membrane as the sensing component to verify selectivity to a particular ion of interest.[9] The frequent growth of heavy metal use in industrial procedure enables ion-selective electrodes dynamic for the accurate sensing and estimation of prospective pollutants.[10-12] Furthermore, modification of the surface of the sensor with different nanomaterials is also important for electroanalytical sensors accredited to the signal improvement given by their high surface to volume ratio, low ohmic resistance, and fast electrode kinetics.[13-16] It has been proved that nanomaterials, such as carbon nanotubes can be employed as excellent ion-to-electron transducers in Ion Selective Electrodes (ISEs) because they improve the signals of potentiometric response and provide stability to the electrical signal.[17-19] Also, availability of CNTs with functionalization of different functional groups have been reported as effective transducers for both electroanalytical and bioanalytical applications.[20-22] Schiff base is a well-known moiety to form a strong coordinating complex and almost all the Schiff bases form 1:1 complex with transition metal ions.[23] Moreover, the existence of N and O donor atoms enhance coordination of these ligands by forming a stable metal complex.[24-27] Therefore, these ligands are well matched to construct sensors based on their electrochemical properties. A few potentiometric sensors containing different types of ligands have been investigated as metal complexing agent for the determination of alkali, alkaline earth and transition metal ions. **Kumar *et al.*[28]** reported N,'N,''N,''' tris(2-pyridyloxymethyl) ethane as an ionophore component in a PVC-based membrane sensor. **Bandi *et al.*[29]** synthesized novel polydentate Schiff bases S_1, and S_2 for the selective identification of Cu^{2+} ions. **Dadkhah *et al.*[30]** reported another Schiff base having imine linkage as an ionophore for selective detection of silver ion. **Isa *et al.*[31]** described potentiometric sensor based on 2,6-diacetylpyridine-(1R)-(-)-fenchonediazine for recognition of copper ions. **Homafar *et al.*[32]** reported 1, 2- bis(salicylidinaminooxy) ethane as a neutral carrier for lead ion. **Arvand *et al.*[33]** reported copper ions detection using imine moiety containing ionophore. **Hajiaghababae *et al.*[34]** reported Hg^{2+} ion-selective electrode based on Schiff base ionophore.

In this work, the optimal conditions of best performance of the electrodes, its selectivity against other metal ions and application of the electrodes were examined using (E)-3-

(((2-((2 aminoethyl)amino)ethyl)imino)methyl)-4H-chromen-4-one **(ICU),** (E)-3-((2-aminoethyl imino)methyl)-4H-chromen-4-one **(IFE)** and (E)-3-((2-(2-(2-aminoethylamino) ethylamino) ethylimino)methyl)-4H-chromen-4-one **(IFE(III))** as ionophores in polyvinylchloride based membrane electrodes. The presence of donor groups like N and O lead to complexation of the ionophores by the metal ions with better selectivity coefficient values.

4.1.2 Experimental

All chemicals used for experiments were of analytical reagent and higher grade. Multi-walled carbon nanotubes-COOH (MWCNT-COOH) with 10-30 nm diameter, 1-10 μm length and >95% purity were obtained from Nanoshel (USA) and used as received. Polyvinyl chloride (PVC), tetrahydrofuran (THF), sodium tetraphenylborate (NaTPB), various plasticizers such as o-nitrophenyl octyl ether (*o*-NPOE), dibutyl amine (DBA), dioctyl phthalate (DOP) were obtained from Sigma-Aldrich (India) and utilized as received. Bis (2-ethylhexyl) sebacate (DOS) was purchased from Alpha Aesar (India). Metal nitrates of concentration 0.1 mol/L were prepared by dissolving in double distilled water. Serial dilutions have been carried out in order to obtained different concentrations of solutions.

Preparation of PVC membranes

Poly vinyl chloride (PVC) based membranes were prepared by dissolving varying amounts of ionophores IFE, ICU and IFE(III) provided by our co-workers, anion excluder NaTPB, MWCNTs, o-NPOE and PVC in 5 mL of THF. The prepared membranes were obtained by adding different amounts of components in terms of weight percentages. The concentrated mixture was obtained by evaporating THF and then transferred in glass rings of 6 mm diameter positioned on smooth glass plates. Solvent evaporation was carefully controlled to attain reproducible characterstics of the membrane; otherwise thickness and morphology of membranes show substantial variations that may eventually affect sensor response. Transparent membrane so obtained was separated cautiously from the glass plate. The developed membrane of 6 mm diameter was cut out and pasted to one end of the 'Pyrex' glass tube. The constructed electrode was finally conditioned for overnight by soaking in a 0.1 mol/L of metal ion solution. It is well-known that characteristics of membrane sensors like sensitivity, selectivity and linearity for a given ionophore rely on the composition and nature of plasticizers used in the study.[6] Hence, numerous membranes of changing composition

were developed and inspected. The membrane that provided reliable results and ideal performance characteristics was selected for thorough studies.

Real-life sample analysis on IFE, ICU and IFE(III) based membranes for the determination of Fe(II), Cu(II) and Fe(III)

Determination of Fe(II) in pharmaceutical samples

The practical ability of ISE no. 3 (Table 3) was further investigated to determine iron in pharmaceutical samples. Samples of finely ground iron capsules and tablets of known weight were treated with 5 mL concentrated HNO_3 acid and heated to near dryness under the cover of fuming hood. After cooling, the residue was leached with 1 mol/L H_2SO_4. After filtration, the resulting solution was diluted with 100 mL distilled water and further analysed with proposed electrode and Atomic Absorption Spectroscopy (AAS).

Determination of Fe(II) in black tea

A sample of black tea (1 g) was accurately balanced into a 100 mL beaker. 15 mL of HNO_3 acid (2 mol/L) and 3 mL of $HClO_4$ acid (0.1 mol/L) were added to the beaker followed by digestion on a hot plate kept in a fuming hood. After that, neutralization was carried out with NaOH (1 mol/L) and 1 mL of 0.01 mol/L hydrazine as a reducing agent. These mixtures were added to the prepared solution. After filtration and dilution with 100 mL distilled water, iron content in black tea was identified with the suggested electrode and Atomic Absorption Spectroscopy (AAS).

Determination of copper (II) in multivitamin capsule

The usefulness of the Cu(II) electrode (Table 6) was further examined to determine copper in multivitamin capsule. One gm from the capsule was exactly weighed into the ceramic crucible. One millilitre of concentrated HNO_3 acid was added to the sample and heated to near dryness under the cover of fuming hood. After cooling, the residue was dissolved again in one millilitre of concentrated nitric acid and the sample solution was slowly evaporated using a water bath. The obtained residue was dissolved in 50 mL of distilled water, heated and filtered off and diluted to 100 mL using a volumetric flask. A factor of desired quantity of this sample was taken and further analysed with the suggested electrode and Atomic Absorption Spectroscopy (AAS).

Determination of Cu(II) in a copper wire sample

A 1g sample of copper electrical wire was fully dissolved in 5mL of concentrated nitric acid by heating on a water bath near to dryness. The experiment was conducted under the cover of a fuming hood and complete safety was ensured. Again, concentrated nitric

acid was added to the mixture and same steps were followed. Then the solution was cooled, filtered off and diluted to 100mL with distilled water in a calibrated volumetric flask. The concentration of copper was identified with the proposed electrode and Atomic Absorption Spectroscopy (AAS).

Determination of copper (II) in black tea

A 1g sample of dry black tea was accurately weighed into a 100mL beaker. 10mL of nitric acid (8M) and 4 mL of perchloric acid were added to the beaker followed by digestion on a hot plate kept in a fuming hood. Oxidization of the sample was carried out till the solution becomes clear. The sample was completely dissolved in 1 mol/L HNO_3 acid, filtered off and diluted to 100 mL using cylindrical volumetric flask. The copper content in black tea was measured with the suggested electrode and Atomic Absorption Spectroscopy (AAS).

Determination of Fe(III) in water samples

To further investigate the potential utility of the sensor (Table 9) real samples of Fe(III) in water were analysed potentiometrically. Before the analysis, the samples were filtered through 0.45 μm membrane filter and centrifuged at 5000 rpm to remove impurities and bulk particles. After that, samples were oxidized in the presence of 1% H_2O_2 and concentrated HNO_3 acid. pH of the solution was maintained at 3.0 and resulting solution was diluted with distilled water in a 100 mL volumetric flask. The Fe(III) content in water sample was measured with the use of calibration method and Atomic Absorption Spectroscopy (AAS).

Determination of Fe(III) in pharmaceutical samples

Samples of well ground pharmaceutical preparations of Fe(III) of known weight were dissolved in 5 mL of concentrated HNO_3 acid and 5 mL of H_2O_2 and heated to near dryness for the oxidation of Fe(II) to Fe(III). After that, samples were filtered and dissolved in 100 mL volumetric flask. pH of the solution was adjusted to 3.0 using concentrated HNO_3 acid. Fe(III) content in the sample solution was analyzed with the proposed electrode and Atomic Absorption Spectroscopy. The findings from suggested method correspond well to the information obtained from the AAS data (Table 3).

Determination of Fe(III) in black tea

For the digestion, 1.0 g of black tea sample was transferred into a 100 mL beaker and leached with 10 mL of HNO_3 acid (2 mol/L) and 4 mL of $HClO_4$ acid (0.1 mol/L). After

digestion, the resulting solution was diluted with 100 mL distilled water and further analyzed with the proposed electrode and Atomic Absorption Spectroscopy.

Potentiometric measurement

All potential measurements were performed at an ambient temperature of 25.0±0.1 ºC with a digital Equip-Tronics potentiometer (EQ-602, accuracy, ±0.1 mV, Mumbai, India) and simultaneously pH of the solution was checked using Equip-Tronics pH meter (EQ-614, Mumbai, India) and conventional glass pH electrode. All the potentiometric experiments were carried out using the following assembly of electrochemical cell.

REF $\|$ M^{2+} test solution | Ionophore membrane | M^{2+} (0.1 mol/L) $\|$ REF

A fixed concentration of metal ion (M^{2+}) was taken as an internal solution (0.1 mol/L) and silver, silver chloride electrode was used as a reference electrode. Performance of the electrodes was explored by evaluating the EMF of primary ion solution within the concentration range of 10^{-9} to 10^{-1} mol L^{-1} by serial dilutions. Selectivity values (K_{AB}^{Pot}) were evaluated using the 'Fixed Interference Method.[35]

4.1.3 Potentiometric characterization of Schiff base ionophores

Ionophores (IFE, ICU and IFE(III)) based on chromen as the basic molecule were synthesized by our coworkers with an aliphatic chain containing amine and imine groups substituted at ortho position to the keto group of pyran ring. The molecule was targeted as an open-ended pseudo cyclic ring where nitrogen atoms of aliphatic chain and the ethereal oxygen would form a pseudo cavity to host some transition metal ions. Based on the concept of hard-soft acid-base, N being a soft base would preferably capture transition metal ions as soft acids. These molecules were studied for its potentiometric characteristics to study its potential as a receptor molecule with a tendency to exhibit host-guest chemistry with target metal ions.

4.1.3.1 Potentiometric study of IFE molecule

Factors affecting performance of the IFE-Cu^{2+} ion selective electrode

Effect of composition

It is well-known that selectivity and sensitivity of an ion-selective electrode rely on the properties of plasticizer, nature of solvent mediator, additive and the amount of ionophore used.[36] The ionophore IFE have a tendency to build a stable complex with Fe(II) by coordinating with N atom of the imine and O atom of the carbonyl group. IFE is soluble in organic solvents and insoluble in aqueous medium, therefore IFE was used as a

detection element in PVC membrane electrode. For the study of composition, twelve newly designed ISEs (designated as ISE No. 1-12) were fabricated using the ionophore IFE, o-NPOE/DBA/DOP or DOS, as the plasticizer and NaTBP (50 mol%) as the anionic additive and the results were briefly described in Table 4.1.1. While using 3.0 % ionophore in membrane matrix the sensitivity, selectivity and linearity of the electrode response was maximum. However, below this rate and more addition of IFE ionophores, the electrode response was slowed and inactive, most likely owing to possible membrane saturations. It is established that plasticizer which is used in the ion selective membrane preparation should exhibit high lipophilicity, polarity, viscosity, high capacity to dissolve the substrate and adequate dielectric constant of the plasticizer. Thus, addition of plasticizer will improve the sensitivity and selectivity of the ion selective electrode.[37]

Effects of plasticizer on performance features of the membrane electrode have also been studied. The use of plasticizers provides the paste certain permanent characteristics and can enhance sensor mechanical stability.[38] It can be seen in Table 4.1.1 (ISE No. 3, 6-8) that due to the wide dielectric constant, o-NPOE is better solvent mediator than DBA, DOS and DOP for the electrode.[39,40] One of the causes of a small electrode detection limit of 1.0×10^{-7} mol/L was o-NPOE's elevated dielectric constant. o-NPOE was therefore selected as the best plasticizer for the electrode used. In the absence of NaTPB, the membrane did not follow a Nernstian response but a good Nernstian slope was observed with the presence of 2% NaTBP. Lipophilic salt's primary role is to increase the ion selective membrane permselectivity, increase sensor selectivity and decrease bulk membrane strength (by identifying the proportion between complex and uncomplex ionophoric concentrations in the membrane).[41,42] The authors can also examine the efficiency of the iron (II) electrode through a strongly available surface with a small distribution size, great electrical conductivity and elevated stability of MWCNT. As shown in Table 4.1.1 (ISE no. 12) and represented in Fig. 4.1.1, the doped electrode with MWCNT (1%) demonstrated increased sensitivity of 2.5×10^{-8} mol/L as opposed to the analogue without MWCNT observed in the reduced detection limit (ISE no. 3).

Effect of pH

The effect of pH on the electrode response was investigated using 1.0×10^{-3} mol L^{-1} Fe(II) at different pH. Nitric acid and sodium hydroxide were used to change pH of the test solution.

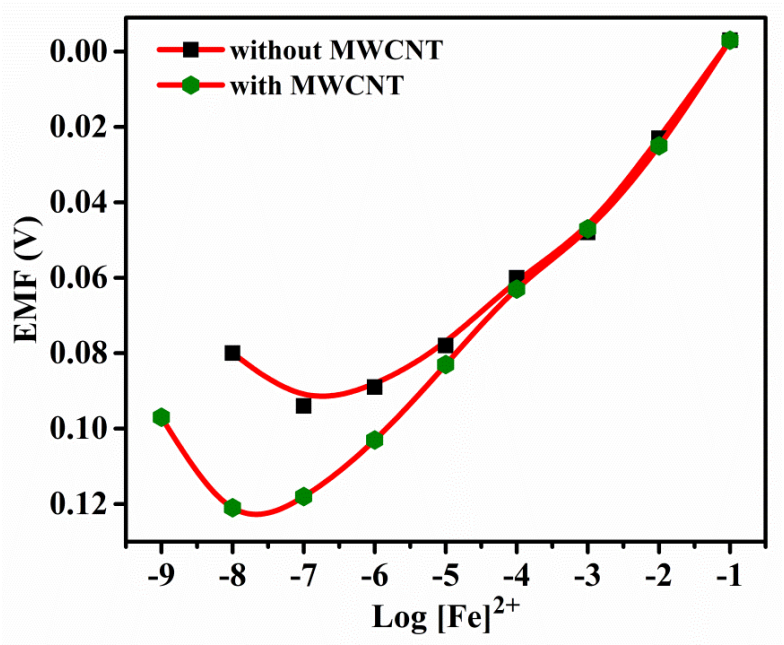

Fig. 4.1.1: Calibration curve for Fe(II)-selective electrode without MWCNTs and with MWCNTs (1%) using IFE based ISE

Table 4.1.1. Composition and characterization of IFE based membrane electrodes

S.No	Composition of Membrane (%w/w)								Detection Limit (mol/L)	Linear Range (mol/L)	Slope (mV/ decade)
	IFE Ionophore	PVC	o-NPOE	DBA	DOP	DOS	NaTPB	MW-CNTs			
1	1	33	64	-	-	-	2	-	1.0×10^{-6}	1×10^{-6}-1×10^{-1}	25
2	2	33	63	-	-	-	2	-	3.9×10^{-6}	1×10^{-5}-1×10^{-1}	33
3	3	33	62	-	-	-	2	-	1.0×10^{-7}	1×10^{-7}-1×10^{-1}	27
4	4	33	61	-	-	-	2	-	5.0×10^{-7}	1×10^{-6}-1×10^{-1}	19
5	5	33	60	-	-	-	2	-	1.2×10^{-6}	1×10^{-5}-1×10^{-1}	33
6	3	33	-	62	-	-	2	-	1.0×10^{-6}	1×10^{-6}-1×10^{-1}	18
7	3	33	-	-	62	-	2	-	1.7×10^{-7}	1×10^{-6}-1×10^{-1}	14
8	3	33	-	-	-	62	2	-	3.1×10^{-7}	1×10^{-6}-1×10^{-1}	11
9	3	33	64	-	-	-	-	-	1.0×10^{-6}	1×10^{-5}-1×10^{-1}	24
10	3	33	62	-	-	-	2	0.5	1.6×10^{-6}	1×10^{-5}-1×10^{-1}	27
11	3	33	62	-	-	-	-	1	1.5×10^{-5}	1×10^{-4}-1×10^{-1}	20
12	3	33	62				2	1	2.5×10^{-8}	1×10^{-7}-1×10^{-2}	26

Potential response of the electrode was plotted against pH of the solution as shown in Fig. 4.1.2. Studies show that the electrode response in the range of pH 2.5 to 6.0 is independent of the pH test solution. The ionophore instability due to the protonation of Nitrogen in ionophores is likely to cause change in potential less than 2. In addition, the electrode response to hydroxide ions will likely cause intensive potential changes in pH higher than 7.0. The electrode containing MWCNT (ISE No. 12) showed stable response in a wide pH range of 3.2 to 8.0 while the electrode No. 9 showed stable response in the pH range 2.5 to 6.0.

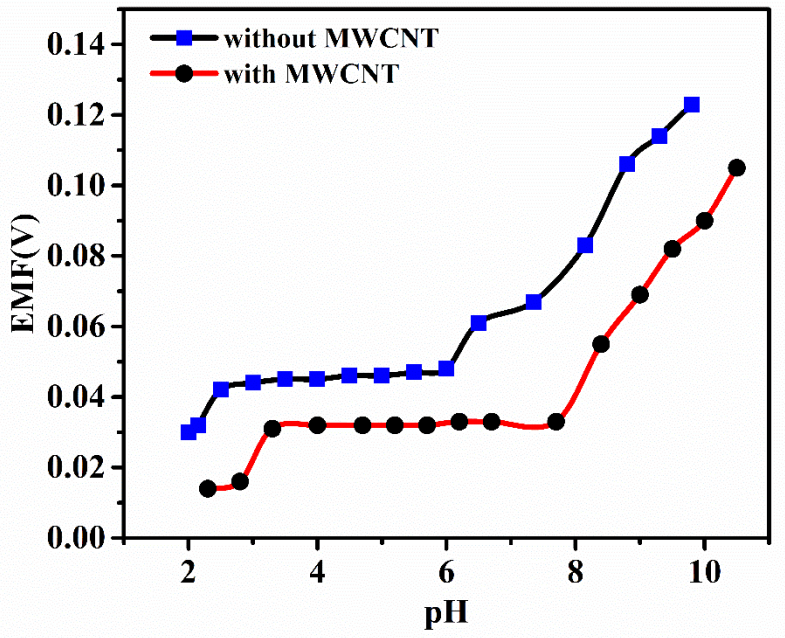

Fig. 4.1.2: Effect of pH on the emf response of the Fe(II) selective electrodes without MWCNT (ISE No. 9) and with MWCNT (ISE No. 12), at 1.0×10^{-4} mol/L concentration of Fe(II) ions

Electrode response time

For any ion selective electrode, dynamic response time is one of the most significant factor in analytical applications. The electrode's response time is the time needed to achieve 90% of the electrode's final steady potential value after successive immersion in Fe(II) solution, each having a 10 fold difference in concentration. In this study, response time of the electrode was measured by varying the Fe(II) concentration ranging from 1×10^{-8} M to 1×10^{-2} mol/L. The potential versus time traces are shown in Fig. 4.1.3. As can be seen from the graph that potential response for electrode no 3 reached the equilibrium in a short response time of ~15 s and remain stable for 3 min after which the divergence was recorded. Whereas, with the addition of MWCNT in the polymer matrix,

the response time for ISE No. 12 reached the equilibrium ~12 s due to the high electrical conductivity of MWCNT.

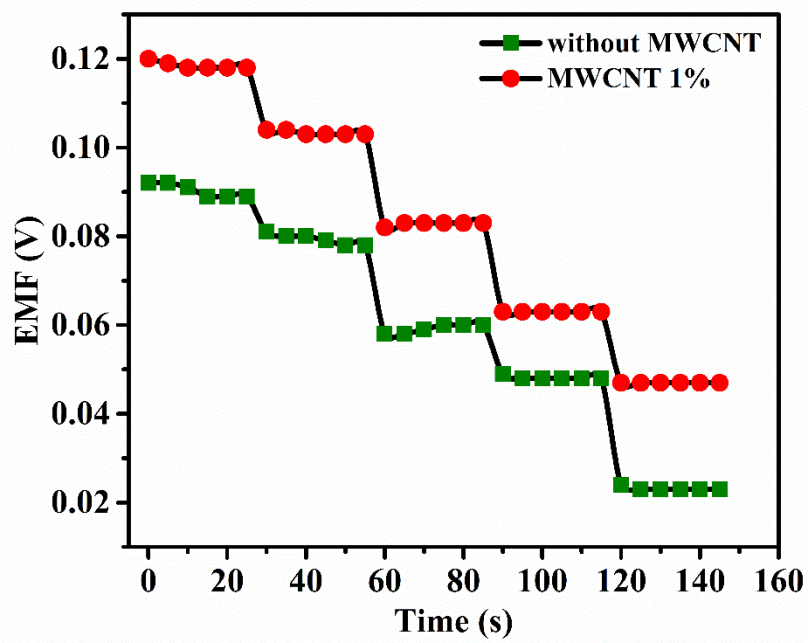

Fig. 4.1.3: Plots of EMF vs response time for Fe(II) selective electrode with and without MWCNTs

Selectivity coefficient

Selectivity of an ion selective electrode is one of the most important characteristics, which explains capability of the electrode to respond to primary ion in respect to other interfering ions. In the present study, selectivity coefficients of the sensor towards different interfering foreign cations was evaluated with the help of fixed interference method (FIM) recommended by IUPAC.[43] The selectivity coefficient value has been assessed by measuring potential responses using the fixed interference method in solutions containing fixed concentration of interfering ion, a_B (2×10^{-3} mol/L) and varying amount of primary ions (Fe(II)), a_A (2×10^{-8} - 2×10^{-1} mol/L). At the intersection of the extrapolated curve of the potential versus logarithm of the activity of the primary ion, the value of a_A in the presence of a diverse ion was calculated that is used to calculate (K_{AB}^{Pot}) according to eqn (1):

$$K_{A,B}^{Pot} = \frac{a_A}{a_B^{\frac{Z_A}{Z_B}}} \qquad 1$$

Table 4.1.2 provides selectivity coefficients for electrode no. 3 and 12. All selectivity values are less than < 1, except Fe^{2+}, for electrode No. 3, while for electrode No. 12 the values of all interfering cations are less than 1 and much lower than electrode No.3. It

shows that the impact of these cations on the functioning of the electrodes is negligible. Also, the ISE No. 12 (containing MWCNT) shows better selectivity for a given set of interfering ions over the ISE No. 3 (without MWCNT). During fabrication of the polymeric membrane, the membrane matrix containing the ionophore and the MWCNTs functionalised with COOH groups besides other components was sonicated and then cast in the polymeric film (see page para). During this process, the ionophore molecules are grafted at the terminal ends. Hence, ionophores are organised in a better way in the membrane loading to better possibilities of interactions with the guest species. Moreover, the side wall defects of the CNTs also lead to formation of sandwich complexes of ionophore receptors with the guest species. In all, the sensing performance of the CNT doped membranes are found to perform with better selectivity.[44,45]

Table 4.1.2. Selectivity coefficient values for the suggested electrodes (ISE No. 3 and ISE No. 12) by fixed interference method

Interfering Ions	**Log K_{AB}^{Pot}**	
	Electrode No. 3 Without MWCNTs	Electrode No. 12 With MWCNTs (1%)
Fe^{2+}	0.00	0.00
Ca^{2+}	-1.64	-2.60
Mg^{2+}	-2.45	-2.69
K^{+}	-2.61	-2.00
Cu^{2+}	-3.00	-3.00
Fe^{3+}	-4.00	-4.33
Cr^{3+}	-3.06	-3.66
Co^{2+}	-3.09	-3.10
Ni^{2+}	-1.20	-1.60
Zn^{2+}	-2.69	-3.94
Ag^{+}	-0.44	-3.00
Pb^{2+}	-1.17	-1.88

Surface characterization of the membrane electrode

To study surface morphology of the membrane, scanning electron microscopic study was done at different steps of its development. Results show that the membrane before adding MWCNT had a smooth surface with small surface defects (Fig. 4.1.4 (a)). Most of the MWCNTs are in the form of tiny bundles or single pipes while incorporating MWCNTs into the membrane matrix. MWCNTs with unique 3-dimensional constructions were placed on the electrode surface (Fig. 4.1.4 (b)). The EDX spectrum of IFE (Fig. 4.1.4 (d)) indicated the presence of Fe, O and C in the membrane matrix. After plunging into the iron solution, the EDX spectrum of the electrode surface is a sign of the effective absorption of Fe^{2+} by the ionophore in the electrode matrix.

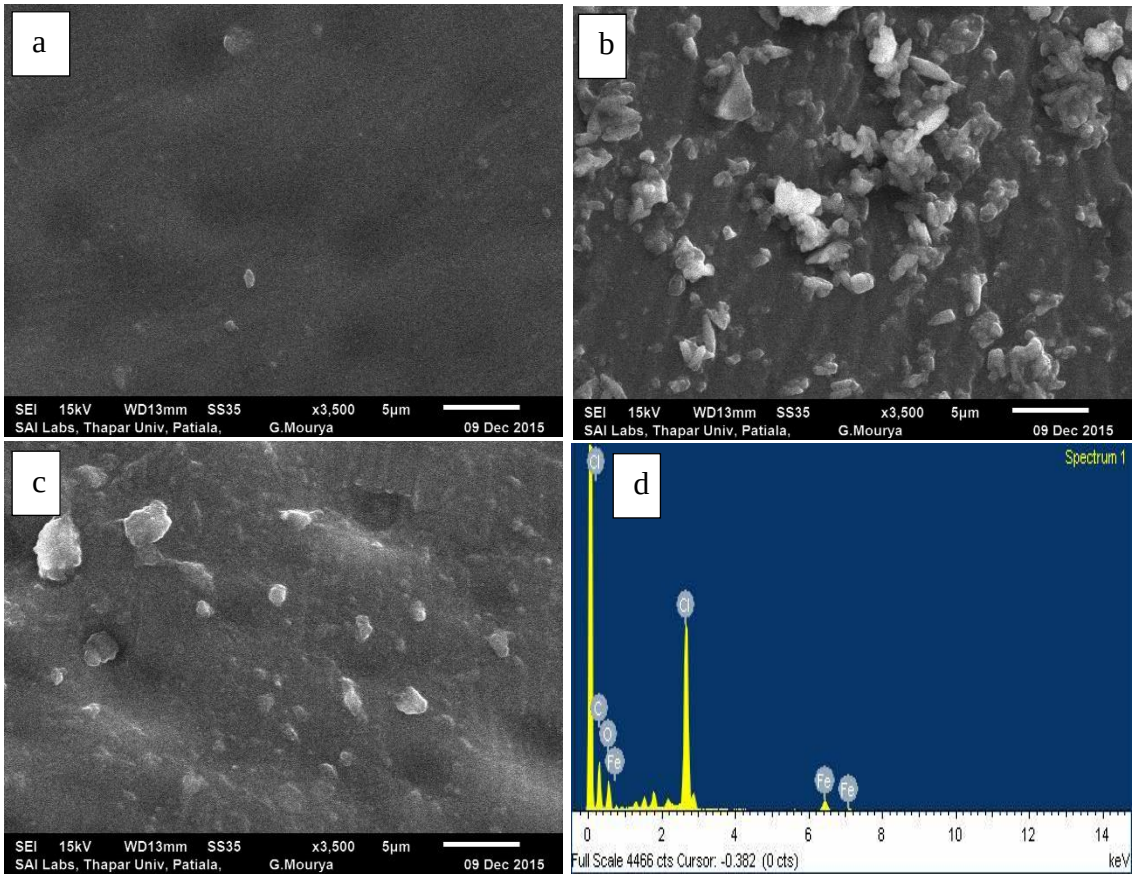

Fig. 4.1.4 (a) SEM images for the Fe^{2+}- ISE before (b) and after the incorporation of 1% MWCNTs (c) After the equilibration of the membrane with iron ions (d) EDX analysis for the same electrode after sorption with iron solution

Analytical Applications

To explore utility of this membrane electrode (ISE No. 3 and 12), potentiometric titration was carried out for the determination of end point. For this, 20 mL of Fe(II) (1×10^{-3} mol/L) was titrated against $K_2Cr_2O_7$ (1×10^{-2} mol/L) (Fig. 4.1.5). The titration plot was

obtained in sigmoid shape and a sharp breakpoint exhibits a 1:1 stoichiometry of the Fe(II) complex. After the end point, the potential response remains stagnant due to decrease in the concentration of Fe(II) ion. To assess practical utility of the proposed potentiometric sensor, these were employed in various real sample matrices such as a pharmaceutical samples and black tea. The findings achieved using Fe(II)-selective electrode and AAS are well-concorded, as demonstrated in Table 4.1.3 obtained from three replicate measurements. Performance characteristics of the IFE potentiometric electrode were compared with previously reported electrodes for the determination of iron ions (Table 4.1.4).[46-52]

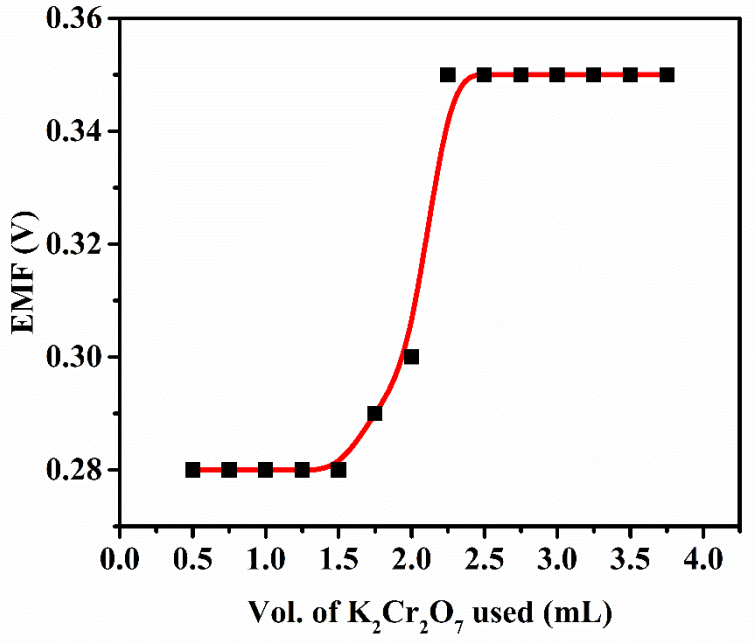

Fig. 4.1.5: Potentiometric titration of 20 mL of Fe(II) (1×10^{-3} mol/L) with $K_2Cr_2O_7$ (1×10^{-2} mol/L) using IFE based electrode

Table 4.1.3. Results of three replicate determinations of Fe (II) in various real-life samples

Sample	Concentration(mol/L)	
	Proposed Method	AAS Method
Multivitamin Tablet	9.2×10^{-4}(±3%)	9.0×10^{-4}(±2%)
Ferrous Sulphate Tablet	1.2×10^{-3}(±3%)	1.2×10^{-3}(±2%)
Iron Capsule	1.3×10^{-2}(±1%)	1.2×10^{-2}(±2%)
Black Tea	2.4×10^{-4}(±2%)	2.5×10^{-4}(±3%)

Table 4.1.4 Comparison of the IFE potentiometric electrode with the previously reported Fe (II) selective electrodes

Ionophore	Electrode	Detection Technique	Detection Limit (mol/L)	Ref.
2,4,6-tri(2-pyridyl)-1,3,5-triazine (TPTZ)	ISE[a]	Potentiometry	4.0×10^{-7}	[46]
N-phenylaza-15-crown-5 (NPA15C5)	ISE	Potentiometry	7.5×10^{-7}	[47]
Chiral 2,6-bis-(carboxamide methyl ester)pyridine	ISE	Potentiometry	4.0×10^{-6}	[48]
(E)-2-acetyl-3-(butyl amino)-N-phenyl buten-2-thioamide	ISE	Potentiometry	1.6×10^{-7}	[49]
5,5'-(propane-1,3-diyl-Bis(sulfa- nediyl))bis(3-benzyl-4H-1,2,4-triazol-4-amine)	Carbon Paste Electrodes	Potentiometry	1.0×10^{-7}	[50]
Dimethyliminocinnamyl linked rhodamine (rhodamine-dimethyliminocinnamyl) (RC)	CGE[b]	Potentiometry	7.43×10^{-8}	[51]
New Crown Ether	ISE	Potentiometry	6.7×10^{-7}	[52]
(E)-3-((2-aminoethylimino)methyl)-4H-chromen-4-one (IFE)	**ISE**	**Potentiometry**	**2.5×10^{-8}**	**This work**

[a] ISE = Ion Selective Electrode
[b] CGE = Coated Graphite Electrode

4.1.3.2 Potentiometric study of ICU molecule

Factors affecting performance of the Cu^{2+} ion selective electrode

Effect of composition

Selectivity and sensitivity of an ion-selective electrode is well-known to rely on plasticizer characteristics, solvent mediator nature, additive and ionophore quantity.[6] Therefore, different aspects of ICU based membrane for Cu^{2+} ion were optimized and the outcomes are summarized in Table 4.1.5. While using 3.0 % ionophore in membrane matrix the sensitivity, selectivity and linearity of the electrode response was maximum. However, below this rate and more addition of IFE ionophores, the electrode response was slowed and inactive, most likely owing to possible membrane saturations.[53] The impact of plasticizers on the efficiency of the membrane electrode is also researched. The use of plasticizers provides the paste certain permeable characteristics and can enhance sensor mechanical stability.[54] It is evident as seen in Table 4.1.5 (ISE No. 3, 6-8) due to the large dielectric constant, o-NPOE is better solvent mediator than DBA, DOS, DOP

for Cu^{2+} ion-selective electrode.[55] The primary reason for reducing the detection limit for the electrode to 5.5×10^{-7} mol/L may be the largest dielectric constant of NPOE. The NPOE was therefore selected as the best plasticizer for working electrode. In the presence of the lipophilic anionic additive NaTPB, the potential response of the membrane was enhanced considerably. It is commonly recognized that lipophilic salts not only decrease the membrane resistance, but also increase electrode response, selectivity and decrease sample anion interference.[56,57] The authors can also examine the efficiency of the copper (II) electrode through a strongly available surface with a small distribution size, great electrical conductivity and elevated stability of MWCNT. As shown in Table 4.1.5 (ISE no. 12) and represented in Fig. 4.1.6, the doped electrode with MWCNT (1%) demonstrated increased sensitivity of 1.0×10^{-7} mol/L as opposed to the analogue without MWCNT observed in the reduced detection limit (ISE no. 3).

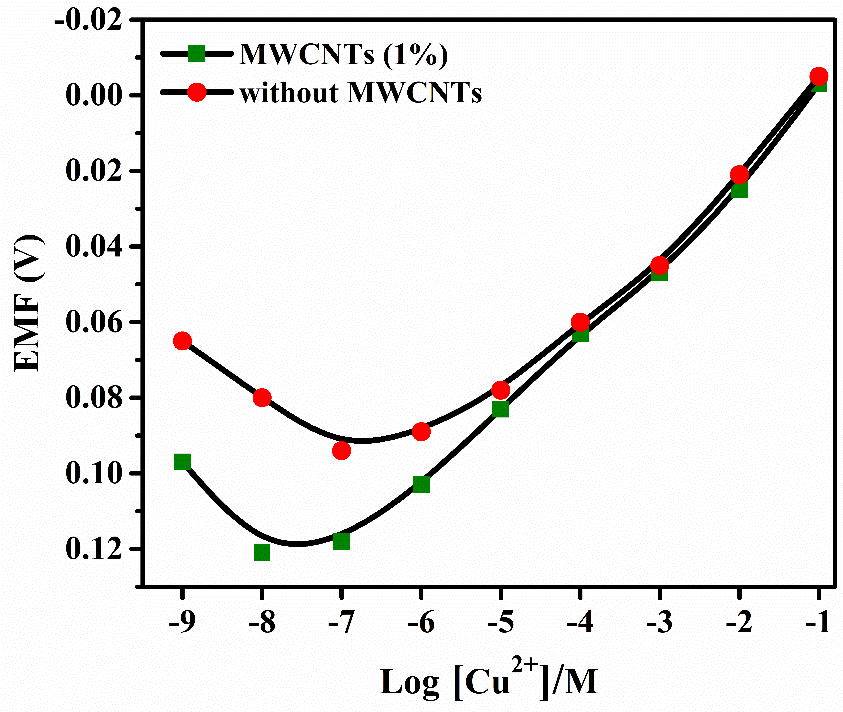

Fig. 4.1.6: Calibration curve for Cu (II)-selective electrode without MWCNTs and with MWCNTs (1%) with ICU based ISE No. 3 and 12

Effect of pH

Emf values were assessed for Cu^{2+} solution (10^{-4} mol/L) with distinct pH values to evaluate the impact of pH on the electrode's response. pH values of solutions were adjusted from 2.0 to 10.0 by adding diluted solutions of HNO_3 or NaOH. The change in emf with pH was plotted as shown in Fig. 4.1.7. The emf stays constant for 4.0-7.0 pH ranges. With greater pH, a sharp shift was noted in emf that could be caused by $Cu(OH)_2$

formation in the solution. A significant change in emf response observed at pH lower than 4 were because of the molecule protonation would reduce its tendency to form a complex. A more or less similar behaviour was observed in the case of addition of MWCNTs.

Table 4.1.5. Composition and characterization of ICU based membrane electrode

S. No	Composition of Membrane (%w/w)								Detection Limit (M)	Linear Range (M)	Slope (mV/ decade)
	Ionophore ICU	PVC	NPOE	DBA	DOP	DOS	NaTPB	MW-CNT			
1	1	33	64	-	-	-	2	-	3×10^{-4}	1×10^{-4}-1×10^{-1}	35
2	2	33	63	-	-	-	2	-	4×10^{-5}	1×10^{-3}-1×10^{-1}	25
3	3	33	62	-	-	-	2	-	3×10^{-6}	1×10^{-6}-1×10^{-1}	25
4	4	33	61	-	-	-	2	-	1×10^{-5}	1×10^{-5}-1×10^{-1}	30
5	5	33	60	-	-	-	2	-	7×10^{-4}	1×10^{-5}-1×10^{-1}	24
6	3	33	-	62	-	-	2	-	1×10^{-4}	1×10^{-4}-1×10^{-1}	24
7	3	33	-	-	62	-	2	-	2×10^{-4}	1×10^{-4}-1×10^{-1}	39
8	3	33	-	-	-	62	2	-	1×10^{-5}	1×10^{-5}-1×10^{-1}	36
9	3	33	64	-	-	-	-	-	7×10^{-4}	1×10^{-5}-1×10^{-1}	32
10	3	33	62	-	-	-	2	0.5	1×10^{-6}	1×10^{-4}-1×10^{-1}	35
11	3	33	62	-	-	-	-	1	1×10^{-4}	1×10^{-4}-1×10^{-1}	23
12	3	33	62				2	1	1×10^{-7}	1×10^{-7}-1×10^{-1}	27

Response Time

Response time of the proposed electrode was measured by its successive immersion in a series of Cu^{2+} solutions, each having a tenfold difference in concentration from 1.0×10^{-5} to 1×10^{-2} mol/L to reach the steady state potential of ±1 mV of the final equilibrium value(s). These dynamic responses were plotted as potential vs. time and are shown in Fig. 4.1.8. Comparison between the two electrodes reveals that the electrode no. 12 reaches equilibrium potential faster (5 s) than the other electrode (10 s) ISE No. 3. It shows a fast diffusion, fast complex formation and the exchange of ions between the aqueous layer and ion-selective electrodes.

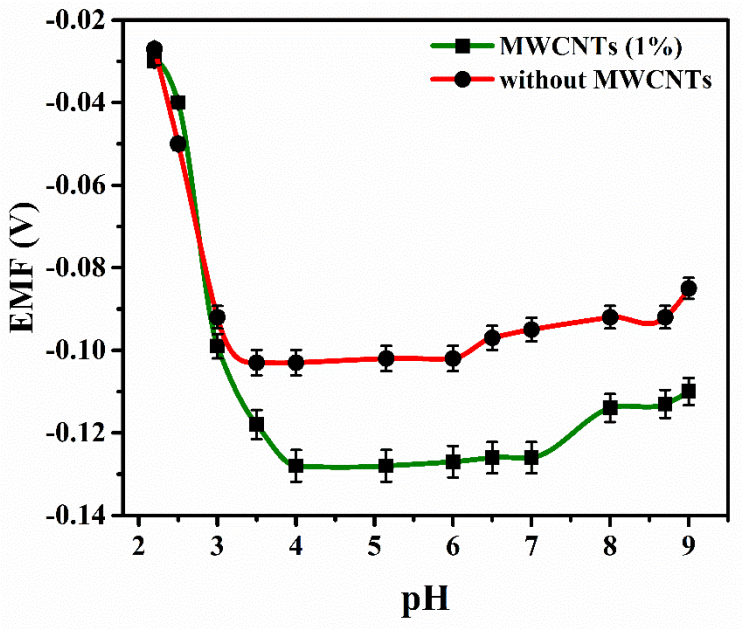

Fig. 4.1.7: Effect of pH on emf response of the Cu^{2+} selective electrode without and with MWCNTs (1%) using copper ion solution (1.0×10^{-4} M)

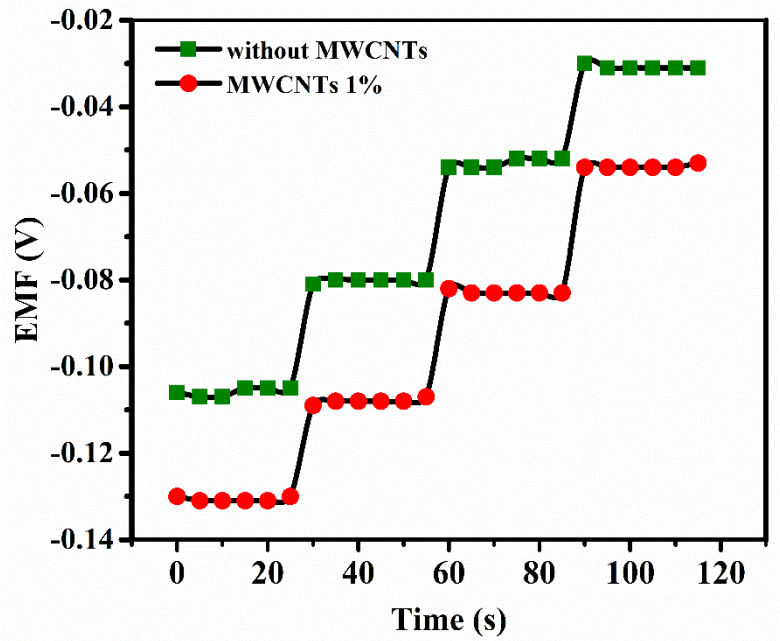

Fig. 4.1.8: Plots of Emf vs response time for Cu^{2+} selective electrode with and without MWCNTs

Selectivity coefficient study

A significant feature of the ion selective electode (ISE) is the primary ions selectivity over other ions present in the solution. For determining the potentiometric selectivity coefficients, fixed interference method (FIM) (recommended by IUPAC) was used.[43] Potentiometric selectivity coefficients, (K_{AB}^{Pot}) can be assessed using a fixed interference

technique by measuring potentials in solutions with a fixed concentration of interference ions, a_B (2×10^{-3} mol/L) and varying concentration of the primary ions, a_A (2×10^{-8} mol/L - 2×10^{-1} mol/L).

The logarithm of the activity of the primary ion was compared to the EMF values. The intersection between the extrapolated linear portions of this curve shows the value of an a_A to be calculated by (K_{AB}^{Pot}) according to Eq. (1)

$$K_{A,B}^{Pot} = \frac{a_A}{a_B^{\frac{Z_A}{Z_B}}} \quad 1$$

Table 4.1.5 provides selectivity coefficients for electrode no. 3 and 12. All selectivity values are less than < 1, except Cu^{2+}, for electrode No. 3, while for electrode No. 12 the values of all interfering cations are less than 1 and much lower than electrode No. 3. It indicates that the function of the suggested electrodes has a negligible disruption. The addition of MWCNT (Table 4.1.6) to the electrode composition showed a clear improvement of the selection pattern.

Table 4.1.6. Selectivity Coefficient Values for the Proposed Electrodes (EL No. 3 and EL No. 12)

Interfering Ions	**Log K_{AB}^{Pot}**	
	Electrode No. 3 Without MWCNTs	Electrode No. 12 With MWCNTs (1%)
Cu^{2+}	-	-
Ca^{2+}	-2.82	-3.77
Mg^{2+}	-3.47	-4.30
K^{+}	-1.07	-2.69
Fe^{2+}	-0.52	-4.30
Fe^{3+}	-3.52	-5.41
Cr^{3+}	-3.92	-7.31
Co^{2+}	-3.00	-4.60
Ni^{2+}	-3.36	-3.30
Zn^{2+}	-3.47	-4.69
Ag^{+}	-2.39	-0.92
Pb^{2+}	-3.72	-4.95

Surface characterization of the membrane electrode

Scanning electron microscope (SEM) is a useful instrument used for characterization of sensor surface morphology. As shown in Fig. 4.1.9, appearance of copper on the surface of membrane containing titled ionophore could be taken as proof for the surface reaction. The membrane was kept immersed in a solution of Cu^{2+} (0.1 M) for 24 hours to facilitate copper ions to enter the ionophore cavity immobilized in the membrane. Energy dispersive X-ray (EDX) is the main technique to detect the sample because every component has a unique atomic structure that permits a distinctive set of peaks on its X-ray spectrum. A sharp and strong peak in the EDX spectrum of the surface of the electrode for copper grows at about 1 keV (Fig. 4.1.9 d). After dipping in copper solution Fig. 4.1.9 (a) is a sign of the effective reaction of the titled ionophore with the Cu^{2+} ions at the electrode surface. Incorporation of CNTs in the membrane are visible clearly in SEM image (Fig. 4.1.9 b) arranged in a flower shape around the central ligand. Fig. 4.1.9 (c) shows presence of Cu species embedded in the matrix of the membrane.

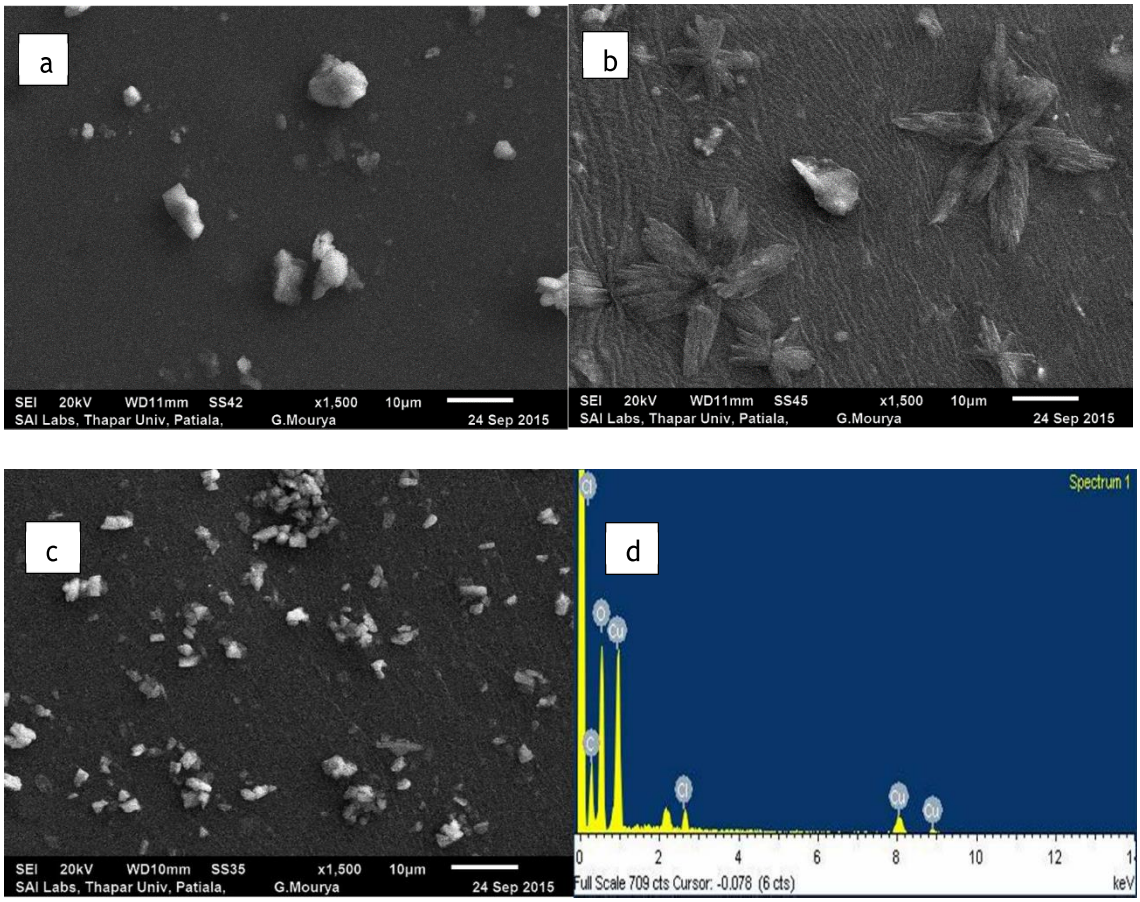

Fig. 4.1.9: SEM images for the Cu^{2+}- ISE (a) membrane without MWCNTs (b) membrane with MWCNTs (1%) (c) After equilibration with copper ions and (D) EDX analysis after equilibration with Cu^{2+} ions

Analytical applications

The electrode was effectively applied to potentiometric titration of Cu(II) ions with EDTA as indicator electrode. (Fig. 4.1.10). A 20 mL solution of Cu (II) (1×10^{-4} M) was titrated against EDTA (1×10^{-3} M) solution at pH 4.2. The end point exhibits 1:1 stoichiometry of the Cu^{2+}-EDTA complex. The suggested membrane electrode may therefore be used in potenometric titrations as an indicator electrode to determine Cu (II) ion concentration. In addition, for direct copper determination in multiple real-life samples, the suggested electrode is being used and compares the outcomes with Atomic Absorption Spectroscopy (AAS). The findings of three replicate measurements given in Table 4.1.7 indicate a satisfactory consistency between the outcomes acquired. Performance characteristics of the proposed ICU potentiometric electrode were compared with previously reported electrodes for the determination of copper ions (Table 4.1.8).[31,58-62]

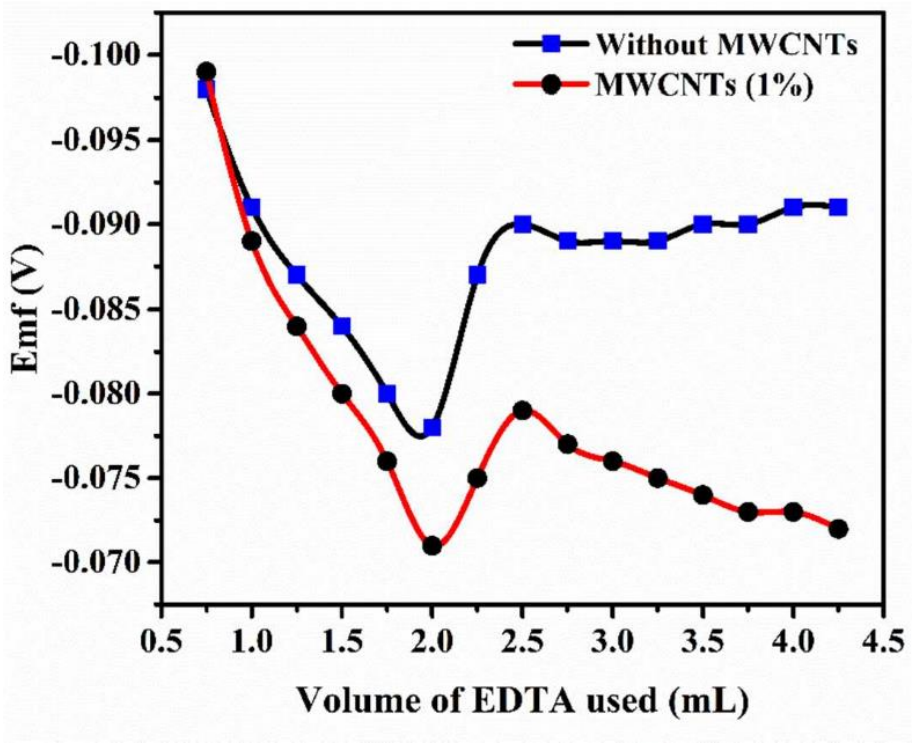

Fig. 4.1.10: Potentiometric titration of 20 mL of $Cu(NO_3)_2$ (1×10^{-3} M) Vs EDTA (1×10^{-4} M) using ICU electrodes without and with MWCNTs (1%)

Table 4.1.7. Real life sample analysis for Cu(II) using proposed method and comparison with AAS

Sample	Concentration(ppm)	
	Proposed Method using ICU electrode	AAS Method
Multivitamin Tablet	1.91(±2%)	1.97(±3%)
Copper wire	5.71(±3%)	5.80(±2%)
Black Tea	0.30(±3%)	0.34(±2%)

Table 4.1.8 Comparison of the ICU potentiometric electrode with the previously reported Cu (II) selective electrodes

Ionohore	**Electrode**	**Detection Technique**	**Detection Limit (M)**	**Ref.**
8-hydroxyquinoline-5-sulfonic acid (8-HQS)	Microneedle Cu (II) selective electrode	Potentiometry	1×10^{-5}	[58]
bis[(2-(hydroxyethylimino) phenolato]copper(II)	ISE[a]	Potentiometry	8.3×10^{-7}	[59]
Pyrrole	GCE/Cu-IP[b]	Potentiometry	5×10^{-7}	[60]
2,6-diacetylpyridine-(1R)-(-)-fenchone diazine	ISE	Potentiometry	2.5×10^{-6}	[31]
6-(bis(pyridin-2-ylmethyl) amino)hexane-1-thiol	Screen Printed ISE	Potentiometry	6.3×10^{-7}	[61]
copper(II)–carmoisine dye complex	Pencil Graphite electrode	Potentiometry	2.0×10^{-6}	[62]
(E)-3-(((2-((2 aminoethyl) amino) ethyl) imino) methyl)-4H-chromen-4-one (ICU)	**ISE**	**Potentiometry**	**1.0×10^{-7}**	**This work**

[a] ISE = Ion Selective Electrode
[b] (GCE/Cu-IP) = Cu (II) imprinted polymer glassy carbon electrode (GCE/Cu-IP)

4.1.3.3 Potentiometric study of IFE(III) electrode

Electrode potential response and factors affecting performance of the IFE(III) electrode

Effect of composition

Nitrogen and oxygen presence in the ionophore structure as heteroatoms and ample insolubility in water allowed IFE(III) to behave for a broad variety of transition, alkaline and alkaline earth metal ions, as appropriate ion carriers in PVC membrane. The sensitivity and selectivity of the potentiometric sensor depend significantly on composition of the ion selective membrane.[63-65] For this purpose, twelve newly designed PVC membrane electrodes with different combinations of ionophore, plasticizer, and anionic additives were prepared to determine the best composition. Results of then performance as membrane electrode are summarized in Table 4.1.9. Based on the lower detection limit of the membrane electrodes 1-5, the membrane composition with 3% ionophore was selected for further studies. The findings indicate that IFE(III) with o-NPOE has a better working range and Nernstian slope, because of its high dielectric constant and polarity, as compared with DBA, DOP and DOS.[38,40] The fact that the lipophilic anionic sites exist in the membrane phase increases the electrode response and selectivity and reduces the ohmic resistance.[41,63,66] As shown in Table 4.1.9, with the addition of anionic additive NaTBP, sensitivity of electrode improved considerably. The effect of MWCNT-COOH on the sensitivity of ion-selective electrodes was also investigated. In each membrane, MWCNT functionalized with COOH group can change the surface of CNTs from hydrophobic to hydrophilic, which facilitates the dispersion within the PVC membrane without altering mechanical stability of the tubes. Incorporation of MWCNTs (1%) in the PVC matrix (Electrode no. 12) showed enhanced selectivity and sensitivity of the electrode with a lower detection limit of 1.6×10^{-7} mol/L (Fig. 4.1.11).

Effect of pH

To investigate the effect of pH on performance of the electrode, electrode potentials were measured for 1×10^{-4} mol/L Fe(III) solution at different pH values. pH values of the solution were adjusted in the range 2 - 10 with sodium hydroxide and hydrochloric acid. The emf response remains constant within the pH range of 3.0-4.5. At pH lower than 3.0, the EMF becomes unstable probably due to protonation of the ionophore, while at pH

>4.5, the potential response changes with pH of the solution which might be a result of hydrolysis of Fe(III) ions.

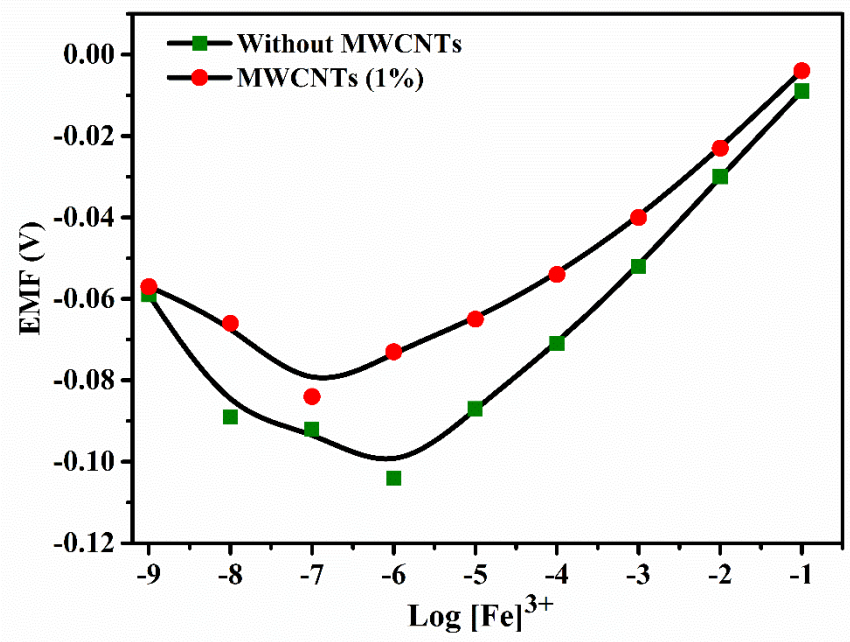

Fig. 4.1.11: Calibration curve for Fe(III)-selective electrode with MWCNTs

Table 4.1.9. Composition and characterization of IFE(III) based membrane electrode

S.No	Composition of Membrane (%w/w)								Detection Limit (mol/L)	Linear Range (mol/L)	Slope (mV/ decade)
	Ionophore IFE(III)	PVC	o-NPOE	DBA	DOP	DOS	NaTPB	MW-CNTs			
1	1	33	64	-	-	-	2	-	1.0×10^{-5}	1×10^{-5}-1×10^{-1}	25
2	2	33	63	-	-	-	2	-	3.2×10^{-5}	1×10^{-4}-1×10^{-1}	23
3	3	33	62	-	-	-	2	-	1.0×10^{-6}	1×10^{-6}-1×10^{-1}	21
4	4	33	61	-	-	-	2	-	4.1×10^{-6}	1×10^{-5}-1×10^{-1}	22
5	5	33	60	-	-	-	2	-	2.5×10^{-5}	1×10^{-4}-1×10^{-1}	28
6	3	33	-	62	-	-	2	-	1.0×10^{-4}	1×10^{-4}-1×10^{-1}	16
7	3	33	-	-	62	-	2	-	1.2×10^{-4}	1×10^{-3}-1×10^{-1}	15
8	3	33	-	-	-	62	2	-	1.4×10^{-6}	1×10^{-5}-1×10^{-1}	13
9	3	33	64	-	-	-	-	-	6.2×10^{-5}	1×10^{-4}-1×10^{-1}	21
10	3	33	62	-	-	-	2	0.5	5.0×10^{-7}	1×10^{-6}-1×10^{-2}	16
11	3	33	62	-	-	-	-	1	4.4×10^{-6}	1×10^{-5}-1×10^{-1}	21

12	3	33	62	-	-	-	2	1	1.6×10^{-7}	1×10^{-6}-1×10^{-2}	17

Response time

Response time is an important parameter in determining usability of the ion-selective electrodes. Response time of an electrode is assessed by measuring the potential when $\Delta E/\Delta t$ becomes equal to 0.5 mV/min, which elapsed from the instant when the IFE(III) based membrane electrode and the reference electrode are brought into contact with the test solution. The concentration of test solution has been changed from 10^{-7}- 10^{-2} mol/L for measuring dynamic response time for the IFE(III)-Fe^{3+} electrode. As shown in Fig. 4.1.12, electrode no. 12 reached its equilibrium time with in a very short response time of 4s. This indicated that Fe^{3+} ionophore at the membrane surface was rapidly exchanging kinetics of the complexing-decomplexing process.

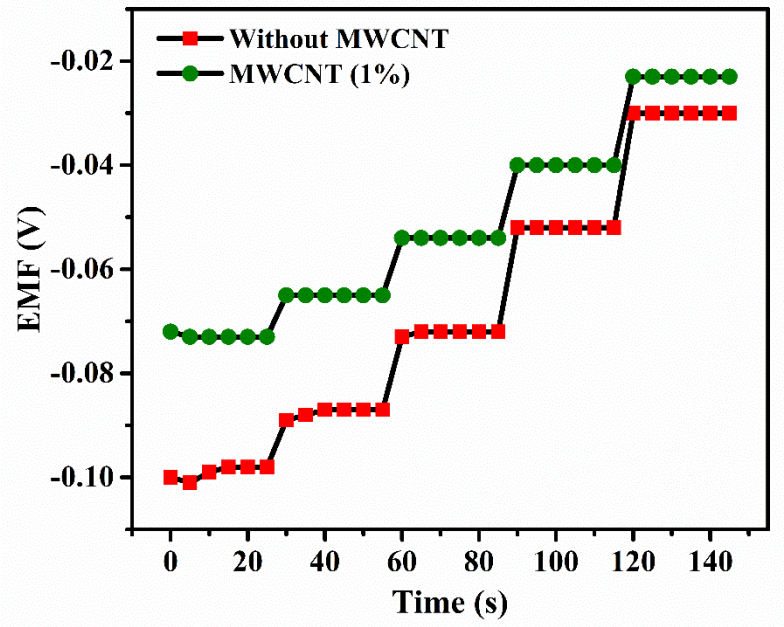

Fig. 4.1.12: Plots of EMF vs response time for IFE(III) based electrode with and without MWCNTs

Potentiometric selectivity coefficients for interfering ions

Potentiometric selectivity coefficient (K_{AB}^{Pot}) represents the impact of interfering ion on response behaviour of an ion selective electrode. It is a numerical impression of the capability of ion selective electrode to counter primary ion against other ions present in the solution. The potentiometric selectivity coefficients for interfering ions relative to Fe^{3+} were determined by using fixed interference method (FIM) (recommended by IUPAC).[35] The selectivity coefficients were evaluated using fixed concentration of

interfering ions a_B (2×10^{-3} mol/L) and varying the concentration of primary ions (Fe(III)), a_A (2×10^{-8} - 2×10^{-1} mol/L).

Table 4.1.10 lists the resulting selectivity coefficient values for electrode no. 3 and 12. The selectivity coefficient values are observed as <1, which indicate negligible effect of foreign ions on the performance of Fe^{3+} ion selective electrode. Most of the values of selectivity coefficients observed for Electrode no. 12 (containing CNTs) are lower than those observed for the Electrode no. 3, due to the incorporation of MWCNT. This may be due to specific arrangement of the ionophore in the membrane mixture with MWCNTs that give chance to capture ion from the surface.

Table 4.1.10. Selectivity coefficient values of IFE(III) based membrane electrode for interfering ions using Fixed Interference Method (FIM)

Interfering Ions	Log K_{AB}^{Pot}	
	Electrode No. 3 Without MWCNT	Electrode No. 12 With MWCNT (1%)
Fe^{3+}	-	-
Ca^{2+}	-0.45	-1.84
Mg^{2+}	-0.30	-1.53
Cu^{2+}	1.12	-1.99
Fe^{2+}	1.80	0.55
Cr^{3+}	-0.59	-3.00
Co^{2+}	-2.93	-1.39
Ni^{2+}	-0.34	-2.14
Zn^{2+}	-1.04	-0.94
Pb^{2+}	-0.74	-1.69
Hg^{2+}	-0.71	-2.06

Surface characterization of the IFE(III) membrane electrode

Surface morphology of the IFE(III) based membrane and its modification with electro-active material like MWCNT was studied by scanning electron microscopy and corresponding SEM images are shown in Fig. 4.1.13 where, the PVC membrane containing ionophore had a uniform layer with small surface defects. On the other hand,

irregular cracks with non-uniform surface was observed upon modification with MWCNT, which increases the adsorption of IFE(III) molecules from the test solution to the surface of membrane (Fig. 4.1.13 (b)). Results obtained from the EDX spectrum of IFE(III) membrane show the presence of Fe, O and C in the membrane matrix (Fig. 4.1.13 (d)). EDX spectrum of the surface of the electrode after equilibration with iron solution shows that the ionophore is complexed with the Fe^{3+} ions at the electrode surface (Fig. 4.1.13 (c)).

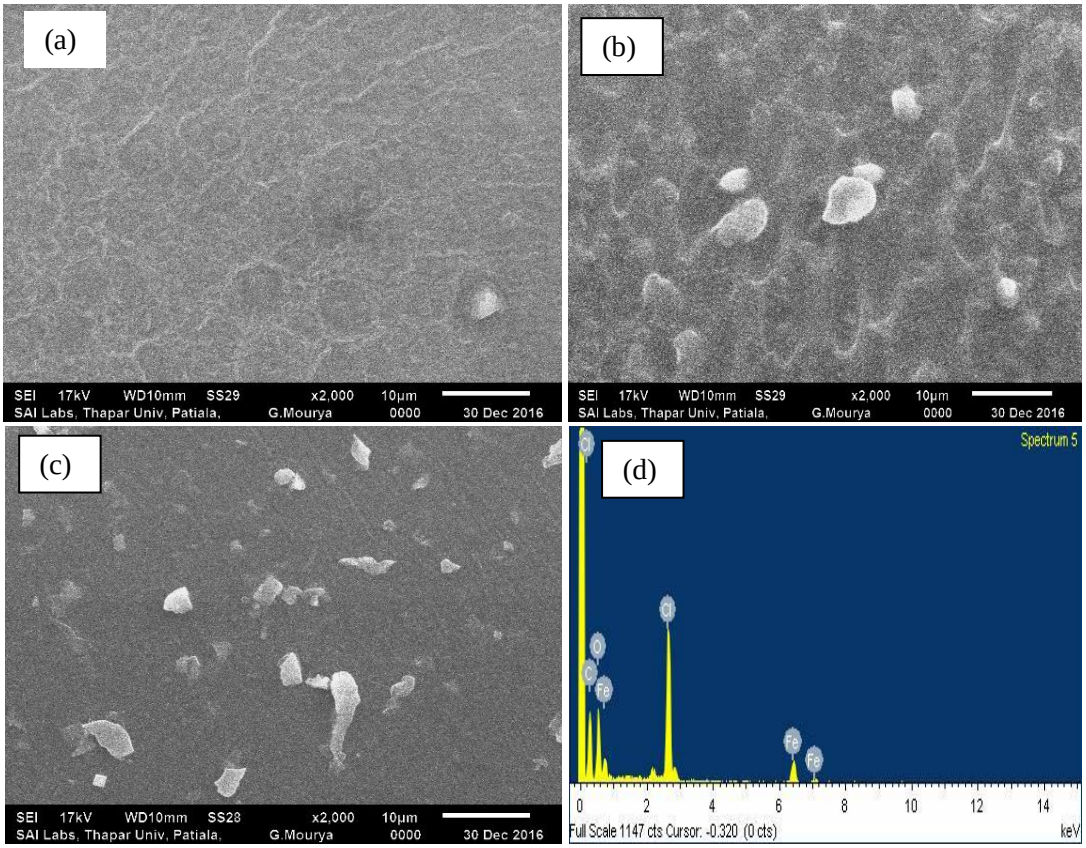

Fig. 4.1.13: (a) SEM images of IFE(III) electrode before and (b) after the incorporation of 1% MWCNTs. (c) After equilibration of electrode with Fe(III) and (d) EDX analysis of the electrode after sorption with iron solution

Analytical applications of IFE(III) electrode

Analytical applicability was evaluated with IFE(III)-Fe^{3+} electrode as an indicator electrode in potentiometric titration of Fe^{3+} solution with EDTA. For this, 20 mL of Fe^{3+} (1×10^{-4} mol/L) was titrated against of EDTA (1×10^{-3} mol/L) solution. As shown in Fig. 4.1.14, with the addition of EDTA to the test solution, a sigmoid shape curve was observed and a sharp end point represents the 1:1 stoichiometry of Fe-EDTA complex. After the endpoint, the electrode response was found to remain almost constant because all iron ions were used up in the formation of Fe^{3+} complex with EDTA. As an indicator

electrode, it has successfully been used in potentiometric titration of Fe^{3+} with EDTA. The iron was determined in pharmaceutical tablets, black tea and tap water to evaluate the practical usefulness of the proposed sensor. Data collected from the proposed Fe(III) selective electrode is in excellent agreement with those obtained from the AAS (Table 4.1.11). Performance characteristics of the proposed IFE(III) potentiometric electrode were compared with previously reported electrodes for the determination of iron ions (Table 4.1.12).[67-71]

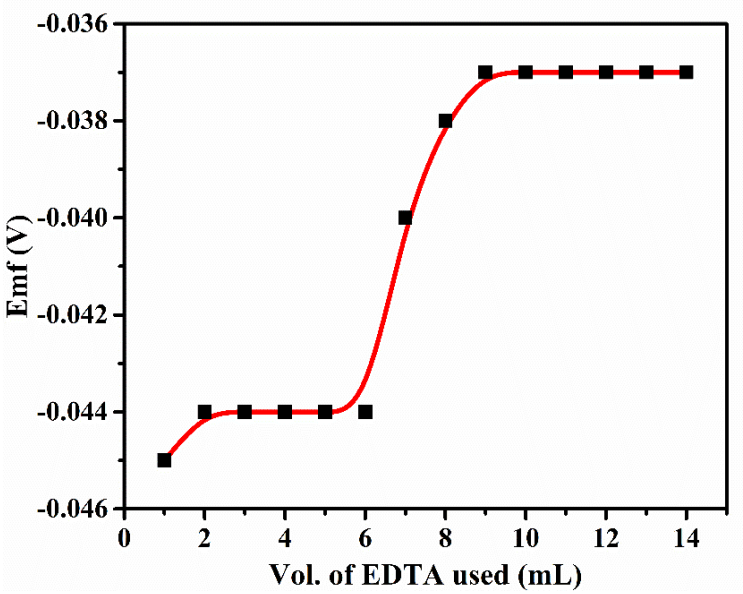

Fig. 4.1.14: Potentiometric titration of 20 mL of Fe(III) (1×10^{-4} mol/L) with EDTA (1×10^{-3} mol/L) using IFE(III) based membrane electrode as an indicator electrode

Table 4.1.11. Results of three replicate determinations of Fe (III) in various real-life samples

Sample	Concentration(mol/L)	
	Proposed Method using IFE(III) based electrode	AAS Method
Multivitamin Tablet	9.1×10^{-4} (±3%)	9.0×10^{-4} (±2%)
Tap Water	9.3×10^{-4} (±3%)	9.5×10^{-4} (±2%)
Green Tea	1.3×10^{-2} (±1%)	1.2×10^{-2} (±2%)
Black Tea	2.4×10^{-4} (±2%)	2.5×10^{-4} (±3%)

Table 4.1.12 Comparison of the IFE(III) potentiometric electrode with the previously reported Fe (III) selective electrodes

Ionophore	Electrode	Detection Technique	Detection Limit (mol/L)	Ref.
5-chloro-3-[4-(trifluoromethoxy)phenylimino]indolin-2-one	ISE[a]	Potentiometry	6.3×10^{-7}	[67]
1,4-Diaminoanthraquinone (DAQ)	ISE	Potentiometry	8.0×10^{-7}	[68]
Fe-phosphotungstate ion-associate	SPISE[b]	Potentiometry	1.57×10^{-7}	[69]
2-[(thiophen-2-yl) methyleneamino]isoindoline-1,3-dione (TMID)	ISE	Potentiometry	5.0×10^{-7}	[70]
1-phenyl-3-pyridin-2-yl-thiourea (PPT)	ISE	Potentiometry	3.9×10^{-7}	[71]
(E)-3-((2-(2-(2-aminoethylamino)ethylamino)ethylimino)methyl)-4H-chromen-4-one (IFE-III),	**ISE**	**Potentiometry**	**1.0×10^{-7}**	**This work**

[a] ISE = Ion Selective Electrode
[b] SPISE = Screen Printed Ion Selective Electrode

4.1.4 Conclusions

In this work, sensitive and selective potentiometric sensors based on (E)-3-((2-aminoethylimino)methyl)-4H-chromen-4-one (IFE), (E)-3-(((2-((2 aminoethyl) amino) ethyl) imino) methyl)-4H-chromen-4-one (ICU) and (E)-3-((2-(2-(2-aminoethylamino) ethylamino) ethylimino)methyl)-4H-chromen-4-one (IFE(III)) were studied as Fe(II), Cu(II) and Fe(III) selective electrodes. The membrane electrodes were optimised with experimental parameters. Incorporation of MWCNT in the membrane matrix showed improved characteristics of the respective ion-selective electrodes. The analytical utility of the membrane electrodes was validated by using these as indicator electrodes in the real life sample analysis for the recognition of Fe(II), Cu(II) and Fe(III) ions.

References

(1) Kumar, S.; Mittal, S. K.; Kaur, N.; Kaur, R. *RSC Advances* **2017**, *7*, 16474-16483.

(2) Kumar, S.; Mittal, S. K.; Singh, J.; Kaur, N. *Analytical Methods* **2016**, *8*, 7472-7481.

(3) K. Mittal, S.; Kumar, S.; Kaur, N. *Electroanalysis*.

(4) Craggs, A.; Moody, G.; Thomas, J. *Journal of Chemical Education* **1974**, *51*, 541.

(5) Morf, W. E. *The Principles of Ion-Selective Electrodes and of Membrane Transport*; Elsevier, 2012; Vol. 2.

(6) Bakker, E.; Bühlmann, P.; Pretsch, E. *Chemical Reviews* **1997**, *97*, 3083-3132.

(7) Freiser, H. *Ion-Selective Electrodes in Analytical Chemistry*; Springer Science & Business Media, 2012.

(8) Bakker, E.; Bühlmann, P.; Pretsch, E. *Electroanalysis: An International Journal Devoted to Fundamental and Practical Aspects of Electroanalysis* **1999**, *11*, 915-933.

(9) Pungor, E.; Tóth, K. *Analyst* **1970**, *95*, 625-648.

(10) Light, T. S. *Journal of Chemical Education* **1997**, *74*, 171.

(11) Birch, B.; Cockcroft, R. *Ion Selective Electrode Reviews* **1981**, *4*, 1-41.

(12) Gupta, V. K.; Ganjali, M.; Norouzi, P.; Khani, H.; Nayak, A.; Agarwal, S. *Critical Reviews in Analytical Chemistry* **2011**, *41*, 282-313.

(13) Zhu, C.; Yang, G.; Li, H.; Du, D.; Lin, Y. *Analytical Chemistry* **2014**, *87*, 230-249.

(14) Trojanowicz, M. *TrAC Trends in Analytical Chemistry* **2006**, *25*, 480-489.

(15) Merkoçi, A. *Microchimica Acta* **2006**, *152*, 157-174.

(16) Scida, K.; Stege, P. W.; Haby, G.; Messina, G. A.; García, C. D. *Analytica Chimica Acta* **2011**, *691*, 6-17.

(17) Crespo, G. A.; Macho, S.; Rius, F. X. *Analytical Chemistry* **2008**, *80*, 1316-1322.

(18) Crespo, G. n. A.; Macho, S.; Bobacka, J.; Rius, F. X. *Analytical Chemistry* **2008**, *81*, 676-681.

(19) Ganjali, M. R.; Khoshsafar, H.; Faridbod, F.; Shirzadmehr, A.; Javanbakht, M.; Norouzi, P. *Electroanalysis: An International Journal Devoted to Fundamental and Practical Aspects of Electroanalysis* **2009**, *21*, 2175-2178.

(20) Parra, E. J.; Crespo, G. A.; Riu, J.; Ruiz, A.; Rius, F. X. *Analyst* **2009**, *134*, 1905-1910.

(21) Kimmel, D. W.; LeBlanc, G.; Meschievitz, M. E.; Cliffel, D. E. *Analytical Chemistry* **2011**, *84*, 685-707.

(22) Gao, C.; Guo, Z.; Liu, J.-H.; Huang, X.-J. *Nanoscale* **2012**, *4*, 1948-1963.

(23) Gupta, V. K.; Singh, A. K.; Mehtab, S.; Gupta, B. *Analytica Chimica Acta* **2006**, *566*, 5-10.

(24) Abdallah, S. M.; Zayed, M.; Mohamed, G. G. *Arabian Journal of Chemistry* **2010**, *3*, 103-113.

(25) Patel, R.; Gundla, V.; Patel, D. *Polyhedron* **2008**, *27*, 1054-1060.

(26) Chattopadhyay, S.; Ray, M. S.; Drew, M. G.; Figuerola, A.; Diaz, C.; Ghosh, A. *Polyhedron* **2006**, *25*, 2241-2253.

(27) Aziz, A. A. A.; Salem, A. N. M.; Sayed, M. A.; Aboaly, M. M. *Journal of Molecular Structure* **2012**, *1010*, 130-138.

(28) Kumar, P.; SK, A. K.; Mittal, S. K. *Journal of Chemical Sciences* **2014**, *126*, 33-40.

(29) Bandi, K. R.; Singh, A. K.; Upadhyay, A. *Materials Science and Engineering: C* **2014**, *34*, 149-157.

(30) Dadkhah, A.; Rofouei, M. K.; Mashhadizadeh, M. H. *Sensors and Actuators B: Chemical* **2014**, *202*, 410-416.

(31) Isa, I. M.; Saidin, M. I.; Ahmad, M.; Hashim, N.; Ghani, S. A.; Si, S. M. *International Journal of Electrochemical Science* **2013**, *8*, 11175-11185.

(32) Homafar, A.; Maleki, F.; Abbasi, Z. *Energy and Environmental Engineering* **2013**, *1*, 99-104.

(33) Arvand, M.; Lashkari, Z. *Spectrochimica Acta Part A: Molecular and Biomolecular Spectroscopy* **2013**, *107*, 280-288.

(34) Hajiaghababaei, L.; Sharafi, A.; Suzangarzadeh, S.; Faridbod, F. *Bioanalytical Electrochemistry* **2013**, *5*, 481-493.

(35) Umezawa, Y.; Umezawa, K.; Sato, H. *Pure and Applied Chemistry* **1995**, *67*, 507-518.

(36) Sokalski, T.; Ceresa, A.; Fibbioli, M.; Zwickl, T.; Bakker, E.; Pretsch, E. *Analytical Chemistry* **1999**, *71*, 1210-1214.

(37) Eugster, R.; Rosatzin, T.; Rusterholz, B.; Aebersold, B.; Pedrazza, U.; Rüegg, D.; Schmid, A.; Spichiger, U. E.; Simon, W. *Analytica Chimica Acta* **1994**, *289*, 1-13.

(38) Pérez, M. a. d. l. A. A.; Marín, L. P.; Quintana, J. C.; Yazdani-Pedram, M. *Sensors and Actuators B: Chemical* **2003**, *89*, 262-268.

(39) Bühlmann, P.; Pretsch, E.; Bakker, E. *Chemical Reviews* **1998**, *98*, 1593-1688.

(40) Bühlmann, P.; Yajima, S.; Tohda, K.; Umezawa, Y. *Electrochimica Acta* **1995**, *40*, 3021-3027.

(41) Telting-Diaz, M.; Bakker, E. *Analytical Chemistry* **2001**, *73*, 5582-5589.

(42) Rosatzin, T.; Bakker, E.; Suzuki, K.; Simon, W. *Analytica Chimica Acta* **1993**, *280*, 197-208.

(43) Umezawa, Y.; Bühlmann, P.; Umezawa, K.; Tohda, K.; Amemiya, S. *Pure and Applied Chemistry* **2000**, *72*, 1851-2082.

(44) Parra, E. J.; Blondeau, P.; Crespo, G. A.; Rius, F. X. *Chemical Communications* **2011**, *47*, 2438-2440.

(45) Kerric, G.; Parra, E. J.; Crespo, G. A.; Rius, F. X.; Blondeau, P. *Journal of Materials Chemistry* **2012**, *22*, 16611-16617.

(46) Mahmoud, W. H. *Analytica Chimica Acta* **2001**, *436*, 199-206.

(47) Aghaie, M.; Giahi, M.; Aghaie, H.; Arvand, M.; Pournaghdy, M.; Yavari, F. *Desalination* **2009**, *247*, 346-354.

(48) Abounassif, M.; Al-Omar, M.; Amr, A. G.; Mostafa, G. *Drug Testing and Analysis* **2011**, *3*, 373-379.

(49) Yazdely, M. A.; Taher, M. A.; Tajik, S. *Analytical & Bioanalytical Electrochemistry* **2013**, *5*, 467-480.

(50) Aglan, R. F.; Rizk, M. S.; Mohamed, G. G.; El-Wahy, A. H.; Mohamed, H. A. *American Journal of Analytical Chemistry* **2014**, *2014*.

(51) Kamal, A.; Kumar, N.; Bhalla, V.; Kumar, M.; Mahajan, R. K. *Sensors and Actuators B: Chemical* **2014**, *190*, 127-133.

(52) Absalan, G.; Arabi, M.; Khalifeh, R.; Sharghi, H.; Tashkhourian, J. *IEEE Sensors Journal* **2013**, *14*, 349-356.

(53) Yang, X.; Kumar, N.; Chi, H.; Hibbert, D. B.; Alexander, P. W. *Electroanalysis* **1997**, *9*, 549-553.

(54) Cummings, E.; Mailley, P.; Linquette-Mailley, S.; Eggins, B.; McAdams, E.; McFadden, S. *Analyst* **1998**, *123*, 1975-1980.

(55) Amemiya, S.; Bühlmann, P.; Umezawa, Y. *Analytical Chemistry* **1998**, *70*, 445-454.

(56) Morf, W.; Kahr, G.; Simon, W. *Analytical Letters* **1974**, *7*, 9-22.

(57) Huser, M.; Gehrig, P. M.; Morf, W. E.; Simon, W.; Lindner, E.; Jeney, J.; Toth, K.; Pungor, E. *Analytical Chemistry* **1991**, *63*, 1380-1386.

(58) Sharifian, M.; Ashraf, N.; Zavar, M. H. A.; Chamsaz, M.; Afzali, F. *Journal of The Electrochemical Society* **2015**, *162*, B57-B61.

(59) Andac, M.; Coldur, F.; Bilir, S.; Birinci, A.; Demir, S.; Uzun, H. *Canadian Journal of Chemistry* **2014**, *92*, 324-328.

(60) Mazloum-Ardakani, M.; Amini, M. K.; Dehghan, M.; Kordi, E.; Sheikh-Mohseni, M. A. *Journal of the Iranian Chemical Society* **2014**, *11*, 257-262.

(61) Li, M.; Zhou, H.; Shi, L.; Li, D.-W.; Long, Y.-T. *Analyst* **2014**, *139*, 643-648.

(62) Ansari, R.; Delavar, A. F.; Aliakbar, A.; Mohammad-Khah, A. *Journal of Solid State Electrochemistry* **2012**, *16*, 869-875.

(63) Khani, H.; Rofouei, M. K.; Arab, P.; Gupta, V. K.; Vafaei, Z. *Journal of Hazardous Materials* **2010**, *183*, 402-409.

(64) Mashhadizadeh, M. H.; Khani, H. *Analytical Methods* **2010**, *2*, 24-31.

(65) Mashhadizadeh, M. H.; Taheri, E. P.; Sheikhshoaie, I. *Talanta* **2007**, *72*, 1088-1092.

(66) Shahrokhian, S. *Analytical Chemistry* **2001**, *73*, 5972-5978.

(67) Demir, E.; Kemer, B.; Bekircan, O.; Y Aboul-Enein, H. *Current Analytical Chemistry* **2015**, *11*, 29-35.

(68) Kazemi, F.; Zamani, H.; Joz-Yarmohammadi, F.; Ebrahimi, M.; Abedi, M. *Bulgarian Chemical Communications* **2017**, *49*, 449-454.

(69) Ali, T. A.; Farag, A. A.; Mohamed, G. G. *Journal of Industrial and Engineering Chemistry* **2014**, *20*, 2394-2400.

(70) Zamani, H. A.; Faridbod, F. *Journal of Analytical Chemistry* **2014**, *69*, 1073-1078.

(71) Motlagh, M. G.; Taher, M. A.; Ahmadi, A. *Electrochimica Acta* **2010**, *55*, 6724-6730.

4.2 Voltammetric studies on Schiff base compounds

Abstract

Voltammetric studies of the ionophores (IFE, ICU and IFE(III)) were done by cyclic voltammetry (CV) and differential pulse voltammetry (DPV) at glassy carbon electrode in TBHP/DMSO solution (0.1 mol L^{-1}) as the electrolyte with a scan rate of 50 mV s^{-1}. The purpose of voltammetric studies was to study the redox properties of IFE, ICU and IFE(III) ionophores. Receptors IFE, ICU and IFE(III) showed cathodic peaks at -1.76 V, -1.77 V and -1.73 V, respectively, because of the reduction of imine group. In case of anodic cycle, peaks were observed due to oxidation of lone pair of electrons on nitrogen atoms of amine groups of the investigated receptors.

4.2.1 Introduction

Some heavy metals are vital as trace elements to maintain the metabolism of the human body.[1,2] However, long-term exposure to heavy metals can cause deleterious health effects in humans.[3-7] A delicate and selective technique to determine heavy metal ion in chemical, biological and environmental samples has therefore to be developed urgently. In order to detect heavy metal ions, several methods have been established using sophisticated analytical instruments such as atomic absorption spectroscopy (AAS),[8,9] inductively coupled plasma-mass spectrometry (ICPMS)[10,11] and spectrophotometry.[12-14] While these techniques provide precise outcomes, they have some practical limitations such as nonportability, being expensive and time-consuming and require sample pre-treatment. To overcome these limitations, electrochemical (voltammetry) methods are preferred that are low cost and portable and have a fast response time, reasonable selectivity, sufficiently low detection limit and specificity.[15] The current-voltage relationship provides basis for the voltammetric sensor. Voltammetry is a method of electroanalysis involving the application of potential (E) to a polarised electrode and recorded the resulting current (i) that flow through the electrochemical cell. Cyclic voltammetry provides evidence for a reaction mechanism. It gives information on the position of redox potentials of electroactive compounds and influence of media on the redox process.[16,17] The voltammetric cell comprise of three electrode: a working electrode, reference electrode and an auxiliary electrode (counter). The three electrode systems are essential to avoid the current flow through the reference electrode, which would otherwise alter their potential through modifications in the species' activities. In a three-electrode system, current is measured between the auxiliary and working electrode

and the reference electrode controls working electrode potential.[18,19] In this work, reduction and oxidation properties of IFE, ICU and IFE(III) were studied using voltammetric measurements.

4.2.2 Experimental

Materials

All chemicals were of analytical reagent grade. Electrolyte tetrabutylammonium hexafluorophosphate was obtained from Sigma-Aldrich. Metal salt solutions of concentration 0.1 mol L^{-1} were prepared by dissolving metal nitrates in DMSO medium and standardized wherever necessary. Working solutions of different concentrations were prepared by serial dilutions.

Voltammetric measurements

To explore the redox properties of IFE-ONPs, electrochemical workstations conducted CV and DPV studies (Autolab/PGSTAT12 /Eco Chemie/Netherlands) using a three-electrode setup consisting of a glassy carbon as working electrode (round disk, diameter 3 mm), Pt electrode as counter electrode and Ag/Ag^+ (0.1 mol/L $AgNO_3$ in DMSO) as reference electrode. The experimental conditions were controlled with NOVA 1.5 software. The CV and DPV studies were performed at a scan rate of 0.03 Vs^{-1}, a pulse amplitude of 0.025 V, a pulse width of 0.05 s and a pulse period of 0.10 s in the potential range of 2.00 V to -2.00 V vs Ag/Ag^+. The working electrode surface was polished with 0.05 micron aluminum before measurements. By using the working electrode on an ultrasonic cleaner for 15 minutes, the remaining particles of alumina were completely removed and dry and cleaned with pure acetonitrile. For all voltammetric measurements, the studies have been completed in an aqueous medium and KCl (0.1 mol/L) as supporting electrolyte. At a temperature of 25.0 ± 1 ºC, the electrochemical measurements were performed. The sample solutions have been deaerated through the stream of nitrogen gas purging for at least 5 minutes in every measurement.

4.2.3 Voltammetric characterization of Schiff base ionophores

4.2.3.1 Discussion on voltammetric studies of IFE

In the cyclic voltammogram of IFE, there were three weak anodic peaks at -0.39 V, -0.12 V and 0.2 V, in addition to a relatively stronger peak at -1.0 V. The stronger peak is due to the supporting electrolyte using glassy carbon electrode as a working electrode. The potential was applied at a scan rate of 50 mV/s. The anodic peaks identified in Fig. 4.2.1

as I, II and III resulted from the anodic reactions. The easiest species to oxidise is the N atom of the terminal amine group that shows anodic peaks at the lower potential. i.e., at -0.3 V followed by the peaks at -0.1 V and +0.2 V respectively due to N atom of imine group and the oxygen atom of pyran ring. For the purpose of further characterization and applications of the ionophore in the anodic DPV, the peak maxima at -0.12 V has been chosen as a model peak.

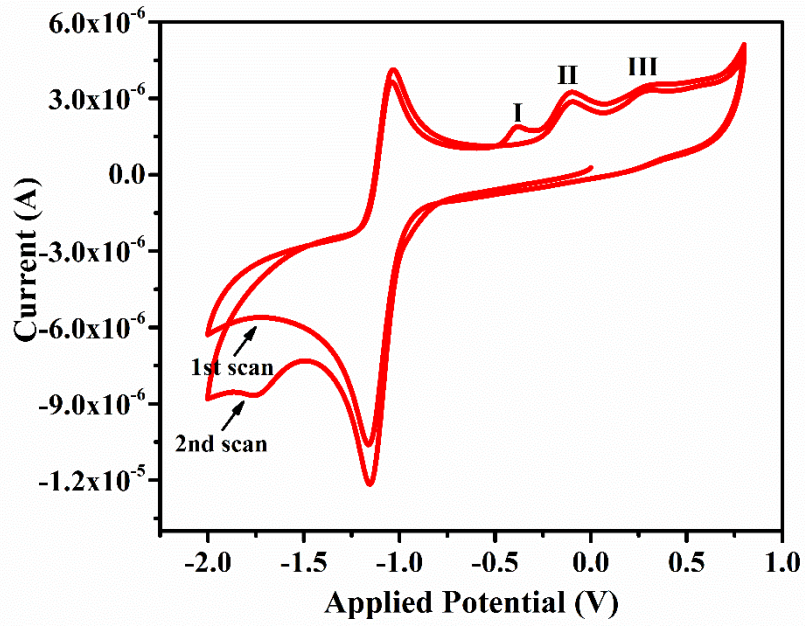

Fig. 4.2.1: Cyclic voltammogram of IFE (5×10^{-4} mol/L) at glassy carbon electrode in DMSO, 0.1 mol/L TBHP. Scan rate: 50 mVs^{-1}

Scan rate study

In order to recognize the procedure involved in electrochemical oxidation of IFE at glassy carbon electrode surface, peak currents of anodic waves were plotted against the square root of scan rate (Fig. 4.2.2 (a)). A linear relationship was found (Fig. 4.2.2 (b)) between peak current I_{pa} and the square root of scan rate. This phenomenon indicates that the oxidation of the IFE is measured by its diffusion towards the electrode surface. When the scan rate rises from 10 mVs s^{-1} to 130 mVs^{-1}, the anodic peak potential moves a little in a positive direction, suggesting that the transfer of the electron is not very quick.

Complexation with metal ions

Experiments were conducted using voltammetric scans of IFE in presence of a number of transition metal ions. It is expected that on complexation with the metal ion, the primary and secondary nitrogen atoms on the aliphatic chain attached to the chromen ring would form a pseudo cavity with the oxygen atom of pyran ring.

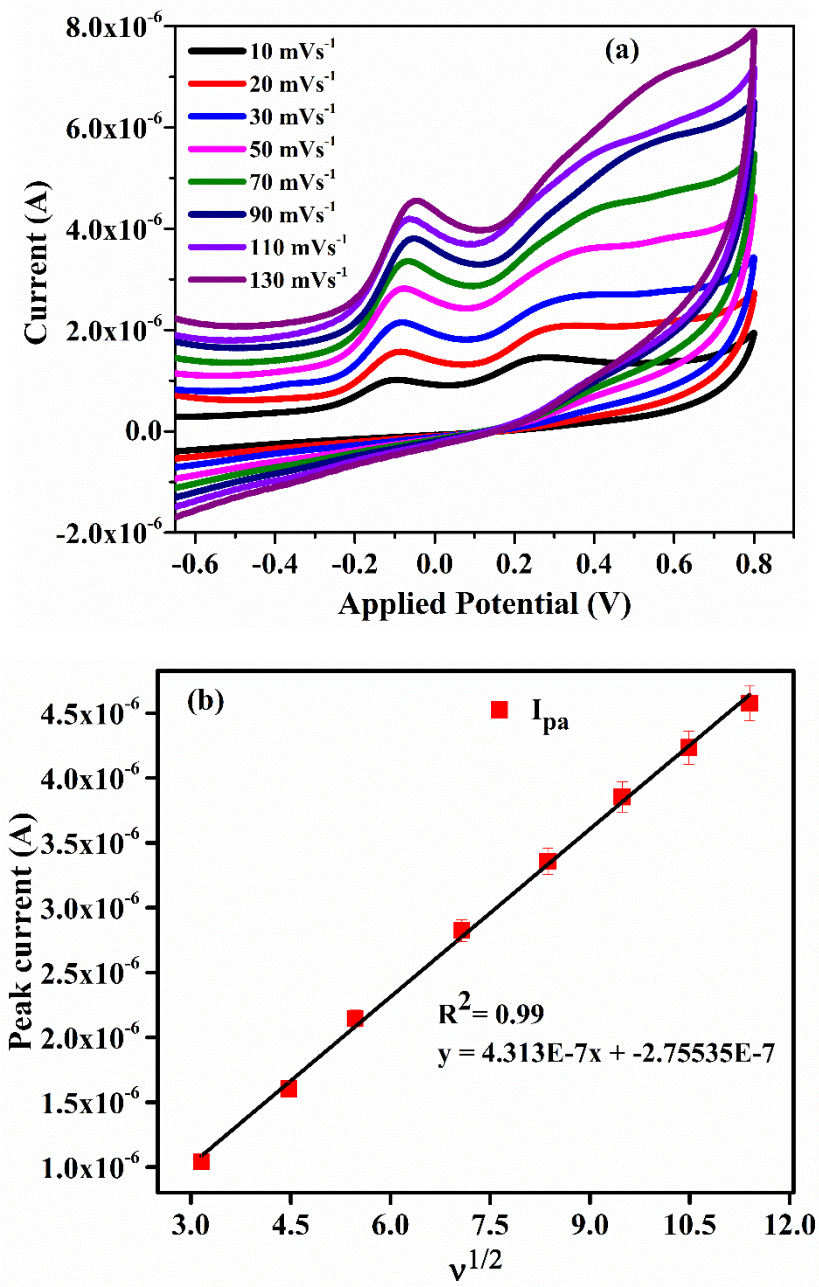

Fig.4.2.2: (a) Cyclic voltammograms of IFE at different scan rates. (b) Calibration plots showing variation of anodic peak current with square root of scan rate (GC as working electrode, Ag/Ag^{+} as reference electrode and TBHP as supporting electrolyte)

As a result of complexation, lone pair on the amine nitrogen would coordinate with the metal ion and does not remain available for any anodic peak. On studying the voltammogram of IFE with each metal ion of the selected group, the peak in anodic region of CV was quenched completely in existence of Fe (II) ions as shown in Fig. 4.2.3, whereas, with most of other metal ions the anodic peaks are still observed clearly, indicating selective complexation of IFE with Fe(II).

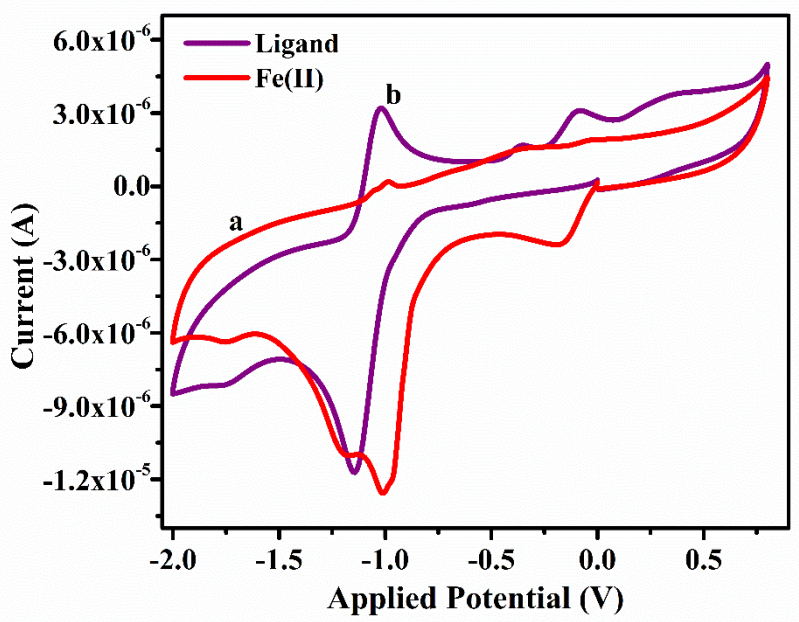

Fig. 4.2.3: Cyclic voltammogram of (a) IFE (5×10^{-4} mol/L) alone (b) IFE (5×10^{-4} mol/L) and Fe(II) (10^{-3} mol/L) at glassy carbon electrode in DMSO, 0.1 mol/L TBHP, scan rate: 50mVs^{-1}

Voltammetric study of IFE in presence of some transition metal ions

Differential pulse voltammograms of IFE were drawn separately with each transition metal ion like K^+, Mg^{2+}, Ca^{2+}, Cr^{3+}, Fe^{3+}, Fe^{2+}, Co^{2+}, Ni^{2+}, Cu^{2+}, Zn^{2+}, Ag^+, Hg^{2+} and Pb^{2+}. As seen from Fig. 4.2.4 there is no major shift in the anodic peak of IFE at -1.0 V with all the tested metal species except with Fe(II), for which the ligand shows new peaks at -0.2 V and -1.0 V. This is a unique observation in DPV plots as well, which indicates a strong complexing ability of IFE with Fe(II). The experiment of ligand complexation was repeated at least 5 times to confirm the observation.

Titration curve of IFE

In order to confirm application potential of the ligand and its kinetic response to the electrode, differential pulse voltammograms were recorded on successive additions of small amounts of Fe(II) to carry out voltammetric titration of IFE with Fe(II) (Fig. 4.2.5). It was observed that on each addition of the titrant volume, a spontaneous increase in current was noticed. The cathodic current stabilized after increasing linearly until the metal-ligand ratio reached 1:1. No further increase in current was noticed indicating 1:1 stoichiometry of the complex with the fast and efficient response of the electrode without any lag in applied potential. Further studies on the compound were carried out to seek its quantitative application by using standard calibration method. DPV of IFE were recorded with different concentrations of Fe(II).

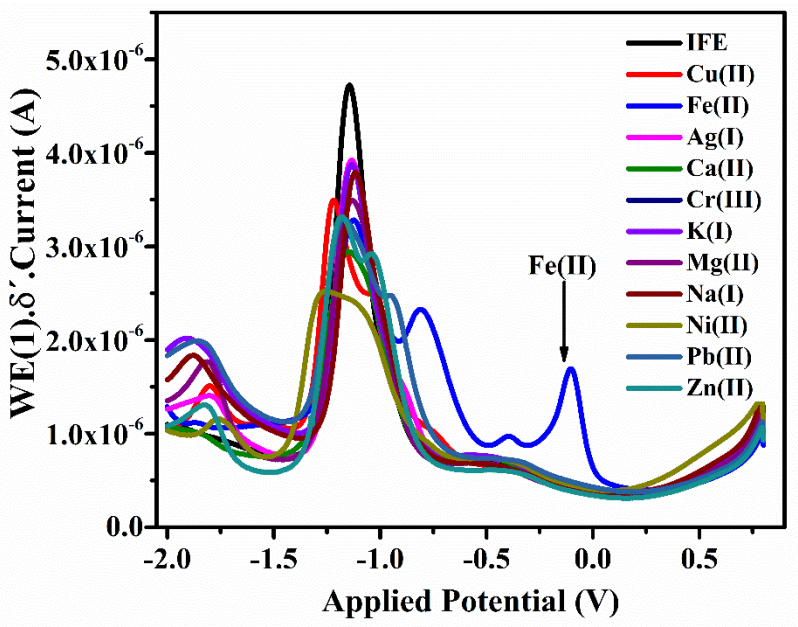

Fig. 4.2.4: Differential pulse voltammogram of IFE in the existence of different metal ions

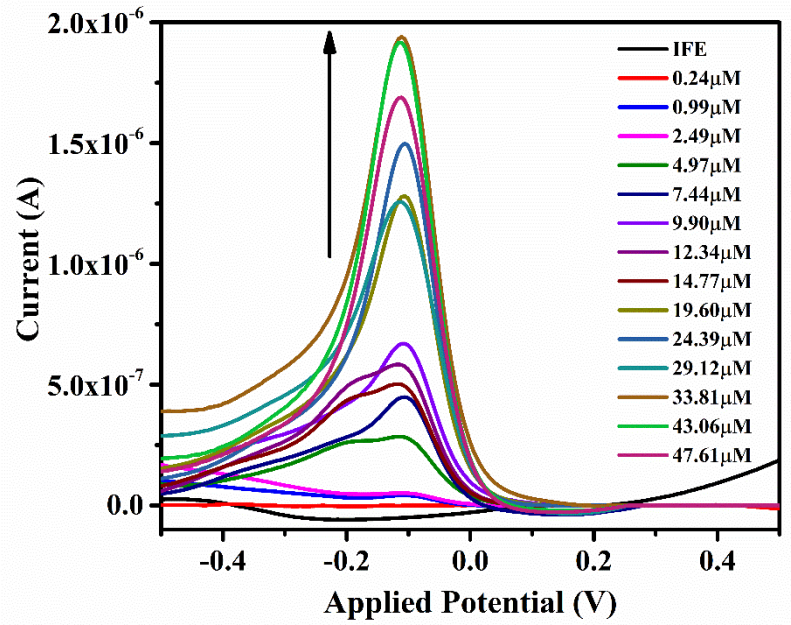

Fig. 4.2.5: Cathodic DPV of IFE (5.0×10^{-4} mol/L) in the presence of increasing amount of Fe (II) ions in DMSO; electrolyte 0.1 mol/L TBHP; Pulse amplitude of 0.05 V; scan rate 0.05 Vs^{-1} within potential range of 0.50 – -0.50 V vs. Ag/Ag^{+}

The plots of current magnitude plotted against different concentrations of Fe (II) are shown in Fig. 4.2.6. The calibration curve is a straight line with a slope of 6.57×10^{-8} mol/L and a standard deviation of 1.85×10^{-9} mol/L. Although, another new peak was observed in presence of Fe(II) at -0.8 V but the peak at -0.1 V was selected for quantitative applications because of its well-defined shape. It has been noted that the

current magnitude increased linearly with the concentration of metal ion. A good linearity was found in the concentration range of 9.9×10^{-7} mol/L – 2.9×10^{-5} mol/L Fe(II) with a correlation coefficient of 0.99. A deviation from linearity occurred at a concentration higher than 2.9×10^{-5} mol/L due to saturation at the electrode surface and detection limit of IFE was estimated as 6.13×10^{-8} mol/L.

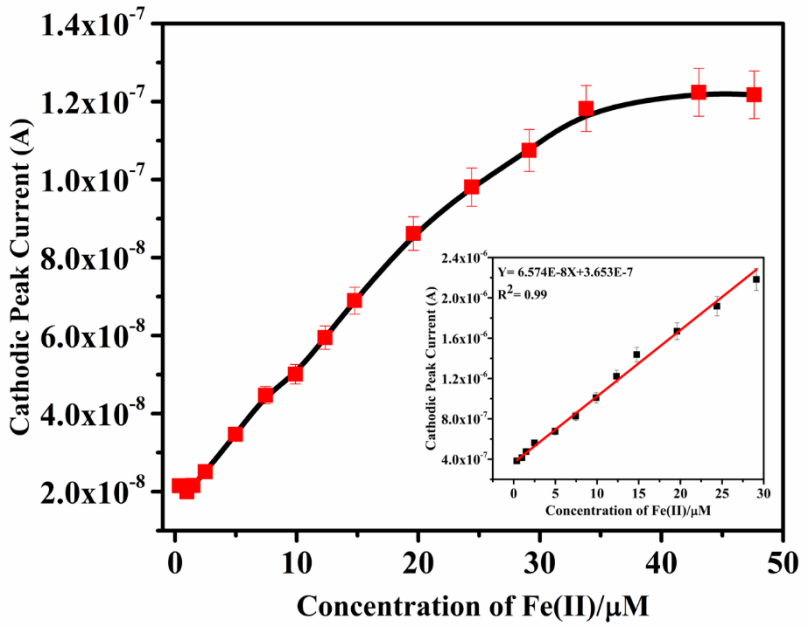

Fig. 4.2.6: Calibration plots between concentration and corresponding current for IFE in electrolyte TBAP (0.1 mol/L), pulse amplitude of 0.05 V; scan rate 0.05 Vs^{-1} vs. Ag/Ag^{+}

Comparison study

The IFE voltammetric sensor shows better selectivity, wide linear range and lower detection limit as compared to the earlier reported electrodes for iron ions as shown in Table 4.2.1.[20-24]

Table 4.1.4 Comparison of the IFE voltammetric electrode with the previously reported Fe (II) selective electrodes

Ionophore	Electrode	Detection Technique	Detection Limit (mol/L)	Ref.
Dimethyliminocinnamyl linked rhodamine (rhodamine-dimethyliminocinnamyl) (RC)	Platinum Electrode	Voltammetry	1.6×10^{-7}	[20]
Iron polysaccharidic complexes.	HDME[a]	Voltammetry	2.7×10^{-6}	[21]
1,10-phenanthroline, 2,2'-dipyridyl	Sol-Gel Electrode	Voltammetry	4.0×10^{-6}	[22]

2-((E)-(4-((E)-4-((E)-2-hydroxy-5-nitrobenzylideneamino) benzyl)phenylimino)methyl)-4-nitrophenol	Screen Printed Electrode	Voltammetry	5.4×10^{-7}	[23]
poly(3,4-ethylenedioxythiophene) polystyrenesulfonate	Glassy Carbon Electrode	Voltammetry	0.2×10^{-7}	[24]
(E)-3-((2-aminoethylimino)methyl)-4H-chromen-4-one (IFE)	**Glassy Carbon Electrode**	**Voltammetry**	**6.13×10^{-8}**	**This work**

[a] HDME= Hanging Dropping Mercury Electrode

4.2.3.2 Discussion on voltammetric studies of ICU

Cyclic voltammetry (CV) and differential pulse voltammetry (DPV) for the identification of Cu(II) ions via glassy carbon as working electrode were explored in electrochemical behaviour of ICU (5 to 10-4 M) in 0.1 M TBHP/DMSO solution with a scan rate of 50 mVs^{-1}. ICU exhibited one anodic peak at -0.055 V and one cathodic peak at -1.779 V vs having different current magnitudes within the potential range of 0.5 V to -2.0 V Ag/Ag^{+}. From the graph it is clear (Fig. 4.2.7) that in the first cycle from positive to a negative potential, cathodic peak was detected which could be assigned to the reduction of chromen ring, which might got oxidized in the anodic scan. It is interesting to note that after the first cycle of the voltammogram the cathodic peak disappeared in the second scan. It might be due to the reason that no site on the molecule was available for reduction; rather oxidized product (after oxidation of lone pair on N atom of amine group) of the first cycle was reduced in the cathodic cycle.

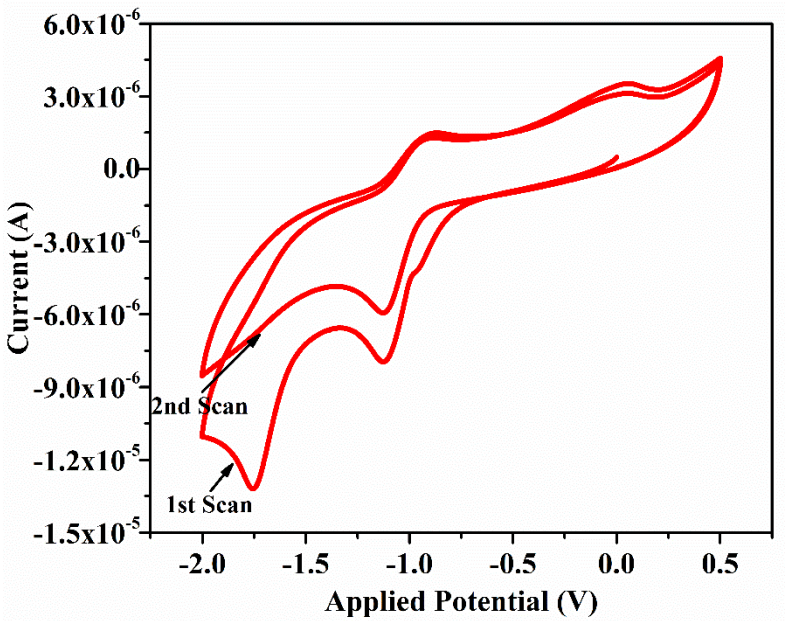

Fig. 4.2.7: Cyclic voltammogram of ICU (5×10^{-4} M) at glassy carbon electrode in DMSO, 0.1 M TBHP. Scan rate: 50mVs^{-1}

Effect of scan rate on peak current

Cyclic voltammograms for ICU have been plotted at different scan rates in the range 10 mVs^{-1} to 130 mVs^{-1} in Fig. 4.2.8 (a). The peak current value of the cathodic peak at -1.15 V is increasing with increasing scan rate, which is also observed in the plots of square root of scan rate ($v^{1/2}$) vs current magnitude. The results indicate that both cathodic and anodic peak current responses are directly related to the square root of a scan rate. It shows that the process of mass transfer on the electrode surface is controlled by the diffusion. Scan rate study can also explain timescale of the experiment. Higher ν value corresponds to shorter timescale, i.e. diffusion- controlled current increased over that for smaller ν value (longer timescale). That is because of increase in the amount of the analyte and concentration gradient to the electrode surface with increasing ν value. Fig. 4.2.8 shows the relationship that is often used by surface-bound or adsorbed redox species to demonstrate the diffusion control of the current.

Metal ion selectivity

To evaluate complexation behaviour of the receptor compound ICU, DPV measurements were carried out upon accumulation of numerous analytes into the solution. Since the peaks were sharper and well-defined using differential pulse voltammetry (DPV) rather than cyclic voltammetry (CV),[25] most of the voltammetric studies were done using differential pulse voltammetry. Fig. 4.2.9 shows the change in current magnitude in DPV after adding 100 µL (10^{-2} M) each of different metal ions such as K^+, Mg^{2+}, Ca^{2+}, Cr^{3+}, Fe^{3+}, Fe^{2+} , Co^{2+}, Ni^{2+}, Cu^{2+}, Zn^{2+}, Ag^+, Hg^{2+} and Pb^{2+} into 2 mL solution of ICU (5×10^{-4} M) in DMSO medium. It was observed that Cu (II) addition shows a sharp change in the DPV, as a new peak appeared at -0.319 V along with the peak at -1.779 V for the ICU ionophore. Metal ions other than copper (II) showed no shift in the peak potential value. In addition, no new peak was observed. From this voltammetric behaviour of ICU, it can be decided that ICU is selective to Cu(II) ions and can be utilized as Cu(II) ion detection in the DMSO medium.

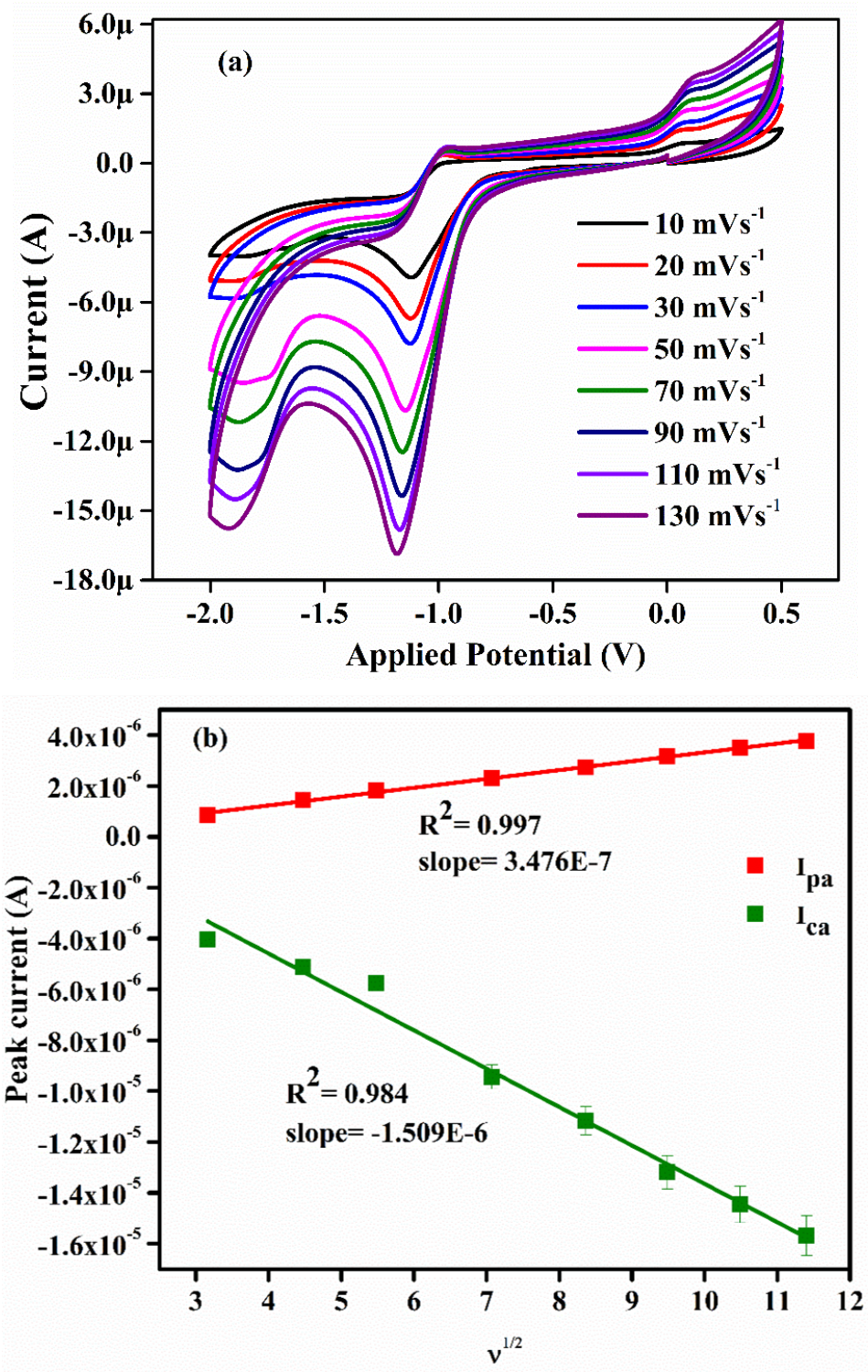

Fig. 4.2.8: (a) Cyclic voltammograms of ICU at different scan rates. (b) Calibration plot showing the variation of peak current with square root of scan rate (GC as working electrode, Ag/Ag^{+} as reference electrode and TBHP as supporting electrolyte)

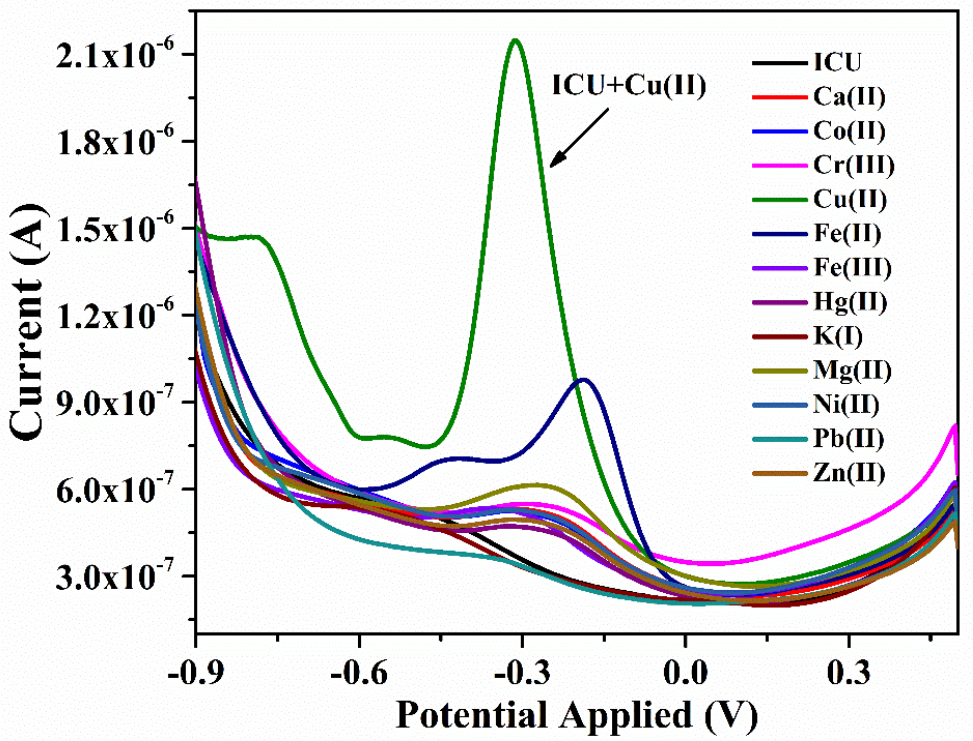

Fig. 4.2.9: Differential pulse voltammograms of ICU in the presence of different metal ions

Copper (II) complexes

To confirm the selectivity and binding ability of ICU towards Cu^{2+}, titrations were carried out using differential pulse voltammetry (Fig. 4.2.10). Two well-defined cathodic peaks I and II were formed at -0.333 V and -0.686 V due to reduction of imine bond, (-C=N-) of the ionophore and -C=O of the chromen ring. In order to achieve complexation with receptor (ICU) molecule, the suggested voltammetric sensor requires more than 1.0 equivalents Cu (II) ions. At -0.049 V, the current intensity of the anodic peak decreased with increase in concentration from 49 µM to 654 µM while a new anodic peak developed at -0,51 V due to the development of the metal-ligand complex. Linear correlation was obtained between the peak height and the Cu (II) molar concentration of the samples in the range of 2.49 µM – 430 µM, a plateau being reached for concentrations greater than 476 µM as shown in Fig. 4.2.11 and exhibit detection limit of 9.32 nM.

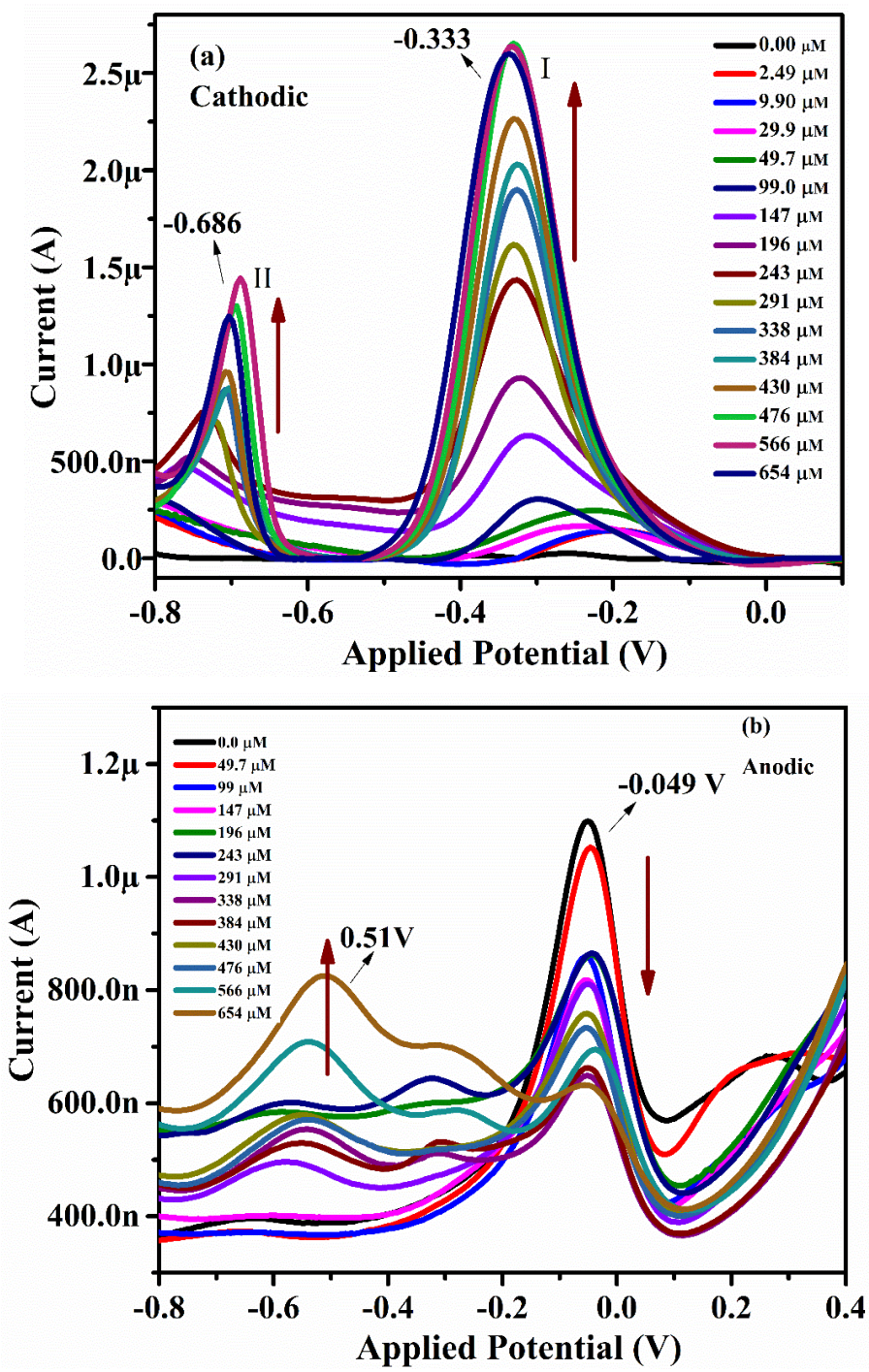

Fig. 4.2.10: (a) Cathodic DPV of ICU (5.0×10^{-4} M) (a) Cathodic (b) Anodic DPV of ICU in the presence of increasing amount of Cu (II) ions in DMSO; electrolyte 0.1 M TBHP; Pulse amplitude of 0.05 V; scan rate 0.05 Vs^{-1} with in potential range of 0.50 – -0.80 V vs. Ag/Ag^{+}

Comparison study

The performance characteristics of proposed electrodes were compared with previously reported electrodes for the determination of Cu(II) and are summarized in Table 4.2.2.[26-30]

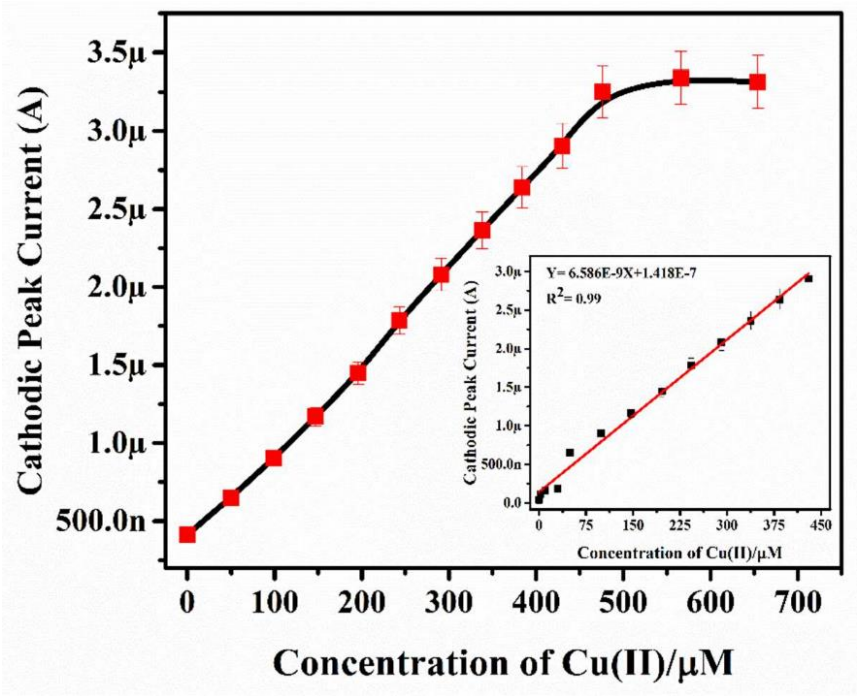

Fig. 4.2.11: Calibration plots between concentration and cathodic current for ICU in TBAP (0.1 M) electrolyte, pulse amplitude of 0.05 V; scan rate 0.05 Vs^{-1} vs Ag/Ag^{+}

Table 4.2.2 Comparison of the ICU voltammetric electrode with the previously reported Cu (II) selective electrodes

Ionohore	**Electrode**	**Detection Technique**	**Detection Limit (M)**	**Ref.**
Maize tassel	Carbon paste electrode	Voltammetry	1.3×10^{-7}	[26]
N,N'-bis(acetylacetone) ethylenediimine	Glassy Carbon electrode	Voltammetry	1.0×10^{-5}	[27]
zeolite NH4-Y	zeolite Y-MWCNT/GCE	Square Wave Voltammetry	1.12×10^{-8}	[28]
Biochar samples	Carbon Paste Electrode	DPADSV[a]	4.0×10^{-7}	[29]
1-butyl-3-methyl-imidazole hexafluorophosphate	Carbon Paste Electrode	DPV[b]	6.6×10^{-7}	[30]
(E)-3-(((2-((2 aminoethyl) amino) ethyl) imino) methyl)-4H-chromen-4-one (ICU)	**Glassy Carbon Electrode**	**Voltammetry**	**9.3×10^{-9}**	**This work**

[a] DPADSV = Differential Pulse Adsorptive Stripping Voltammetry
[b] DPV = Differential Pulse Voltammetry

4.2.3.3 Discussion on voltammetric studies of IFE(III)

The purpose of voltammetric experiments was to investigate redox behaviour of IFE(III) in DMSO medium using TBHP as supporting electrolyte in the applied potential range 1.0 V to -2.0 V at a scan rate of 50 mV/s. IFE(III) exhibits an irreversible peak with a cathodic reduction peak at -1.73 V corresponding to the one-electron reduction process, which arises from the reduction of imine group -CH=N- to amine -CH_2-NH-. As the potential is scanned to 1.0 V, two anodic peaks were observed at 0.12 and 0.60 V, respectively due to oxygen atom of pyran ring and N atom of amine group. In addition, a strong peak at -1.1 V was observed due to supporting electrolyte. (Fig. 4.2.12).

Effect of scan rate on voltammetric measurement

Cyclic voltammetric curve of IFE(III) in DMSO medium at different scan rates from 10 mVs^{-1} to 150 mVs^{-1} are shown in Fig. 4.2.13 (a). Scan rate studies were carried out in order to confirm whether the mass transfer at the working electrode process was diffusion or absorption-controlled. At high scan rate, anodic as well as cathodic peak currents indicate a linear relationship with the square root of scan rate which reveals that the mass transfer taking place at the electrode surface is a diffusion-controlled process (Fig. 4.2.13 (b)).

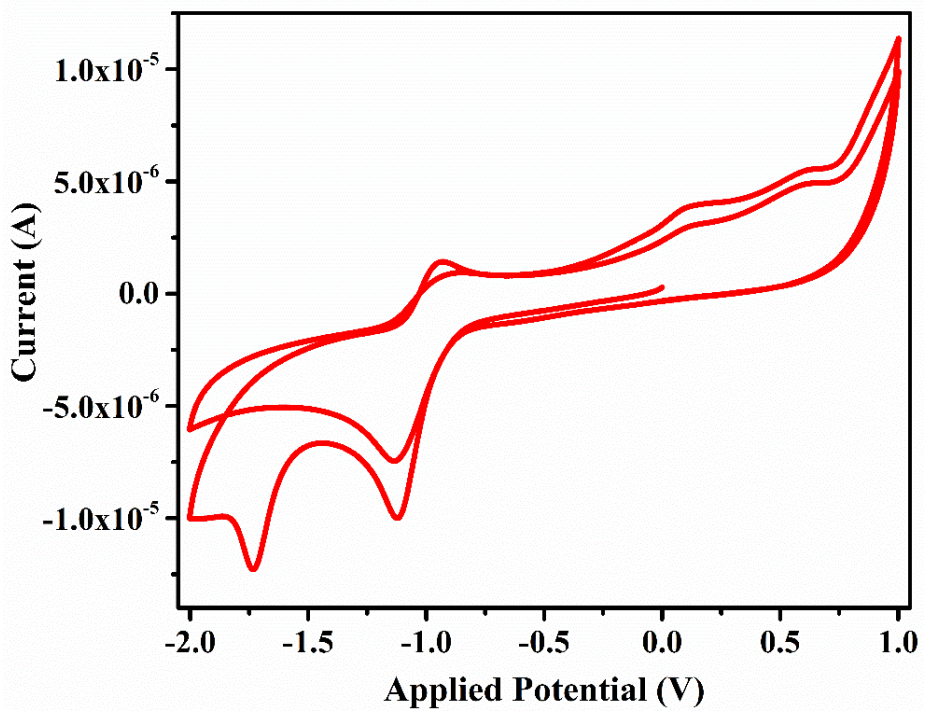

Fig. 4.2.12: Cyclic voltammograms of IFE(III) (5×10^{-4} mol/L) at glassy carbon electrode in DMSO, 0.1 mol/L TBHP, Scan rate: 50 m Vs^{-1}

Complexation of IFE(III) with metal ions

The ionophore (E)-3-((2-(2-(2-aminoethylamino)ethylamino)ethylimino)methyl)-4H-chromen-4-one (IFE(III)) with two oxygen atoms and four nitrogen atoms of the Schiff base is insoluble in aqueous medium. Therefore, complexation of the ionophore with metal ions was studied in DMSO medium. During metal-ligand interactions only electronic factor seems to be playing a part as the DFT studies indicate metal bonding to only two heteroatoms on one side of the plane while the other side remains open. Moreover, the possibility of another molecule of IFE(III) joining from the backside of the metal is also ruled out as the Job's plot indicate 1:1 stoichiometry between the metal and ligand. Now, the question of preference of the ionophores IFE, ICU, and IFE(III) for Fe(II), Cu(II) and Fe(III), respectively has to be answered only on the basis of electronic character of the guest metal ion. As per the HSAB concept of Ahrland et al.,[31] the less electropositive metal ions like Fe(II), Fe(III) and Cu(II) would preferably bind with soft bases like O in preference to N, which is a hard base. Moreover, binding of transition metals is encouraged in the given series of receptor molecules due to the availability of empty π-bonding orbitals of imine and carbonyl double bonds. Hence, in general, the conjugated environment of double bonds of the IFE, ICU, and IFE(III) compounds encourage electrostatic bonding with elements of first transition series (second half) due to the possibility of accommodating electron from the metal atom to the ligand (back bonding). Regarding relative preference of the given series of receptors IFE, ICU and IFE(III), respectively for Fe(II), Cu(II) and Fe(III), the most important factor is the electronic environment rather than the steric one, since the receptor molecules are podands and there are no strict constraints of space.

The three receptors do not differ much in their electronic environment around the pseudo cavity near imine and carbonyl groups, as the hydrocarbon chain with imine linkage is not in conjugation. Hence, the selective behaviour of the receptor molecules IFE, ICU and IFE(III) is decided by the guest species.

The receptor IFE(III) preferably binds with Fe(III) (Fig. 4.2.14) as it generates more cathodic current than the other two metal ions (Cu(II) and Fe(II)) which is most electropositive of all the metal ion species as guest ions. Secondly, the two amine N atoms are likely to converge over the Fe(III) guest ion from the back side. Electronically, Fe(III) would also offer vacant e_g orbitals facilitating the coordination of Fe(III) with lone pairs on the N atoms and an oxygen atom of the carbonyl group.

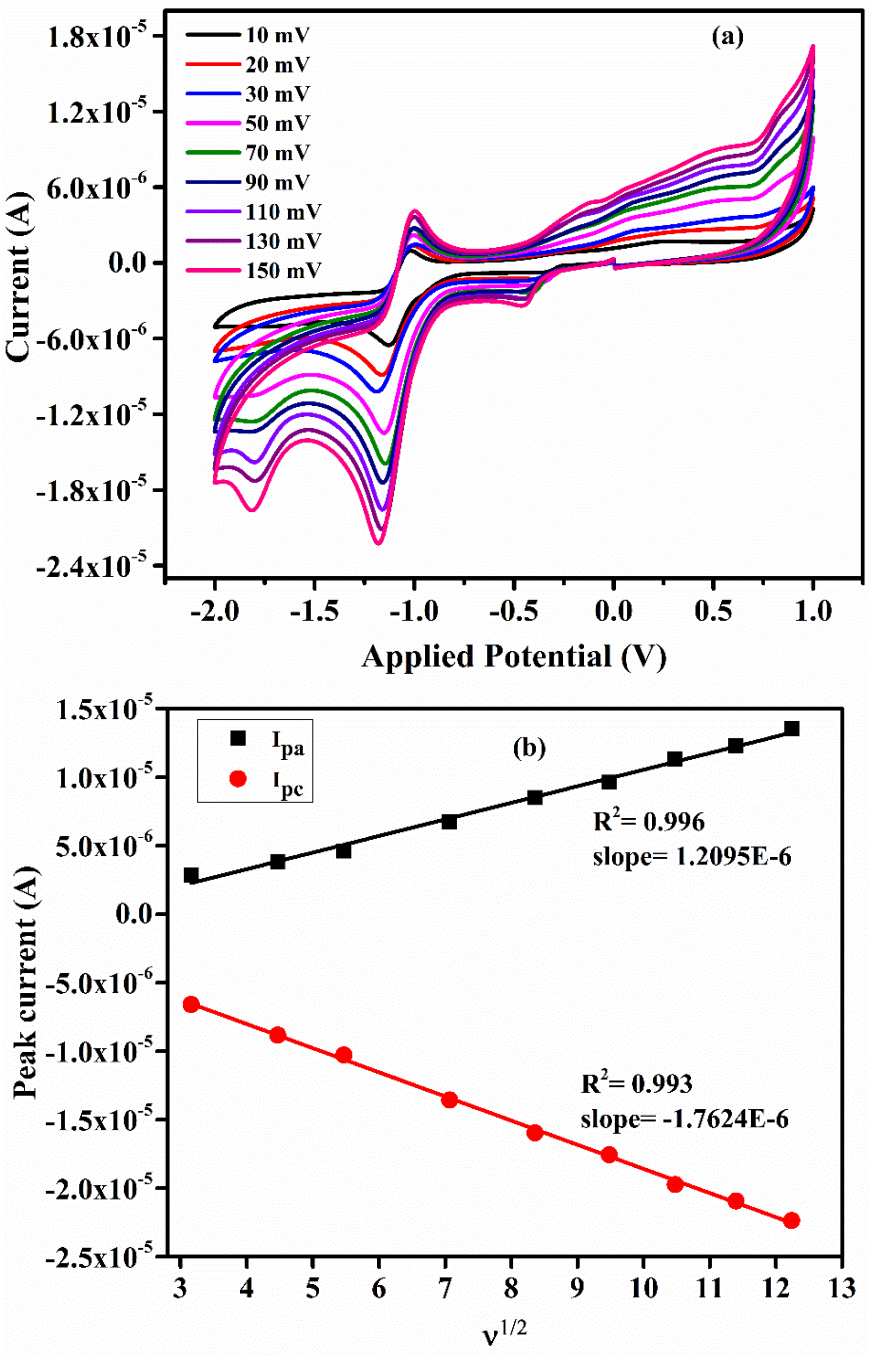

Fig. 4.2.13: (a) Cyclic voltammograms of IFE(III) at different scan rates. (b) Calibration plot showing the variation of peak current with square root of scan rate (GC as working electrode, Ag/Ag^+ as reference electrode and TBHP as supporting electrolyte)

The receptor IFE(III) also binds with Cu(II) and Fe(II) with lower cathodic peak current height in that order (Fig. 4.2.14). The position of cathodic peak maxima for all the three guest metal ions Fe(III), Cu(II) and Fe(II) are related to their respective cathodic peak potentials.

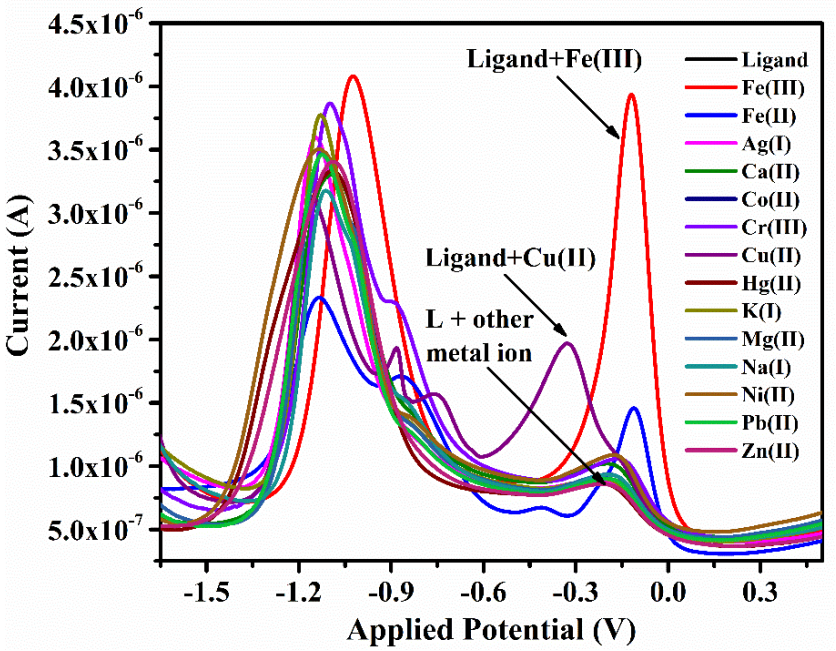

Fig. 4.2.14: Cathodic differential pulse voltammograms of IFE(III) in the presence of different metal ions

Calibration curve for Fe(III) ion determination

In order to use IFE(III) as a voltammetric sensor for Fe(III) ions, differential pulse voltammograms of IFE(III) were recorded after successive additions of a calculated amount of Fe(III) ions in the concentration range 0.0 to 53.6 µM in about 20 steps. It can be seen from Fig. 4.2.15 that peak current intensity of the cathodic peak potential at -0.9 V increased simultaneously, with successive addition of the peak current values. There was building up of a new peak at -0.15 V which gradually reaches to a maxima at 41.5 µM concentration of the guest Fe^{3+} ions. On further addition of Fe^{3+} solution, there was no further increase in the current, indicating a 1:1 stoichiometry of the IFE(III)-Fe^{3+} complex. Taking into consideration the intensity of cathodic peak current at -0.15 V, a calibration curve was plotted (Fig. 4.2.16) against concentration of the Fe(III) ion added to the solution. The calibration curve shows good correlation coefficient (0.96) between the relative peak current and concentration of Fe(III) in the range of 16.3-44.5 µM. The limit of detection of the proposed voltammetric sensor was observed as 5.2×10^{-8} mol/L for the Fe(III) determination.

Comparison study

In table 4.2.3, we compare some recent electrochemical sensor in Fe^{3+} detection. It should be noted that proposed sensors show relatively better selectivity, lower detection limit

and wide concentration range as compared to the previously reported methods for the determination of Fe(III).[24,32-36]

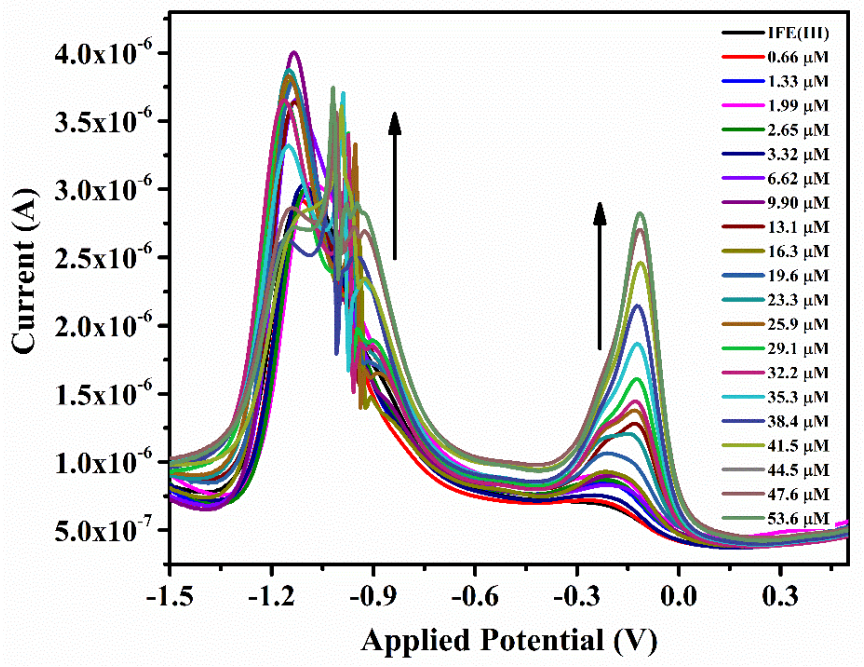

Fig. 4.2.15: Cathodic DPV of IFE(III) (5.0×10^{-4} mol/L) in the presence of increasing amount of Fe (III) ions in DMSO; electrolyte TBHP (0.1 mol/L); Pulse amplitude of 0.05 V; scan rate 0.05 Vs^{-1} within potential range of 0.50 – -0.50 V vs. Ag/Ag^{+}

Table 4.2.3 Comparison of the IFE(III) voltammetric electrode with the previously reported Fe (III) selective electrodes

Ionophore	Electrode	Detection Technique	Detection Limit (mol/L)	Ref.
Carbon nanodots	SPCE[a]	Voltammetry	7.9×10^{-5}	[32]
Ferrocene appended quinoline-triazole(FAQT) derivative	Platinum	Voltammetry	2.3×10^{-7}	[33]
Ruthenium oxide hexacyanoferrate film (RuOHCF/CFM).	CFM[b]	Amperometry	2.2×10^{-7}	[34]
PPY/PEDOT-S composite	Glassy Carbon	Amperometry	8.0×10^{-7}	[35]
poly(3,4-ethylenedioxythiophene) polystyrenesulfonate	Glassy Carbon	Voltammetry	1.0×10^{-7}	[24]
4-(2,4-Dinitrophenoxy)-3-methoxybenzaldehyde	Glassy Carbon	Voltammetry	4.2×10^{-4}	[36]

(E)-3-((2-(2-(2-aminoethylamino)ethylamino)ethylimino)methyl)-4H-chromen-4-one (IFE-III),	**Glassy Carbon Electrode**	**Voltammetry**	**5.2×10^{-8}**	**This work**

[a] SPCE = Screen Printed Carbon Electrode
[b] CFM = Carbon Fiber Microelectrode

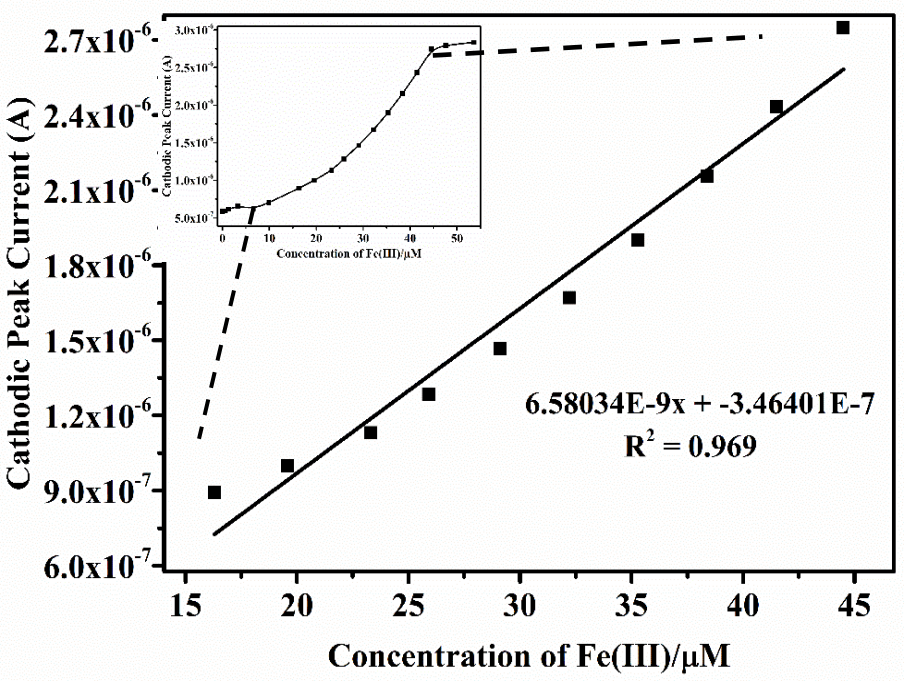

Fig. 4.2.16: Calibration plots between concentration of Fe(III) and corresponding peak current for IFE(III) in electrolyte TBAP (0.1 mol/L), pulse amplitude of 0.05 V; scan rate 0.05 Vs^{-1} vs. Ag/Ag^{+}

4.2.4 Conclusions

In this work, voltammetric characterization of compounds (IFE, ICU and IFE(III)) are described and their binding ability with metal ions such as Fe(II), Cu(II) and Fe(III) were determined by voltammetric measurements without any major interference from other various metal ions. The proposed voltammetric sensors have many advantages such as low cost, easy preparation, wide concentration range and good detection limits.

References

(1) Fisher, N. S.; Jones, G. J.; Nelson, D. M. *Journal of Experimental Marine Biology and Ecology* **1981**, *51*, 37-56.

(2) Xiang, C.; Oliver, D. J. *The Plant Cell* **1998**, *10*, 1539-1550.

(3) Jaishankar, M.; Tseten, T.; Anbalagan, N.; Mathew, B. B.; Beeregowda, K. N. *Interdisciplinary Toxicology* **2014**, *7*, 60-72.

(4) Martin, S.; Griswold, W. *Environmental Science and Technology Briefs for Citizens* **2009**, *15*, 1-6.

(5) Sharma, R. K.; Agrawal, M. *Journal of Environmental Biology* **2005**, *26*, 301-313.

(6) Duruibe, J. O.; Ogwuegbu, M.; Egwurugwu, J. *International Journal of Physical Sciences* **2007**, *2*, 112-118.

(7) Yi, Y.; Yang, Z.; Zhang, S. *Environmental Pollution* **2011**, *159*, 2575-2585.

(8) Willis, J. *Analytical Chemistry* **1962**, *34*, 614-617.

(9) Tüzen, M. *Microchemical Journal* **2003**, *74*, 289-297.

(10) Moor, C.; Lymberopoulou, T.; Dietrich, V. J. *Microchimica Acta* **2001**, *136*, 123-128.

(11) Dai, B.; Cao, M.; Fang, G.; Liu, B.; Dong, X.; Pan, M.; Wang, S. *Journal of Hazardous Materials* **2012**, *219*, 103-110.

(12) Vuković, J.; Matsuoka, S.; Yoshimura, K.; Grdinić, V.; Grubešić, R. J.; Županić, O. *Talanta* **2007**, *71*, 2085-2091.

(13) Medinilla, J.; Ales, F.; Sanchez, F. G. *Talanta* **1986**, *33*, 329-334.

(14) Wen, X.; Yang, Q.; Yan, Z.; Deng, Q. *Microchemical Journal* **2011**, *97*, 249-254.

(15) Jain, R.; Gupta, V. K.; Jadon, N.; Radhapyari, K. *Analytical Biochemistry* **2010**, *407*, 79-88.

(16) Kissinger, P. T.; Heineman, W. R. *Journal of Chemical Education* **1983**, *60*, 702.

(17) Compton, R. G.; Banks, C. E. *Understanding Voltammetry*; World Scientific, 2011.

(18) Mabbott, G. A. *Journal of Chemical Education* **1983**, *60*, 697.

(19) Nicholson, R. S. *Analytical Chemistry* **1965**, *37*, 1351-1355.

(20) Kamal, A.; Kumar, N.; Bhalla, V.; Kumar, M.; Mahajan, R. K. *Sensors and Actuators B: Chemical* **2014**, *190*, 127-133.

(21) Merli, D.; Profumo, A.; Dossi, C. *Journal of Pharmaceutical Analysis* **2012**, *2*, 450-453.

(22) Stozhko, N. Y.; Morosanova, E.; Kolyadina, L.; Azarova, Z. M. *Journal of Analytical Chemistry* **2004**, *59*, 865-870.

(23) Rana, S.; Mittal, S. K.; Kaur, N.; Banks, C. E. *Sensors and Actuators B: Chemical* **2017**, *249*, 467-477.

(24) Sundramoorthy, A. K.; Premkumar, B. S.; Gunasekaran, S. *ACS Sensors* **2016**, *1*, 151-157.

(25) Bard, A. J.; Faulkner, L. R.; Leddy, J.; Zoski, C. G. *Electrochemical Methods: Fundamentals and Applications*; Wiley New York, 1980; Vol. 2.

(26) Moyo, M.; Okonkwo, J. O.; Agyei, N. M. *Environmental Monitoring and Assessment* **2014**, *186*, 4807-4817.

(27) Feier, B.; Băjan, I.; Fizeșan, I.; Floner, D.; Cristea, C.; Geneste, F.; Săndulescu, R.; Hatieganu, I. *International Journal of Electrochemical Science* **2015**, *10*, 121-139.

(28) Senthilkumar, S.; Saraswathi, R. *Journal of Applied Electrochemistry* **2011**, *41*, 909-917.

(29) Oliveira, P. R.; Lamy-Mendes, A. C.; Rezende, E. I. P.; Mangrich, A. S.; Junior, L. H. M.; Bergamini, M. F. *Food Chemistry* **2015**, *171*, 426-431.

(30) Liu, R.; Lei, C.; Zhong, T.; Long, L.; Wu, Z.; Huan, S.; Zhang, Q. *Analytical Methods* **2016**, *8*, 1120-1126.

(31) Ahrland, S.; Chatt, J.; Davies, N. *Quarterly Reviews, Chemical Society* **1958**, *12*, 265-276.

(32) Tan, S. C.; Chin, S. F.; Pang, S. C. *Journal of Sensors* **2017**, *2017*.

(33) Kamal, A.; Kumar, S.; Kumar, V.; Mahajan, R. K. *Sensors and Actuators B: Chemical* **2015**, *221*, 370-378.

(34) Peña, R. C.; de Souza, A. P. R.; Bertotti, M. *Journal of Electroanalytical Chemistry* **2014**, *731*, 49-52.

(35) Sobkowiak, M.; Gabrielsson, R.; Inganäs, O.; Milczarek, G. *Synthetic Metals* **2014**, *194*, 170-175.

(36) Sharma, R.; Chhibber, M.; Mittal, S. K. *RSC Advances* **2015**, *5*, 21831-21842.

4.3 Schiff base ionophores as optical sensors for metal ions

Abstract

Schiff base complexes of Fe(II), Cu(II) and Fe(III) with (E)-3-((2-aminoethylimino)methyl)-4H-chromen-4-one (IFE), (E)-3-(((2-((2 aminoethyl) amino) ethyl) imino) methyl)-4H-chromen-4-one (ICU) and (E)-3-((2-(2-(2-aminoethylamino) ethylamino) ethylimino)methyl)-4H-chromen-4-one (IFE(III)), respectively have been characterized by UV-Visible spectroscopy for their binding stoichiometry through Job's plot method.

4.3.1 Introduction

Schiff base ligands are used as essential measuring system for optical and electrochemical sensors in many analytical devices.[1-6] Schiff bases are well known compounds for their strong coordinating ability with the transition metal ions.[7-10] Schiff bases containing N, O and S donor atoms produce most stable transition complexes and possess interesting physiological properties such as antibacterial, antifungal, anticancer and diuretic activities.[11-14] Schiff base compounds have wide applications in analytical chemistry, coordination chemistry, food industry, agriculture and medicinal industry.[15-20] In a preliminary spectrophotometric study, experiments were carried out with Schiff base ionophores on UV-vis spectrophotometer to know the interaction of molecules with the transition metal ions. The detectable changes in the UV-Vis spectra indicate the formation of ionophore-metal complex. The complexation ability of the ionophores was examined in DMSO medium. After the confirmation, it was decided to incorporate the target metal ions into PVC membrane electrode by equilibration in aqueous medium. The binding stoichiometry for ICU, IFE, and IFE(III) with respective target metal ions was confirmed with Job's plot method. The Job's function A_{Job} is calculated according to the equation $A_{Job}= (1-X)A_0-A$.

4.3.2 Experimental

Experiments in UV-Visible experiments were conducted with standard stock solutions of ligands (1.0×10^{-3} mol/L) and target metal ions (1.0×10^{-2} mol/L) by dissolving suitable and accurately weighed pure solid compounds (with an precision of 0.1 mg) in conventional calibrated volumetric flasks and diluted with acetonitrile to 25.0 mL. For the UV-Visible studies working solutions of different concentrations were prepared by serial dilution of stock solutions. Using a pre-calibrated micropipette, the metal ion detection of ligand solutions was carried out according to UV-Visible spectrum as

illustrated in Figs 4.3.1-4.3.3, by adding a quantity of the microliter of the concentrated standard solution of metal ions (1.0×10^{-2} mol/L) in DMSO medium.

4.3.3 Ion recognition studies of IFE, ICU and IFE(III)

The relationship between IFE, ICU and IFE(III) and different metal ions like Cu^{2+}, Ag^{+}, Fe^{3+}, Cd^{2+}, Co^{2+}, Cr^{3+}, K^{+}, Mg^{2+}, Ca^{2+}, Ni^{2+}, Zn^{2+} and Fe^{2+} was investigated through UV-Vis spectroscopy. To investigate the absorbance of IFE, ICU and IFE(III) for different metal ions UV visible studies were carried out in the absence and presence of these cations. All the experiments were carried out in DMSO medium. The absorption spectra of the ligands and their respective complexes were recorded over the wavelength range of 200-700 nm. As seen from Fig. 4.3.1-4.3.3, the major absorption band for IFE (Fig. 4.3.1), ICU (Fig. 4.3.2) and IFE(III) (Fig. 4.3.3) was observed at 295, 315 and 320 nm due to $\pi \rightarrow \pi^*$ transitions due to aromatic ring present in the molecules.

A UV-Visible spectra of IFE-Fe(II) complex upon addition of 20 equivalents of Fe(II) ion showed an increase in the intensity of absorption band at 295 nm while a new band appeared at 360 and 395 nm due to complexation of IFE with Fe(II) ions. However, no significant changes were detected with all the other metal ions. In case of ICU, upon addition of 20 equivalents of Cu(II) to the ligand solution, a small shoulder appeared at 350 nm with simultaneous increase in the intensity of the peak at 314 nm. Appearance of new band and other changes in the spectra indicate the formation of ICU-Cu(II) complex. Interference studies were carried out in the presence of all the other metal ions and no visible changes were observed. Similarly, complexation studies were carried out with IFE(III) receptor on UV-Visible spectrophotometer. A new band appeared at 414 nm in the UV-Visible spectrum along with enhancement of 320 nm band due to complexation of Fe(III) with IFE(III) molecule. Experiments with all the other metal ions did not show any interference in the detection of Fe(III) ions. After the ion recognition studies, IFE, ICU and IFE(III) molecules were incorporated into a PVC membrane as a sensing elements for the monitoring of Fe(II), Cu(II) and Fe(III) ions.

4.3.4 Job's plot analysis

In most cases, Job's method is reliable for the determination of stoichiometry in host-guest complex. The binding stoichiometry of IFE, ICU and IFE(III) with metal ions was analysed by the method of continuous variation (Job's method)[21]. Absorbances were measured at 320 nm, 340 nm and 320 nm respectively for IFE-Fe(II), ICU-Cu(II) and

IFE(III)-Fe(III). The total concentration of receptors and metal ions were kept constant at 4.0×10^{-4} mol/L during the titration by mixing the stock solutions (2×10^{-5} mol/L) of each compound in different ratios.

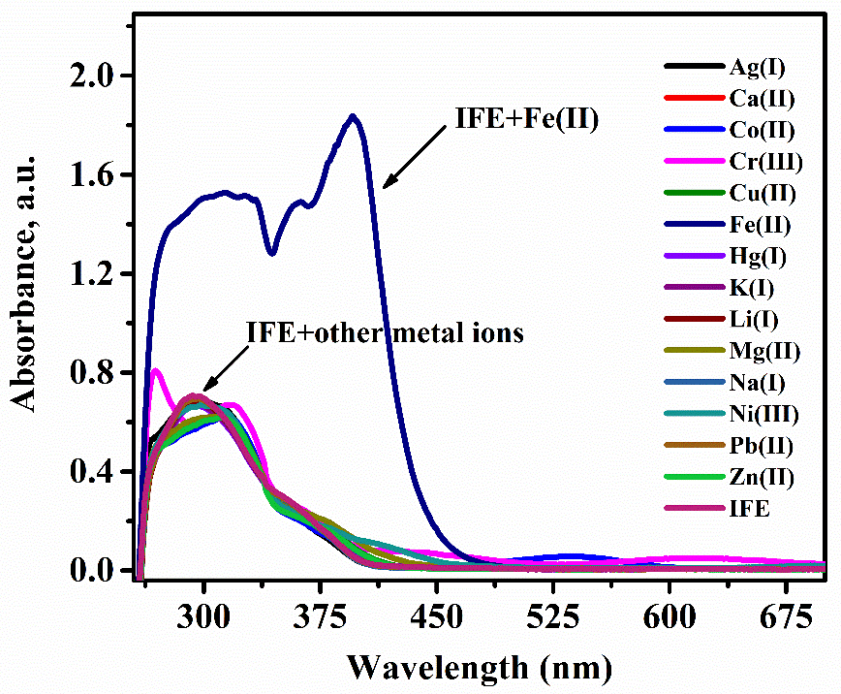

Fig. 4.3.1: UV-Vis spectra of IFE (2×10^{-5} mol/L) in presence of different metal ions (4.0×10^{-4} mol/L)

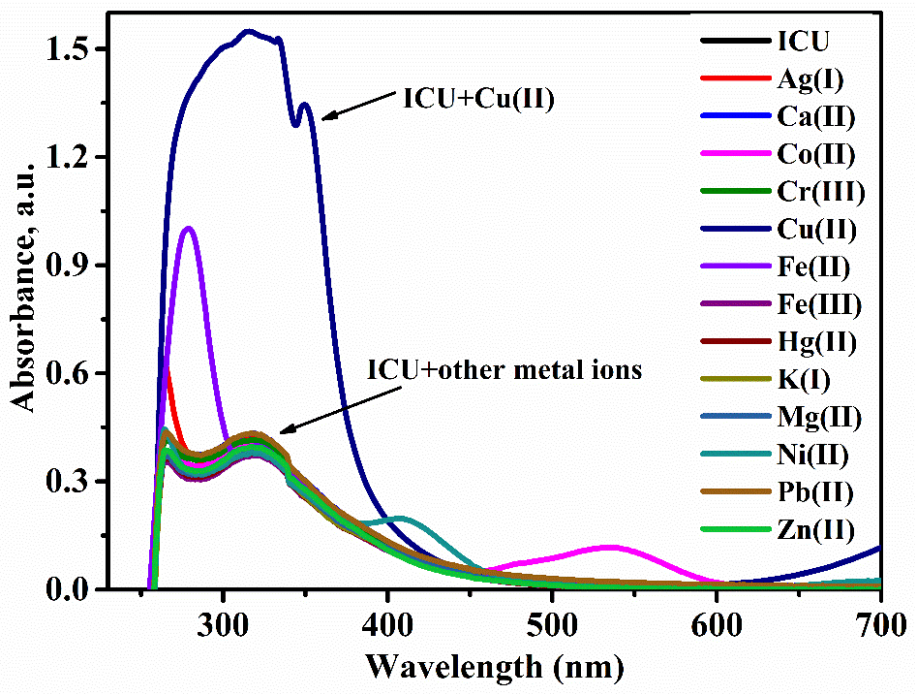

Fig. 4.3.2: UV-Vis spectra of ICU (1.6×10^{-5} mol/L) in presence of different metal ions (4.0×10^{-4} mol/L)

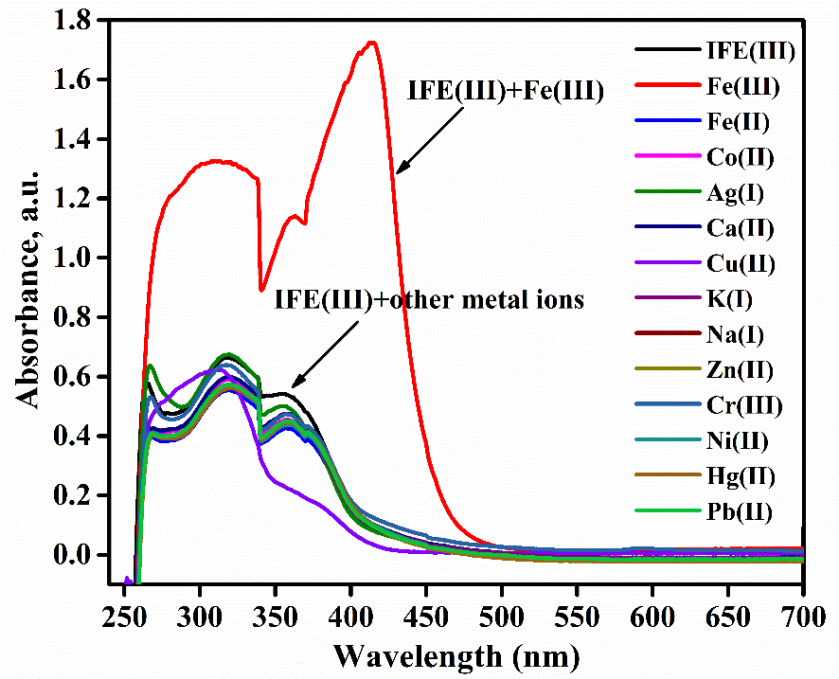

Fig. 4.3.3: UV-Vis spectra changes of IFE(III) (2×10^{-5} mol/L) in presence of different metal ions (4.0×10^{-4} mol/L)

The binding stoichiometry for IFE, ICU and IFE(III) and selected metal ions (Fe^{2+}, Cu^{2+} and Fe^{3+}) was analyzed by plotting the Job's plot (Fig. 4.3.4, 4.3.5 and 4.3.6) The Job's function A_{Job} is calculated according to the equation $A_{Job} = (1 - X)A_0 - A$. The maximum absorbance at a molar fraction of 0.5 clearly reveals the formation of a metal complexes in 1:1 stoichiometry.

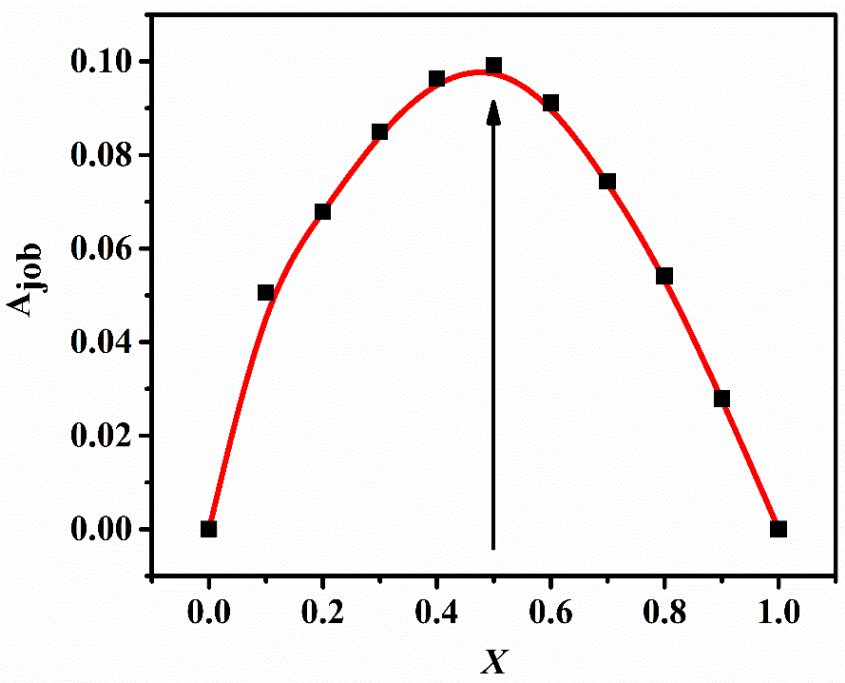

Fig. 4.3.4: Job's plot for determining the binding stoichiometry of IFE with Fe(II)

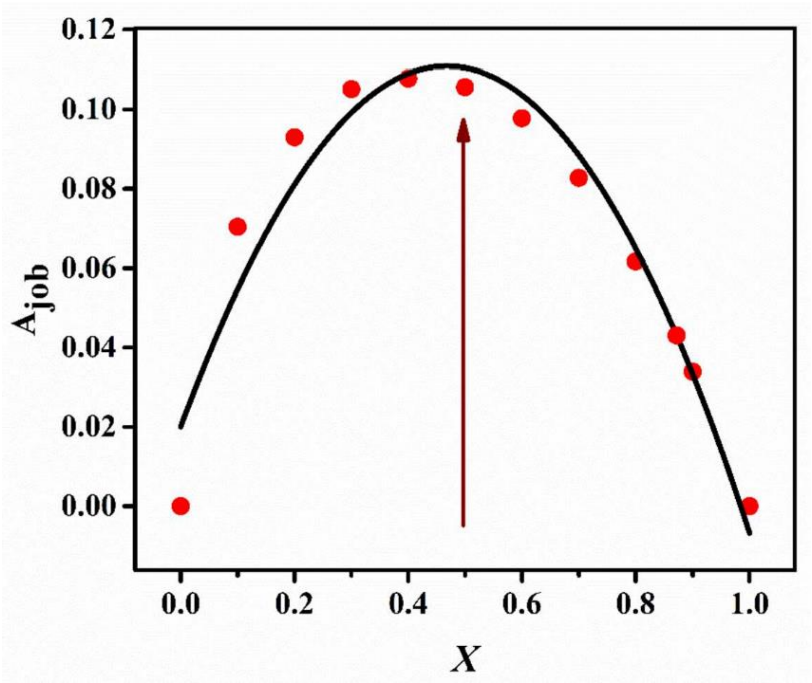

Fig. 4.3.5: Job's plot for determining the binding stoichiometry of ICU with Cu^{2+}

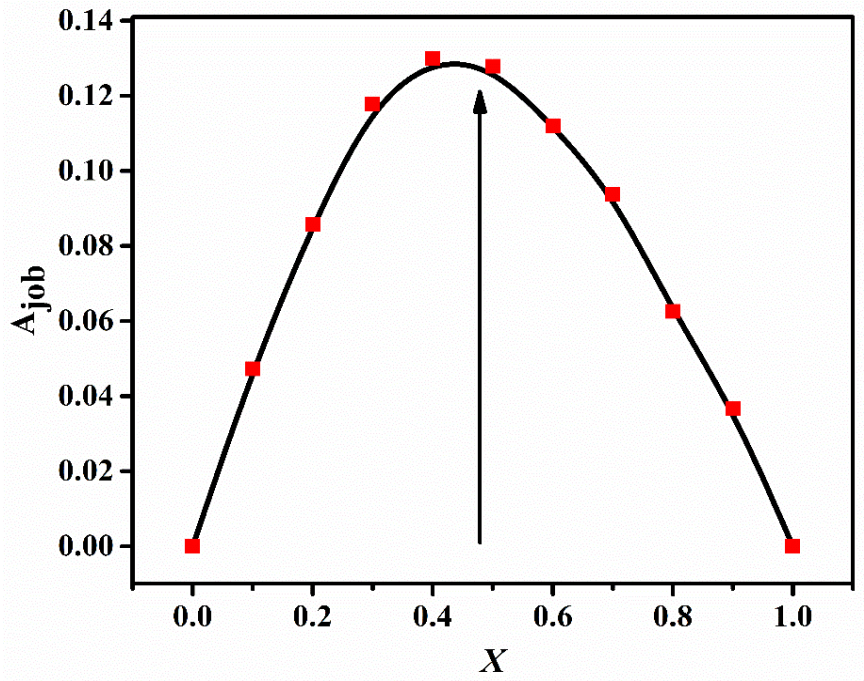

Fig. 4.3.6: Job's plot for determining the binding stoichiometry of IFE(III) with Fe(III)

4.3.5 Conclusions

This chapter described the spectrophotometric properties of novel Schiff base compounds. Optical chemosensors for the detection of Fe(II), Cu(II) and Fe(III) based on imine based Schiff base compounds are reported. Moreover, stoichiometry of Schiff base complexes was determined from Job's plot method and it was found to be 1:1 for all the compounds.

References

1 Kavitha, P.; Saritha, M.; Reddy, K. L. *Spectrochimica Acta Part A: Molecular and Biomolecular Spectroscopy* **2013**, *102*, 159-168.

2 Shokrollahi, A.; Ghaedi, M.; Ghaedi, H. *Journal of the Chinese Chemical Society* **2007**, *54*, 933-940.

3 Huang, N.; Zhang, S.; Yang, L.; Liu, M.; Li, H.; Zhang, Y.; Yao, S. *ACS Applied Materials & Interfaces* **2015**, *7*, 17935-17946.

4 Kumari, S.; Chauhan, G. S. *ACS Applied Materials & Interfaces* **2014**, *6*, 5908-5917.

5 Afkhami, A.; Moosavi, R.; Madrakian, T.; Keypour, H.; Ramezani-Aktij, A.; Mirzaei-Monsef, M. *Electroanalysis* **2014**, *26*, 786-795.

6 Arabahmadi, R.; Orojloo, M.; Amani, S. *Analytical Methods* **2014**, *6*, 7384-7393.

7 Cozzi, P. G. *Chemical Society Reviews* **2004**, *33*, 410-421.

8 Chandra, S.; Jain, D.; Sharma, A. K.; Sharma, P. *Molecules* **2009**, *14*, 174-190.

9 Zishen, W.; Zhiping, L.; Zhenhuan, Y. *Transition Metal Chemistry* **1993**, *18*, 291-294.

10 Belal, A.; El-Deen, I.; Farid, N.; Zakaria, R.; Refat, M. S. *Spectrochimica Acta Part A: Molecular and Biomolecular Spectroscopy* **2015**, *149*, 771-787.

11 Lekha, L.; Raja, K. K.; Rajagopal, G.; Easwaramoorthy, D. *Journal of Molecular Structure* **2014**, *1056*, 307-313.

12 Mazlan, N. A.; Ravoof, T. B. S.; Tiekink, E. R.; Tahir, M. I. M.; Veerakumarasivam, A.; Crouse, K. A. *Transition Metal Chemistry* **2014**, *39*, 633-639.

13 Saha, S.; Sasmal, A.; Choudhury, C. R.; Gómez-Garcia, C. J.; Garribba, E.; Mitra, S. *Polyhedron* **2014**, *69*, 262-269.

14 Chandra, S. *Spectrochimica Acta Part A: Molecular and Biomolecular Spectroscopy* **2013**, *103*, 338-348.

15 Segura, J. L.; Mancheno, M. J.; Zamora, F. *Chemical Society Reviews* **2016**, *45*, 5635-5671.

16 Begum, A. B.; Rekha, N.; Kumar, B. V.; Ranganatha, V. L.; Khanum, S. A. *Bioorganic & Medicinal Chemistry Letters* **2014**, *24*, 3559-3564.

17 Liu, Q.; Yang, X.; Huang, Y.; Xu, S.; Su, X.; Pan, X.; Xu, J.; Wang, A.; Liang, C.; Wang, X. *Energy & Environmental Science* **2015**, *8*, 3204-3207.

18 Al Zoubi, W.; Ko, Y. G. *Applied Organometallic Chemistry* **2017**, *31*, e3574.

19 Wang, Q.; Gao, W.; Liu, Y.; Yuan, J.; Xu, Z.; Zeng, Q.; Li, Y.; Schröder, M. *Chemical Engineering Journal* **2014**, *250*, 55-65.

20 Ghorbani-Choghamarani, A.; Darvishnejad, Z.; Tahmasbi, B. *Inorganica Chimica Acta* **2015**, *435*, 223-231.

21 Huang, C. Y. In *Methods in enzymology*; Elsevier, **1982**, pp 509-525.

4.4 Theoretical studies on Schiff base compounds IFE, ICU and IFE(III)

4.4.1 Introduction

Theoretical calculations can be used to determine the molecular geometries and analyse their interaction with guest atoms.[1,2] Ab initio Hartree-Fock (HF) and DFT calculations successfully suggest the behaviour of donor and acceptor atoms of ligands and the coordination sphere of a compound.[3,4] Density functional theory calculations provide excellent investigation about vibrational frequencies and molecular structure than HF calculations.[5-7] Density functional theory is widely used in the chemistry and physics community. The development of powerful optimization technique based on density functional theory method has made it possible to carry out full geometry optimization of stable molecule.[1,8] DFT can be successfully employed to obtain molecular structure, dipole moments, highest occupied molecular orbital (HOMO), lowest unoccupied molecular orbital (LUMO), force fields and frequencies, NMR, UV and Infrared spectra.[9-11] In this chapter, density functional theory on a series of imine-based compounds is discussed. Theoretical prediction of Schiff bases was done in Gaussian software based on energy gap (ΔE) between host and guest. Our goal is to investigate the intermolecular charge transfer in host-guest system and analyse the influence of carbon-nitrogen, carbon-oxygen and carbon-carbon linkage between donor and acceptor in molecular performance.

4.4.2 Experimental

The GAUSSIAN 03W package was used for density functional theory (DFT) and Hartree-Fock (HF) calculations. Full-unconstrained geometry optimization of (E)-3-((2-aminoethylimino)methyl)-4H-chromen-4-one (IFE), (E)-3-(((2-((2 aminoethyl) amino) ethyl) imino) methyl)-4H-chromen-4-one (ICU) and (E)-3-((2-(2-(2-aminoethylamino) ethylamino) ethylimino)methyl)-4H-chromen-4-one (IFE(III)) was carried out using B3LYP/6-31G level of theory while metal complexation experiments were conducted using LAN2DZ method using B3LYP function.

4.4.3 Results and discussion on the theoretical studies

Three metal complexes of Fe(II), Cu(II) and Fe(III) ions with Schiff base compounds have been investigated. The coordination of the selected metal ions towards IFE, ICU and IFE(III) receptor molecules takes place through –C=N and –C=O groups.

Theoretical calculations of IFE

The calculations of density functional theory (DFT) provided for a better understanding of the nature of the Fe(II) coordination with IFE, energy-optimized structures of IFE and corresponding Fe(II) complexes (Fig. 4.4.1) at the B3LYP level using 6-31G basis set for simple ionophore (IFE) and metal complexes using the Gaussian 03W software.

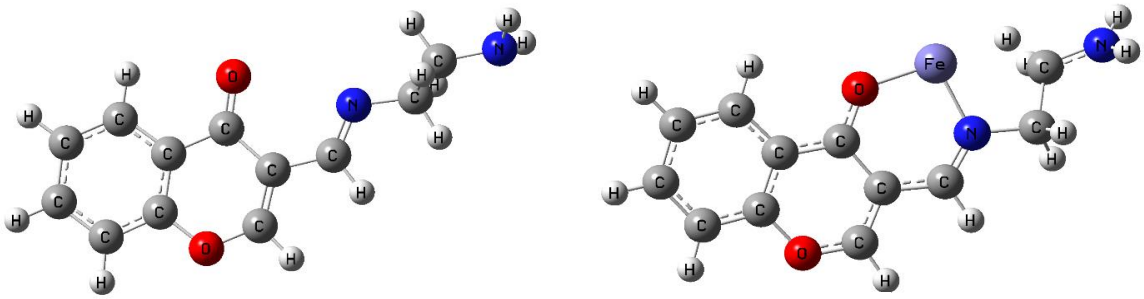

(a) **(b)**

Fig. 4.4.1: DFT computed optimized structure of receptor (a) IFE and (b) its complex with Fe(II)

The spatial distributions and orbital energies of highest occupied molecular orbital (HOMO) and lowest unoccupied molecular orbital (LUMO) of IFE and its complex IFE-Fe(II) were also determined (Fig. 4.4.2). The energy gap between HOMO and LUMO energy levels is an important parameter in determining the reactivity of the molecule.[12] Quantitatively, the calculated values of energy of HOMOs and LUMOs are -0.210 eV and -0.063 eV for the free ligand (a) and -0.501 eV and -0.408 eV for the Fe(II) complex (b). The energy difference between the LUMO and HOMO is defined as the band gap energy (Eg), which can be calculated as

$$E_g = E_{LUMO} - E_{HOMO}$$

The results clearly indicate that the binding of Fe(II) to IFE lowered the HOMO-LUMO energy gap and stabilized the system through electron transfer. Thus, they show a favourable complexation according to proposed coordination. Given the experimental proof, during IFE binding with Fe(II) there was a three-dimensional molecular structure and charge transfer process occured. The Density Functional Theory (DFT) calculations were investigated by using the B3LYP functional, and 6-31 G basis set for Fe atom as indicated in the Gaussian 03W computational code as shown in the Figure. 4.4.1.

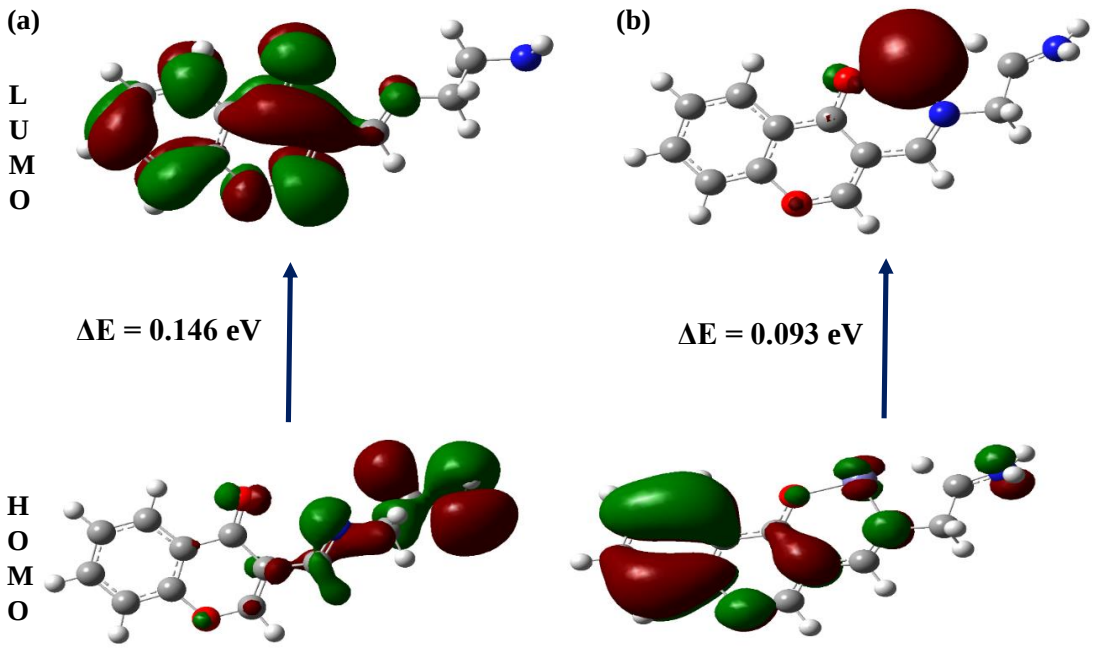

Fig. 4.2.2: DFT computed HOMO and LUMO Diagram of (a) IFE and its (b) IFE–Fe(II) Complex

Theoretical calculations of ICU

Density functional theory-based electronic structure calculation has an excellent predictability strength for the multiple structural and thermodynamic characteristics of molecular system.[13] Density Functional Theory (DFT) and Hartree Fock (HF) calculations were done to understand the host-guest interaction between the Schiff base and numerous metal cations. To obtain the information about the tendency of the Ligand (ICU) to form a complex with Cu^{2+} and Ligand (ICU) calculations were performed using Gaussian 03 software.

The first stage was to complete geometry optimization of the free ligand (ICU) by using the 6-31 G basis set at B3LYP level of DFT theory with a single point energy calculation for the optimized structure.[14,15] Energy calculations for the optimized structure using the 6-31G++ basis set with Hartree Fock (HF) Theory were done. The same procedure is then repeated with the effective core potentials of the LANL2DZ basis for the ratio of ligand (ICU)-Cu complex (1:1). The optimized structures are shown in Fig. 4.4.3, 4.4.4 for Cu Complex (b), for the free ligand (a).

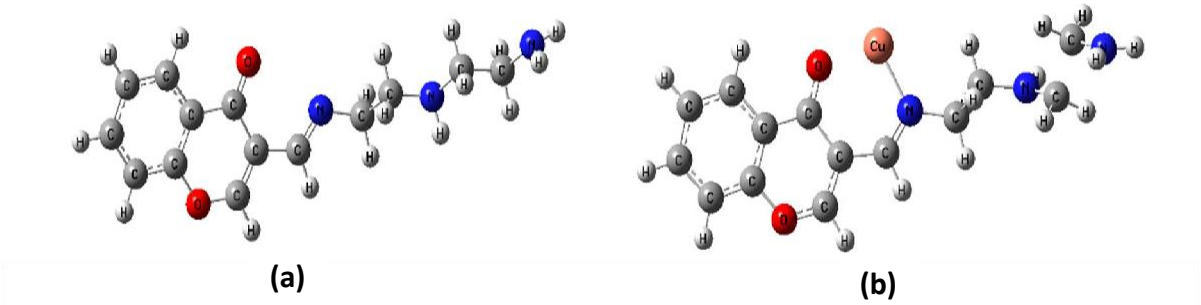

Fig. 4.4.3: DFT computed optimized structure of receptor ICU (a) and its complex with Cu^{2+} (b)

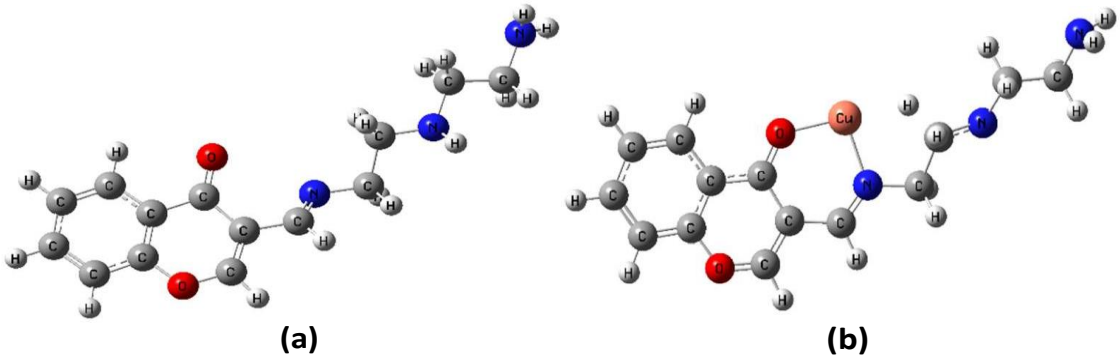

Fig. 4.4.4. HF computed optimized structure of receptor ICU (a) and its complex with Cu^{2+} (b)

For a chemical reaction to occur there should be an interaction between reactants, which happens through frontier molecular orbital.[16] It is well recognized that HOMO is able to donate electrons whereas LUMO is able to accept electrons. Using DFT, the calculated value of energy for HOMOs and LUMOs are -0.199 eV and -0.064 eV for free ligand (a) and -0.446 eV and -0.302 eV for Cu complex (b). While energy for HOMOs and LUMOs are -0.329 eV and 0.076 eV for free ligand and -0.551 eV and -0.239 eV for Cu complex were found using HF thoery.

According to DFT calculations, the values for the proposed free ligand and its Cu^{2+} complex are 0.135 eV and 0.144 eV respectively (Fig. 4.4.5). It is clear from the result that complex possesses more E_g value reveals the more stability of Cu^{2+} complex relative to the free ligand. However, same calculations when done using HF theory, the corresponding values obtained were 0.406 eV and 0.311 eV, respectively indicating relatively lesser stability of the complex as compared to ligand (Fig. 4.4.6). Since, DFT calculations are accepted more widely than HF theory, the former results are accepted.[17] Experimentally also, the complexation of ligand with Cu (II) is very well observed and

recorded by voltammetric technique. In view of the experimental evidence, during binding of Cu^{2+} by ICU the 3-D molecular structure and charge transfer process took place. The basis sets 6-31 G (for electrons C, H, N and O) and LANL2DZ (for atom Cu) are accessible in the Gaussian 03W computational code. Density function theory (DFT) calculations were explored by using B3LYP functional computational codes as indicating in Fig. 4.4.3.

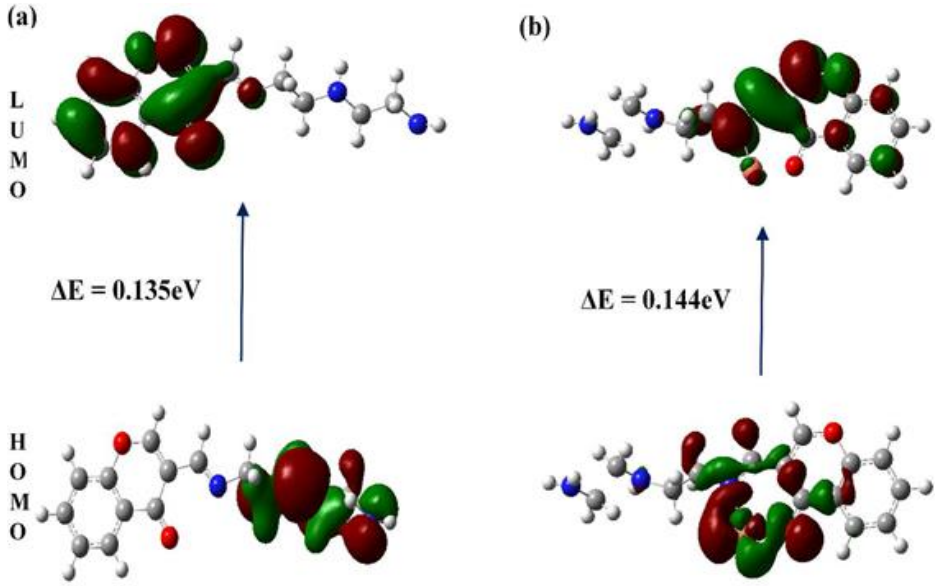

Fig. 4.4.5: DFT computed HOMO and LUMO Diagram of (a) ICU and its (b) ICU–Cu^{2+} Complex

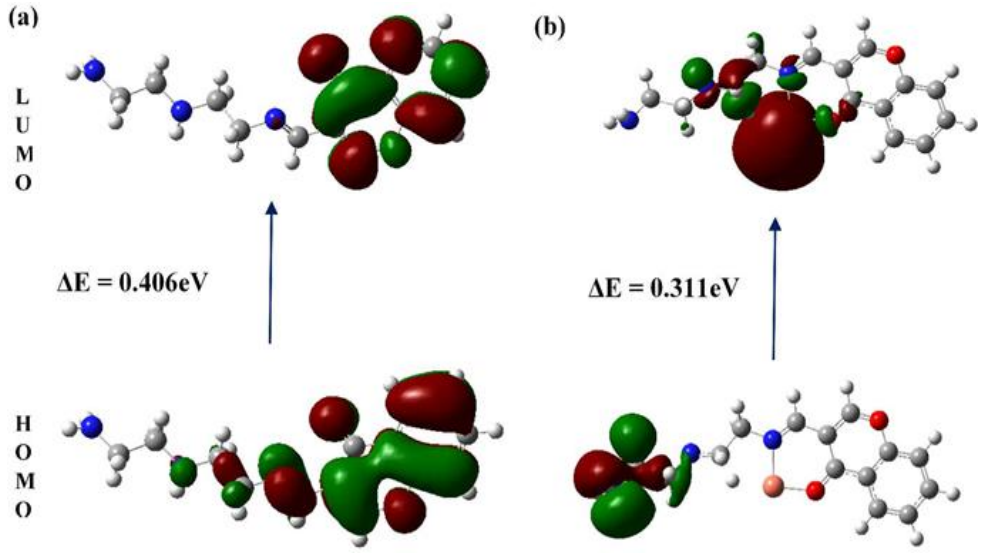

Fig. 4.4.6: HF computed HOMO and LUMO Diagram of (a) ICU and its (b) ICU–Cu^{2+} Complex

Theoretical calculations of IFE(III)

Density functional theory-based electronic structure calculations were used to understand the coordination of Fe^{3+} with IFE(III). In order to get stable structure IFE(III) and its complex were optimized using B3LYP functional with 6-31G basis set for ligand and LanL2DZ for IFE(III)-Fe^{3+} complex (Fig 4.4.7). For IFE(III)-Fe^{3+} complex, HF optimized model of IFE(III) was generated and placing the Fe^{3+} in the core of benzopyrancarbonyl O and imine N as donor moieties at a noninteracting distance. This model was optimized using HF/LanL2DZ basis set for Fe^{3+} ion.

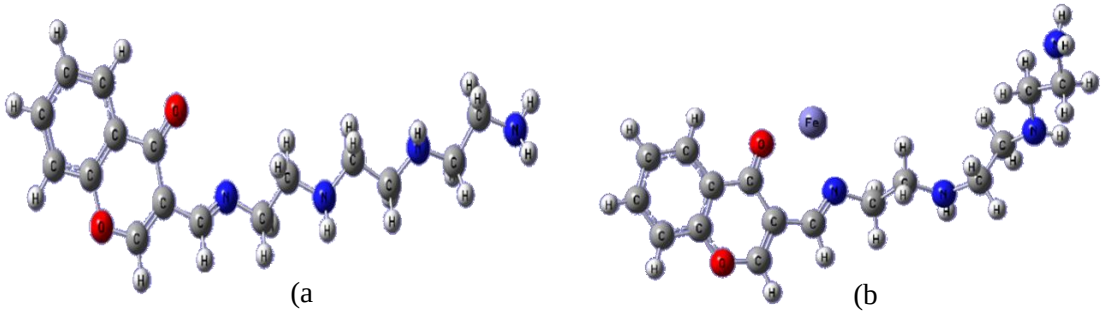

Fig. 4.4.7: HF computed optimized structure of receptor IFE(III) (a) and its complex with Fe^{3+} (b)

The TD-DFT results show the frontier molecular orbitals i.e. HOMO and LUMO related to the molecular electronic structure of ligand and metal complex (Fig. 4.4.8). Generally, it is implicit that HOMO accounts for its ability to donate electrons while the LUMO has the capability of accepting electrons.[18,19] The HOMO and LUMO energy of the ligand (IFE(III)) found to be -8.91 and 2.26 eV and for the complex (IFE(III)-Fe^{3+}) -14.13 and -11.01 eV, respectively. The energy gap $\Delta E = (E_{HOMO}-E_{LUMO})$, between HOMO and LUMO for the ligand and its complex were 11.17 and 3.12 eV, respectively. The decreased value in the energy gap between HOMO and LUMO describes the possible charge carrying interaction within the molecules.

In view of the experimental evidence, the density functional theory (DFT) calculations for stoichiometry was further encouraged by using the B3LYP functional and LanL2DZ for Fe atom is based on a computational code available in the Gaussian 03W as shown in Fig. 4.4.7.

4.4.4 Conclusions

In this chapter, the results of ab initio HF and DFT studies of transition metal complexes of (E)-3-((2-aminoethylimino)methyl)-4H-chromen-4-one (IFE), (E)-3-(((2-((2

aminoethyl) amino) ethyl) imino) methyl)-4H-chromen-4-one (ICU) and (E)-3-((2-(2-(2-aminoethylamino) ethylamino) ethylimino)methyl)-4H-chromen-4-one (IFE(III)) with Fe(II), Cu(II) and Fe(III) have been reviewed. Theoretical calculations clearly indicate that the binding of Fe(II), Cu(II) and Fe(III) to IFE, ICU and IFE(III) lowered the HOMO–LUMO energy gap and stabilized the system through electron transfer. Therefore, they show a favourable complexation according to projected coordination.

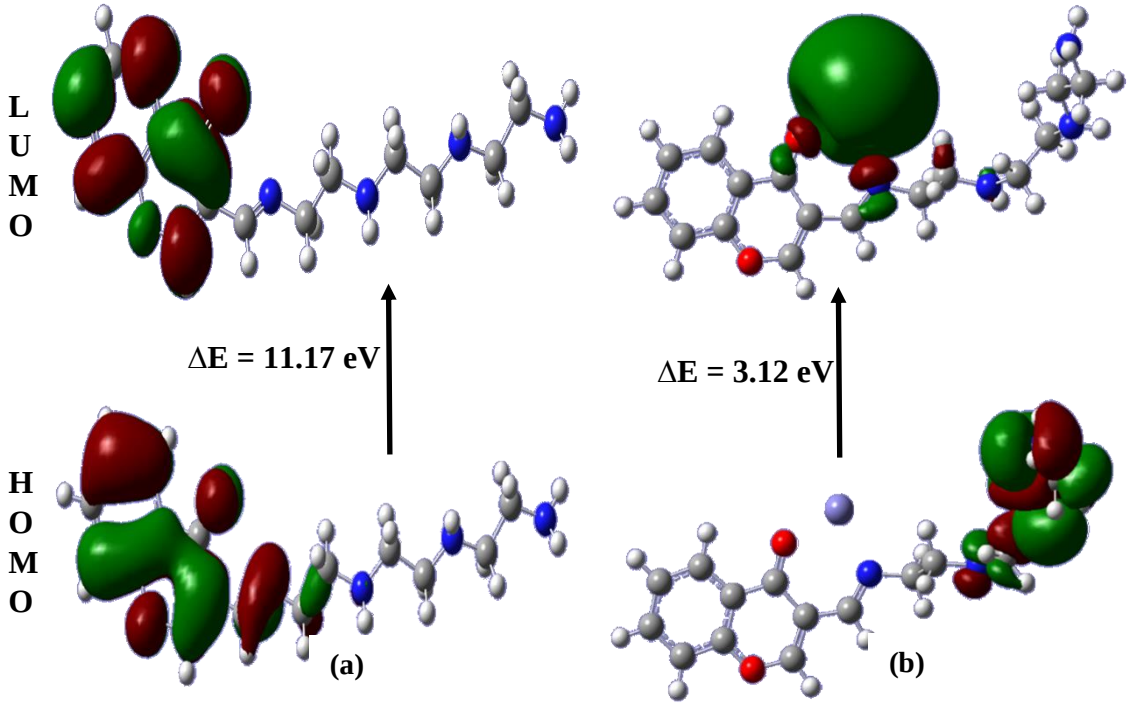

Fig. 4.4.8: HF computed HOMO and LUMO Diagram of (a) IFE(III) and its (b) IFE(III)–Fe^{3+} Complex

Reference

1 St-Amant, A.; Salahub, D. R. *Chemical Physics Letters* **1990**, *169*, 387-392.

2 Ziegler, T. *Chemical Reviews* **1991**, *91*, 651-667.

3 Kühl, O. *Coordination Chemistry Reviews* **2005**, *249*, 693-704.

4 Ireta, J.; Neugebauer, J.; Scheffler, M. *The Journal of Physical Chemistry A* **2004**, *108*, 5692-5698.

5 Sundaraganesan, N.; Kalaichelvan, S.; Meganathan, C.; Joshua, B. D.; Cornard, J. *Spectrochimica Acta Part A: Molecular and Biomolecular Spectroscopy* **2008**, *71*, 898-906.

6 Sundaraganesan, N.; Ilakiamani, S.; Subramani, P.; Joshua, B. D. *Spectrochimica Acta Part A: Molecular and Biomolecular Spectroscopy* **2007**, *67*, 628-635.

7 Sundaraganesan, N.; Meganathan, C.; Joshua, B. D.; Mani, P.; Jayaprakash, A. *Spectrochimica Acta Part A: Molecular and Biomolecular Spectroscopy* **2008**, *71*, 1134-1139.

8 Andzelm, J.; Kölmel, C.; Klamt, A. *The Journal of Chemical Physics* **1995**, *103*, 9312-9320.

9 El-Azhary, A. A. *Spectrochimica Acta Part A: Molecular and Biomolecular Spectroscopy* **1996**, *52*, 33-44.

10 Karabacak, M.; Şahin, E.; Çınar, M.; Erol, I.; Kurt, M. *Journal of Molecular Structure* **2008**, *886*, 148-157.

11 Karabacak, M.; Cinar, M. *Spectrochimica Acta Part A: Molecular and Biomolecular Spectroscopy* **2012**, *86*, 590-599.

12 Bereket, G.; Hür, E.; Öğretir, C. *Journal of Molecular Structure: THEOCHEM* **2002**, *578*, 79-88.

13 Parr, R.; Yang, W.; *Oxford University Press, New York*, **1989**.

14 Hohenberg, P.; Kohn, W. *Physical Review* **1964**, *136*, B864.

15 Kohn, W.; Sham, L. J. *Physical Review* **1965**, *140*, A1133.

16 Bereket, G.; Hür, E.; Ö retir, C. *Journal of Molecular Structure: THEOCHEM* **2002**, *578*, 79-88.

17 Zhang, G.; Musgrave, C. B. *The Journal of Physical Chemistry A* **2007**, *111*, 1554-1561.

18 Li, G.-Y.; Chu, T. *Physical Chemistry Chemical Physics* **2011**, *13*, 20766-20771.

19 Gece, G.; Bilgiç, S. *Corrosion Science* **2009**, *51*, 1876-1878.

4.5 Organic nanoparticles of Schiff based ionophores for enhanced voltammetric performance

Abstract

In aqueous dispersion, organic nanoparticles of (E)-3-(2-aminoethylimino) methyl)-4H-chromen-4-one (IFE) were synthesized with an average particle size of 50-65 nm.[1] Dynamic light scattering (DLS) and Transmission electron microscopy (TEM) described characterization of organic nanoparticles. Based on voltammetric measurements, organic nanoparticles (ONPs) of IFE exhibited good response towards sensing and selective detection of Cu(II) ions in aqueous medium. Even in the presence of other alkali, alkaline and transitional metal ions, the sensor shows excellent Cu(II) response under optimum conditions. Differential pulse voltammetry was introduced to the optimized electrode and a linear dynamic range between 2.5×10^{-6} to 1.4×10^{-5} mol/L with a detection limit of 8.22×10^{-8} mol/L obtained. This system was also used as a voltammetric sensor in multiple real-life samples to determine Cu(II) ions.

4.5.1 Introduction

Metal and semiconductor nanoparticles have been studied in earlier years due to their exceptional properties such as optical, optoelectronic, electronic and magnetic.[2-4] On the other hand, organic nanoparticles (ONPs) are likely to hold the higher potentials due to their variability and flexibility in materials synthesis and nanoparticle preparation.[5,6] Improvement in the field of organic nanoparticles has attracted researcher to develop chemosensor by using organic compound that aggregate into small size organic nanoparticles.[7,8] Organic nanoparticles have excellent optical and electronic properties, which prompted their use in novel luminescent material, chemical sensors, medicine and optoelectronic devices. Due to their excellent properties such as low cost, good photostability, large diversity in molecular structure and quantum size effect, organic nanoparticles have attracted interest of analytical scientists in the last few years.[5,6,9,10] Therefore, electrochemistry is an alternative approach to optical method which provides more efficient and cost-effective method for characterization of organic nanoparticles. To develop organic nanoparticles of a Schiff base ionophore (IFE) (Fig. 1) as chemosensor in an aqueous medium, their cation recognition behavior was evaluated by recording the voltammetric performance of ONPs.

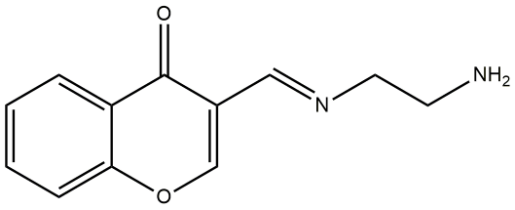

Fig. 4.5.1: Structure of receptor IFE

Experimental

4.5.2 Materials

All chemical used in this study were of analytical reagent grade and utilized as received from the commercial suppliers. Metal ion solutions of 0.1 mol/L concentration were prepared by dissolving metal nitrates in double distilled water. Dimethyl sulphoxide obtained from Sigma-Aldrich (India). Potassium chloride was obtained from the Sd Fine (India). Serial dilutions were carried out in order to obtained working solutions of different concentrations. The average particle size and shape of nano-aggregates were determined using dynamic light scattering (DLS) probe and transmission electron microscopy (TEM) analysis. The UV-visible spectral measurements were recorded on Analytic Jena Specord PC 205 spectrophotometer with a quartz cuvette of path length, 1 cm.

Preparation of organic nanoparticle

The preparation of ONPs in aqueous medium was achieved by production of uniform sized organic nanoparticles using one step reprecipitation method.[5] This method is a solvent displacement method in which target molecule dissolved in organic solvent is added to aqueous medium accompanied with vigorous stirring. This variation in the solubility of solvent is the driving force for the generation of nanoparticles. ONPs of IFE was prepared by mixing solution of Schiff base compound (1 mM) in DMSO solvent. This solution was introduced into the 100 mL distilled water with continuous sonication for about 15 minutes and maintained the temperature below 10 ℃. After that, resulting solution was further sonicated for 10 minutes to yield a colloidal suspension and size of the prepared nanoparticles were determined by using DLS probe. The reproducibility of the technique has been checked by using this experiment 5 times.

Electrochemical Studies

To explore the redox properties of IFE-ONPs, electrochemical workstations conducted cyclic voltammetric and differential pulse voltammetric studies (Autolab/PGSTAT12

/Eco Chemie/Netherlands) using a three-electrode setup consisting of a Glassy Carbon as working electrode (round disk, diameter 3 mm), Pt electrode as counter electrode and Ag/Ag^+ (0.1 mol/L $AgNO_3$ in H_2O) as reference electrode. The experimental conditions were controlled with NOVA 1.5 software. The CV and DPV studies were performed at a scan rate of 0.03 Vs^{-1}, a pulse amplitude of 0.025 V, a pulse width of 0.05 s and a pulse period of 0.10 s in the potential range of 2.00 V to -2.00 V vs Ag/Ag^+. The working electrode surface was polished with 0.05 micron aluminum before measurements. By using the working electrode on an ultrasonic cleaner for 15 minutes, remaining alumina particles were completely removed and dry and cleaned with pure acetonitrile. For all voltammetric measurements, the studies have been completed in an aqueous medium and KCl (0.1 mol/L) as supporting electrolyte. At a temperature of 25.0 ± 1 ºC, the electrochemical measurements were performed. The sample solutions have been deaerated through the stream of nitrogen gas purging for at least 5 minutes in every measurement.

Real life sample analysis

To validate practical ability of the sensor, IFE-ONPs were utilized to detect Cu(II) ion in various real-life samples such as tap water, tea, and pharmaceutical tablet analyzed by the proposed method.

1.0 g sample were precisely weighed in a 100 ml beaker for the assessment of tea samples. The beaker was supplemented by 10 ml nitric acid and 5 ml perchloric acid followed by hot plate digestion till the sample had been fully oxidized. After filtration with Whatman filter paper, the solution was dissolved with nitric acid 0.1 mol/L and then diluted to 100 mL using calibrated volumetric flask..

The sample of tap water was acquired from the laboratory. To eliminate all suspended particles, the sample has been filtered and pH of the solution was adjusted at 5.0 with 0.20 mol/L acetate buffer solution. Since copper was not detected in the solution, so different volumes of the Cu(II) stock solution were spiked into the solution and analyzed with the proposed method and Atomic Absorption Spectroscopy (AAS).

The utility of IFE-ONPs was further investigated to determine copper in multivitamin capsules. A multivitamin capsule has been precisely weighed and put in a ceramic crucible. It was heated to almost near to dryness under the cover of a fume hood with a millilitre of nitric acid. After cooling, the remaining residue has been dissolved in another millilitre, and the solution has been carefully evaporated via a water bath. Residue was

once again heated, filtered and diluted with a 50 mL distilled water using volumetric flask. An aliquot was taken from the sample and further analyzed with the proposed electrode and Atomic Absorption Spectroscopy (AAS).

4.5.3 Results and discussion

Fabrication of organic nanoparticle

Organic nanoparticles can be assembled from two approaches: bottom-up and top-down approaches. Former approach has been commonly used for the preparation of nanoparticle, in which a single atom or molecule combines to form nano-sized particles. Reprecipitation is categorized in a bottom-up approach. Second, the top-down approach includes breaking down of molecular aggregates into nano-sized particles and is of limited application to organic material as they have lower melting point and thermal instability.[11,12] Development of IFE-ONPs was executed by simple reprecipitation technique. According to this procedure, Schiff base ionophore (IFE) (1 mM) was dissolved in a polar solvent like DMSO and slowly injected into the aqueous medium over a period of 15-20 minutes using micro-syringe followed by continuous sonication to obtain the nanoparticles. To evaluate size and morphology of the prepared IFE-ONPs, characterization was done by DLS (dynamic light scattering) and TEM analysis (transmission electron microscopy). DLS study reveals that the average particle size of 50 nM was obtained while monitoring the size and variation of nanoparticle during the mixing of solutions (Fig. 4.5.2). The size and morphology of the nanoparticles were also monitored from the TEM analysis (Fig. 4.5.3). Spherical shaped nanoparticles were evenly distributed and size from 50-65 nm comparable to that observed from the DLS study. This procedure has been repeated five times to verify the method's reproducibility and optimization of parameters like temperature, sonication time, injection rate, and concentration was done.

Effect of water content

UV-Visible spectra of IFE compound in DMSO and its organic nanoparticles dispersed in aqueous medium were recorded at a concentration of 1.0×10^{-4} mol/L each (Fig. 4.5.4). There is a decrease in absorption maxima occurring on changing the solvent system from DMSO to water, which can be attributed to the development of nano-aggregation.

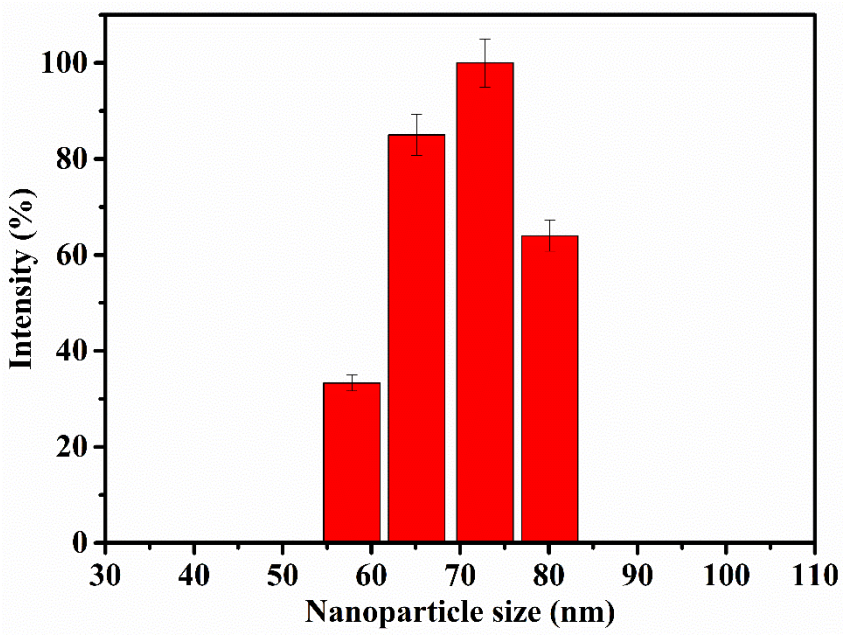

Fig. 4.5.2: DLS histograms of IFE-ONPs (showing average particle size of 72 nm) in DMSO/H_2O (1:99, v/v)

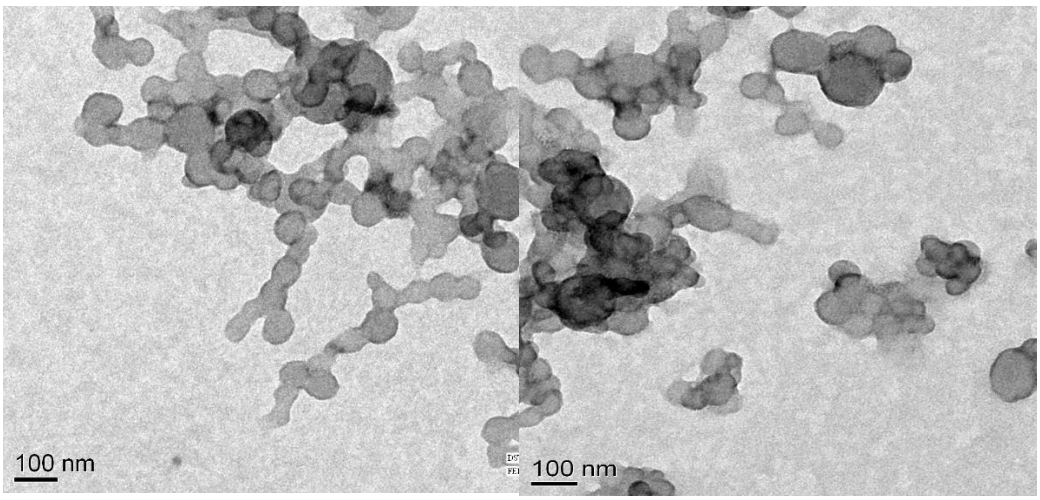

Fig. 4.5.3: TEM image of size distribution of ONPs of receptor IFE prepared in aqueous solution

Electrochemical characterization

In previous study,[13] the electrochemical behavior of IFE molecule in a non-aqueous medium has been discussed which shows its high selectivity towards Fe(II) ions. In this work, electrochemical measurements of ONPs were carried out in an aqueous medium with glassy carbon electrode at a scan rate of 30 mV/s. In the cyclic voltammogram of IFE-ONPs, there are two cathodic peaks; at -1.5 V and another weak and broad peak at -0.60 V and one weak anodic peak at 0.15 V. In comparison to our previous study, IFE-ONPs show remarkable variation with enhanced peak current observed in both cathodic and anodic regions due to the excellent electron transfer capability of the ONPs with

more active sites available for the binding (Fig. 4.5.5). Conversion of a bulk material to nanoparticles is accompanied by a lot of structural changes. Hence, it is likely to change its preference for target species.[14] In conclusion, ONPs electrocatalyzed the better oxidation/reduction reaction with enhanced current.

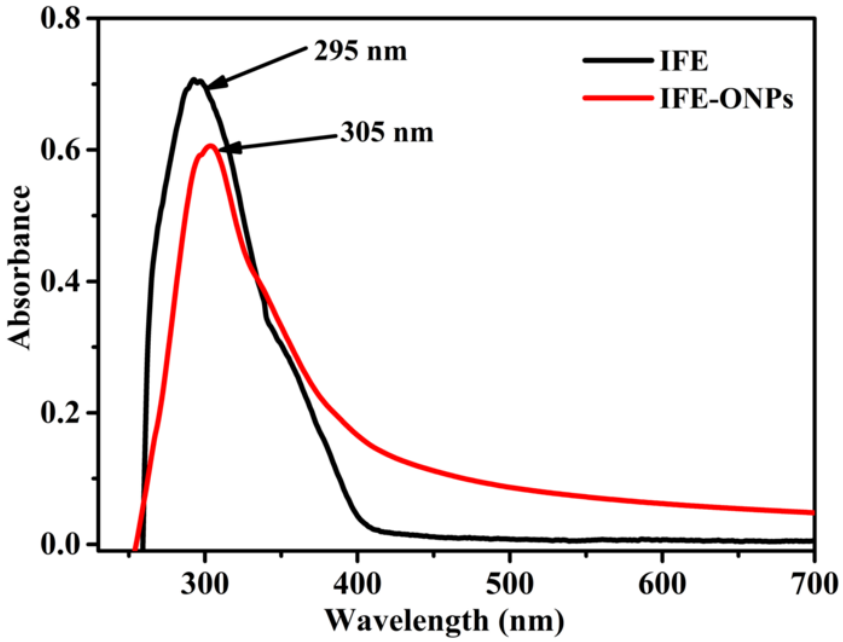

Fig. 4.5.4: Absorption spectra of ligand IFE in DMSO and its ONPs in an aqueous medium

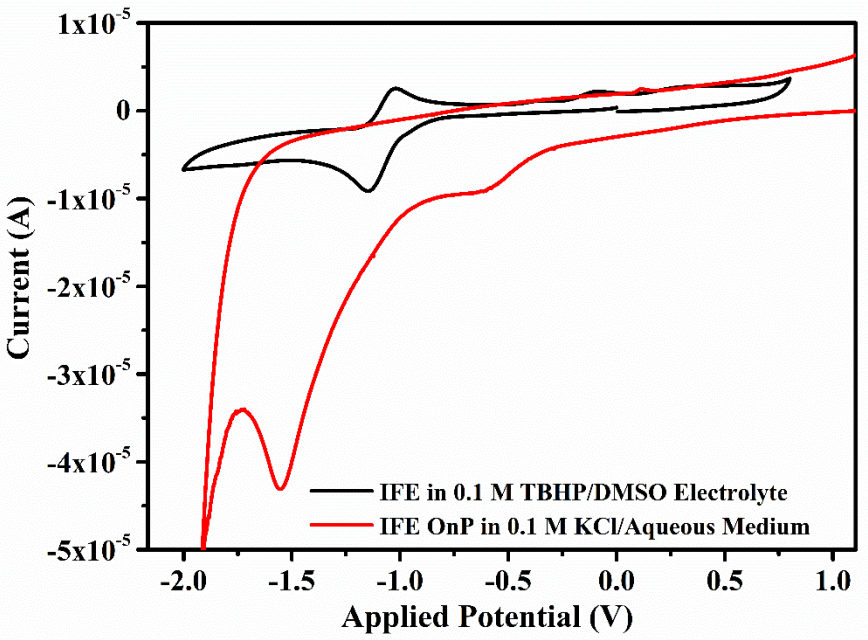

Fig. 4.5.5: Cyclic voltammograms of IFE-ONPs (8×10^{-5} mol/L) at the glassy carbon electrode in (1:99) DMSO: H_2O, 0.1 mol/L KCl. Scan rate: 30 mV s^{-1}

Scan Rate

Behavior of IFE-ONPs at different scan rates (20-130 mV/s) performed with cyclic voltammetric studies is shown in Fig. 4.5.6 (a). The peak current at -0.17 V increased with increase in scan rate. Experimental findings confirmed the linear dependence between the peak current and square root of the scan with a coefficient of correlation of 0.99, which shows a diffusion-controlled process at the electrode area. Fig. 4.5.6 (b).

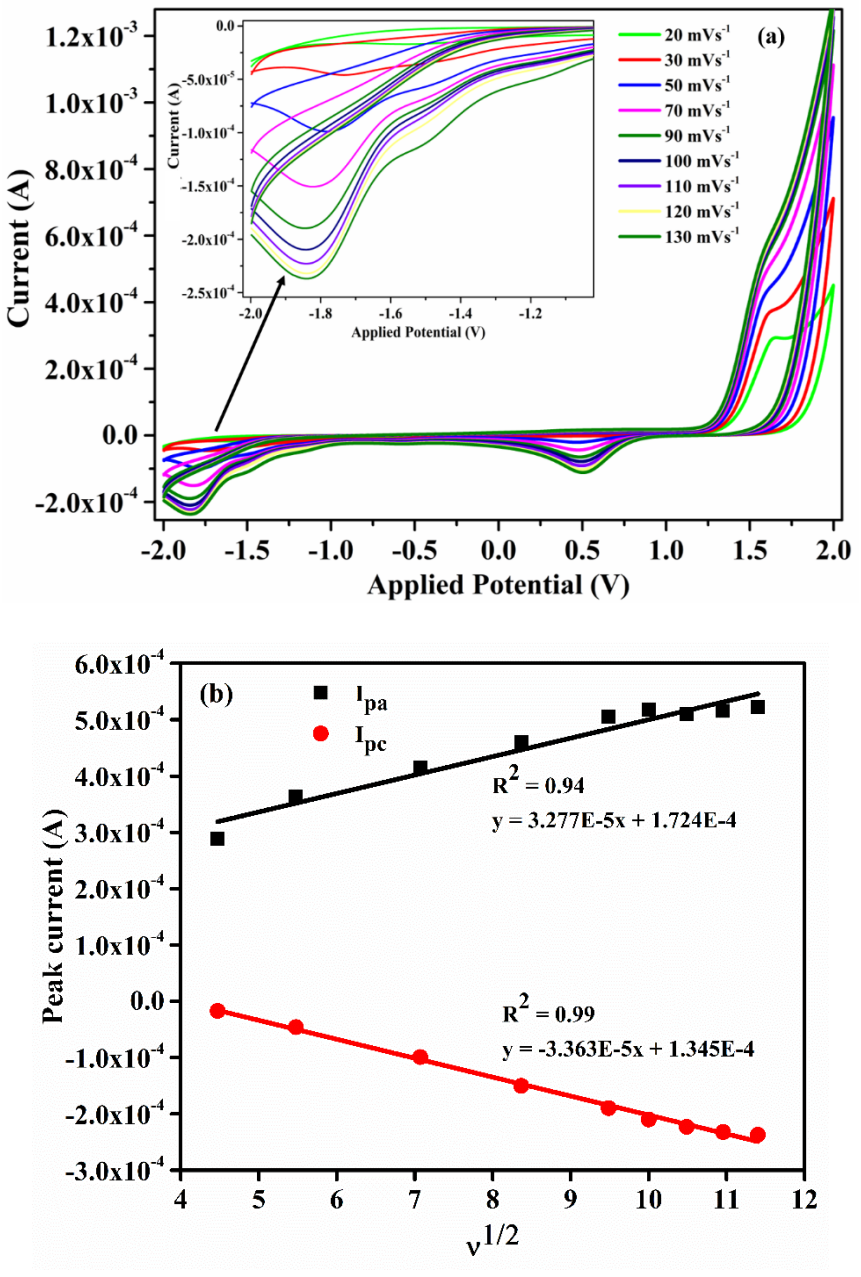

Fig. 4.5.6: (a) Cyclic voltammograms of IFE-ONPs at different scan rates. (b) Calibration plots showing the variation of peak current with square root of scan rate (GC as a working electrode, Ag/Ag^{+} as a reference electrode and KCl as supporting electrolyte)

Selectivity of IFE-ONPs for metal ions

The electro-analytical experiments were carried out in the presence of varying metal ions; like K^{+}, Mg^{2+}, Ca^{2+}, Cr^{3+}, Fe^{3+}, Fe^{2+}, Co^{2+}, Ni^{2+}, Cu^{2+}, Zn^{2+}, Ag^{+}, $Hg^{2+,}$ and Pb^{2+} to examine the selectivity response of the suggested sensor. Fig. 4.5.8 shows differential pulse voltammograms of IFE-ONPs in existence of metal ions at the GC electrode in the applied potential range of 2.0 V to -2.0 V with a scan rate of 30 mV/s. Nearly all metal ions have not affected IFE-ONPs current peak response. No observable influence in voltammograms was recorded indicating good selectivity of the IFE-ONP for Cu(II) ions over other different metal ions. Four cathodic peaks were observed at 0.50 V, 0.01 V, -0.45 V and -1.20 V while no major change was observed in the anodic region (Fig. 4.5.7). There was a slight shift in the cathodic peak at -1.20 V which might be due to the quasi-reversible behavior of the electrochemical reaction at the electrode surface. In addition, two new peaks at 0.01 V and 0.50 V were observed indicating copper interaction with IFE-ONPs.

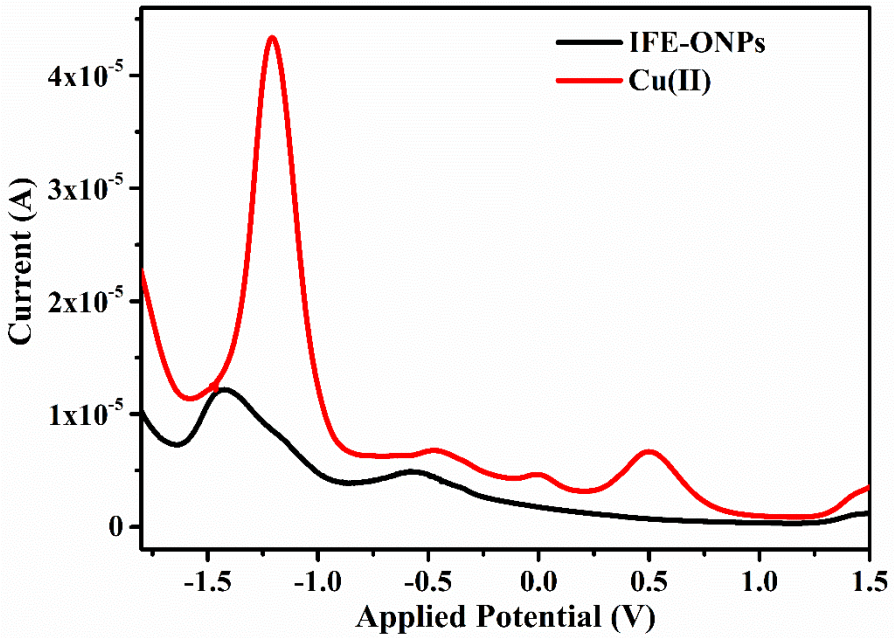

Fig. 4.5.7: Cathodic differential pulse voltammograms of (a) IFE-ONPs (8×10^{-5} mol/L) (b) and Cu(II) (10^{-3} M) at glassy carbon electrode in an aqueous medium, 0.1 mol/L KCl. Scan rate: 30 mVs^{-1}

Selectivity of IFE-ONP for various anionic species

In order to know about the interaction of IFE-ONPs with anions, voltammetric studies were carried out in DMSO: H_2O (1:100) medium (Fig. 4.5.9). Typically, anions in the form of tetrabutylammonium salts were added to the solution of IFE-ONPs in an aqueous

medium. Under the same conditions as used for the detection of Cu(II), no significant changes were observed in cyclic voltammograms with any of the anions. Hence, results showed no selectivity for the anion.

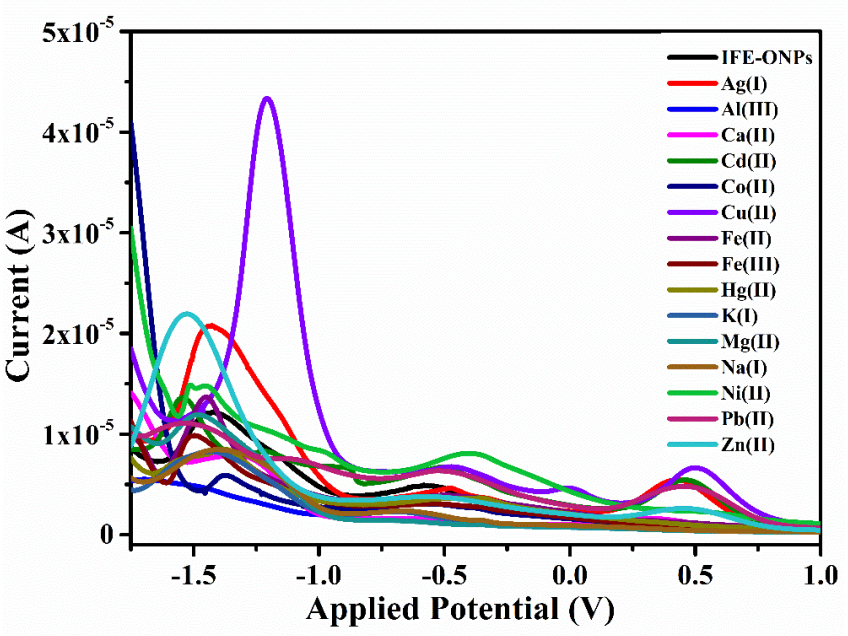

Fig. 4.5.8: Cathodic differential pulse voltammogram of IFE-ONPs in the presence of different metal ions

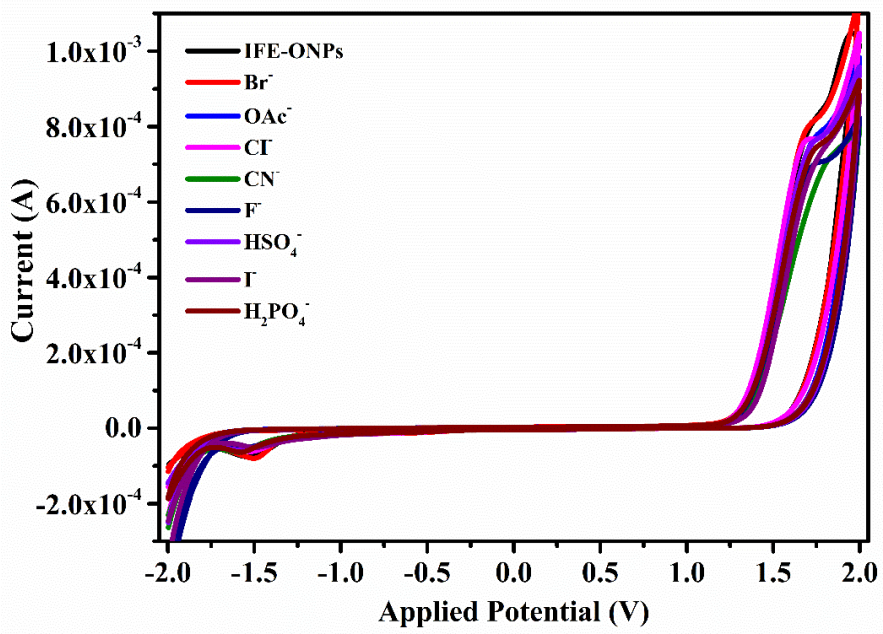

Fig. 4.5.9: Cyclic voltammograms of IFE-ONPs ($8x10^{-5}$ M) in presence of different anions at glassy carbon working electrode in 0.1M KCl/H_2O solution with a scan rate of 0.03 Vs^{-1}

Voltammetric studies on IFE-ONP-Cu complex

Formation of the complex was assessed in function of the changes in the voltammetric spectra of IFE-ONPs and Cu(II). A much greater current sensitivity and a much better resolution than cyclic voltammetry, differential pulse voltammetry (DPV) was chosen for further studies. To gain more insight into the complexation properties of Cu(II) and IFE-ONPs, differential pulse voltammetric titrations were carried out. As shown in Fig. 4.5.10, successive additions of Cu(II) ion in the IFE-ONP solution, the peak current at 0.50 V, -0.45 V, and -1.20 V increased due to binding of Cu(II) with IFE-ONPs. The peak current in DPV titration was dependent on Cu(II) ion concentration in the linear range of 2.49 µM to 14.77 µM and correlation coefficient (R^2) of 0.99 (Fig. 4.5.11). The limit of detection was calculated using the formula 3σ/m, which was found to be 8.22×10^{-8} mol/L. Therefore, this sensitivity of current range can be used for the detection of Cu(II) in real life samples.

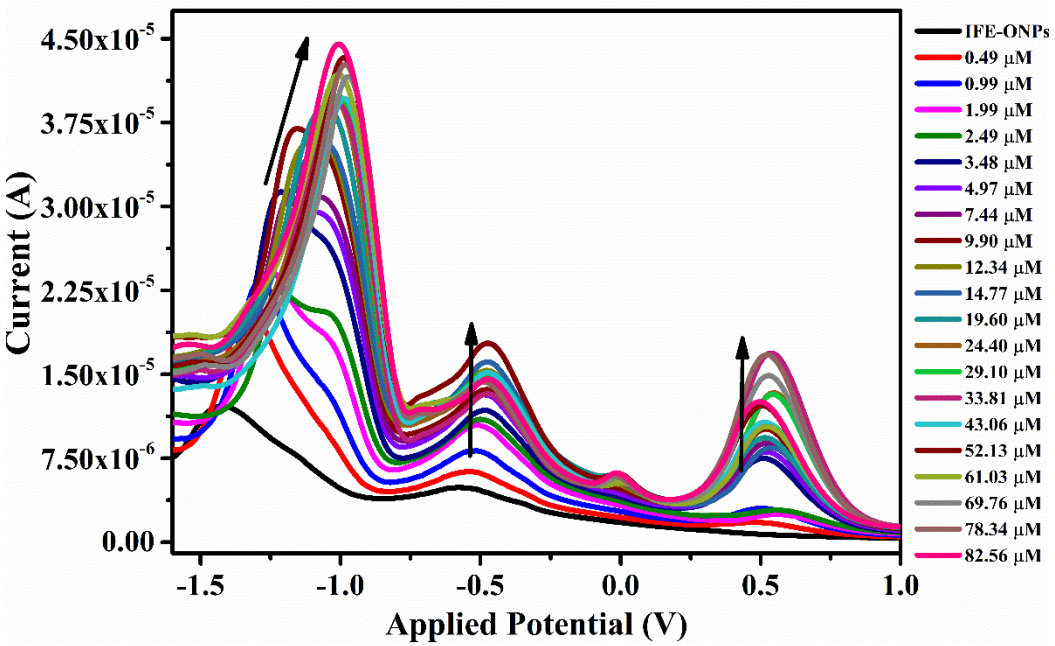

Fig. 4.5.10: Cathodic DPV of IFE-ONPs (8.0×10^{-5} mol/L) in presence of increasing amounts of Cu(II) ions in aqueous medium; electrolyte 0.1 mol/L KCl; Pulse amplitude of 0.05 V; scan rate 0.03 Vs^{-1} within the potential range of -1.5 – 1.0 V vs. Ag/Ag^{+}

Interference Study

Voltammetric measurements have been performed to assess the response of interfering metal ions for sensitive and selective Cu(II) ion detection. Interference studies were carried out with an equal concentration of interfering metal ions mixed with Cu(II) as primary ions. The voltammogram shows well-defined peaks for Cu(II) co-exist with

competitive metal ions without any significant changes in the peak current. This specified that the IFE-ONPs respond to the Cu(II) ion in a well-defined manner. Table 4.5.1 shows the current response of IFE-ONPs in absence and presence of interfering metal ions.

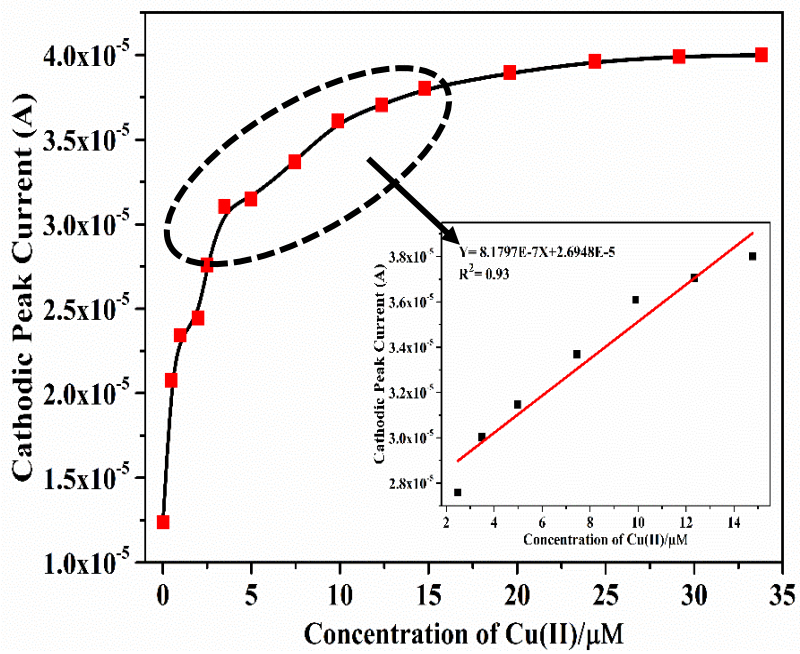

Fig. 4.5.11: Calibration plots between concentration and corresponding current for IFE-ONPs in electrolyte KCl (0.1 mol/L), pulse amplitude of 0.05 V; scan rate 0.03 Vs^{-1} vs. Ag/Ag^{+}

Table 4.5.1. Changes in cathodic/anodic peak current at -1.5 V on the addition of various interfering ions

Interfering Ions	% Change in peak current at -1.5 V
Li(I)	-0.5
Na(I)	-1.9
Mg(II)	+0.5
K(I)	-2.6
Ca(II)	+0.8
Cr(III)	-0.6
Fe(II)	+0.2
Co(II)	-0.7
Ni(II)	-3.1
Zn(II)	+1.1
Pb(II)	+0.9

Real Sample Analysis

IFE-ONPs worked well under laboratory conditions. Some of the effective applications of the proposed sensor for selective and sensitive monitoring of Cu(II) ion in different biological and environmental samples are given below. The samples (tap water, tea and pharmaceutical tablet) were treated by the recommended procedure as described in experimental section. All the measurements were carried out three times. The results obtained from the voltammetric measurement are in good agreement with the results obtained from the AAS (Table 4.5.2). This demonstrates that the IFE-ONPs are potentially applicable for the determination of Cu(II) in real-life samples.

Table: 4.5.2. Results of comparison of Cu (II) determination with proposed method and AAS method in various real-life samples

Sample	Concentration(ppm)	
	Proposed Method	AAS Method
Multivitamin Tablet	1.91(±2%)	1.97±3%
Black Tea	0.30(±3%)	0.34(±2%)
Tap Water	0.21(±3%)	0.20(±3%)

4.5.4 Comparison of performance characteristics of IFE-ONPs with those of previously reported sensors

When compared with other reported methods,[14-20] the proposed method for Cu(II) determination shows better selectivity, wide linear concentration range, and lower detection limit. In literature, different sensing elements were detected by using the organic nanoparticles of different probes and are summarized in Table 4.5.3.

4.5.5 Conclusions

Theory and experiments on a novel IFE-ONP voltammetric sensor are reported for the determination of Cu(II) based on synthesized ionophore (E)-3-((2-aminoethylimino)methyl)-4H-chromen-4-one (IFE). The performance of voltammetric sensor shows good selectivity for Cu(II) ion without any interference from the cations and exhibited the detection limit of 8.2×10^{-8} mol/L. The analytical utility of the electrode was validated by using it as a voltammetric sensor for real-life sample analysis for the determination of Cu(II).

Table: 4.5.3. Comparison of proposed method for Cu(II) determination with some reported literature using organic nanoparticles

Ionophore	Solvent	Metal Ion	Detection Technique	Detection Limit (mol/L)	Ref.
Chromone	H_2O	Cu(II)	Fluorescence	2.1×10^{-8}	[13]
Anthracene-N-phenylethylenediamine nanoparticles	EtOH-HEPES buffer	Cu(II)	Fluorescence	1.8×10^{-5}	[14]
N_3O_2 macrocycle	EtOH/ H_2O	Al(III)	Fluorescence	2.8×10^{-7}	[15]
Naphthalimide moiety	H_2O	Cr(III)	Fluorescence	6.4×10^{-8}	[16]
Disulfide based receptor	H_2O	Cu(II)	Voltammetry	1.9×10^{-7}	[17]
Pyrene based Bigineilli compound	H_2O	Fe (III)	Fluorescence	7.9×10^{-6}	[18]
Naphthalene–thiourea–thiadiazole	H_2O	Ag (I)	Fluorescence	4.7×10^{-8}	[19]
(E)-3-((2-aminoethylimino)methyl)-4H-chromen-4-one (IFE)	**H_2O**	**Cu(II)**	**Voltammetry**	**8.2×10^{-8}**	**This Work**

References

1 Kumar, S.; Mittal, S. K.; Kaur, N. *Analytical Methods* **2019**, *11*, 359-366.

2 Katz, E.; Willner, I.; Wang, J. *Electroanalysis: An International Journal Devoted to Fundamental and Practical Aspects of Electroanalysis* **2004**, *16*, 19-44.

3 Georgakilas, V.; Gournis, D.; Tzitzios, V.; Pasquato, L.; Guldi, D. M.; Prato, M. *Journal of Materials Chemistry* **2007**, *17*, 2679-2694.

4 Wang, F.; Hu, S. *Microchimica Acta* **2009**, *165*, 1-22.

5 Jana, A.; Devi, K. S. P.; Maiti, T. K.; Singh, N. P. *Journal of the American Chemical Society* **2012**, *134*, 7656-7659.

6 An, B.-K.; Kwon, S.-K.; Jung, S.-D.; Park, S. Y. *Journal of the American Chemical Society* **2002**, *124*, 14410-14415.

7 Singh, A.; Raj, T.; Aree, T.; Singh, N. *Inorganic Chemistry* **2013**, *52*, 13830-13832.

8 Suk, J.; Bard, A. J. *Journal of Solid State Electrochemistry* **2011**, *15*, 2279-2291.

9 Kaur, R.; Kaur, A.; Singh, G.; Kumar, M.; Kaur, N. *Analytical Methods* **2014**, *6*, 5620-5626.

10 Yang, Y.; Wang, X.; Cui, Q.; Cao, Q.; Li, L. *ACS Applied Materials & Interfaces* **2016**, *8*, 7440-7448.

11 An, B. K.; Kwon, S. K.; Park, S. Y. *Angewandte Chemie International Edition* **2007**, *46*, 1978-1982.

12 Verma, S.; Gokhale, R.; Burgess, D. J. *International Journal of Pharmaceutics* **2009**, *380*, 216-222.

13 Kumar, S.; Mittal, S. K.; Kaur, N.; Kaur, R. *RSC Advances* **2017**, *7*, 16474-16483.

14 Raj, T.; Saluja, P.; Singh, N. *Sensors and Actuators B: Chemical* **2015**, *206*, 98-106.

15 Bhardwaj, S.; Maurya, N.; Singh, A. K. *Sensors and Actuators B: Chemical* **2018**, *260*, 753-762.

16 Gangopadhyay, M.; Jana, A.; Rajesh, Y.; Bera, M.; Biswas, S.; Chowdhury, N.; Zhao, Y.; Mandal, M.; Singh, N. P. *ChemistrySelect* **2016**, *1*, 6523-6531.

17 Azadbakht, R.; Talebi, M.; Karimi, J.; Golbedaghi, R. *Inorganica Chimica Acta* **2016**, *453*, 728-734.

18 Saini, A.; Bhasin, A. K.; Singh, N.; Kaur, N. *New Journal of Chemistry* **2016**, *40*, 278-284.

19 Singh, J.; Huerta-Aguilar, C. A.; Singh, H.; Pandiyan, T.; Singh, N. *Electroanalysis* **2015**, *27*, 2544-2551.

20 Qu, F.; Liu, J. a.; Yan, H.; Peng, L.; Li, H. *Tetrahedron Letters* **2008**, *49*, 7438-7441.

Conclusions

In this thesis work, two main categories of electrochemical techniques such as potentiometry and voltammetry have been employed for the detection of target metal ions. These methods find applications in real life sample analysis. Potentiometric and voltammetric measurements based on (E)-3-((2-aminoethylimino)methyl)-4H-chromen-4-one (IFE), (E)-3-(((2-((2 aminoethyl) amino) ethyl) imino) methyl)-4H-chromen-4-one (ICU) and (E)-3-((2-(2-(2-aminoethylamino) ethylamino) ethylimino)methyl)-4H-chromen-4-one (IFE(III)) were carried out to determine the Fe(II), Cu(II) and Fe(III) ions, respectively.

MWCNT can effectively act as ion-to-electron transducer in ion selective electrodes (ISE). Incorporation of MWCNT in the membrane matrix showed improved characteristics of ion selective electrodes. The electrodes doped with MWCNT (1%) showed enhanced sensitivity observed by the lower detection limit 2.5×10^{-8}, 1.0×10^{-7} and 1.6×10^{-7} mol/L compared with its analogue without MWCNT 1.0×10^{-7}, 5.0×10^{-7} and 1.0×10^{-6} for IFE, ICU and IFE(III) respectively. Analytical applications of the membrane electrodes were confirmed by using these as indicator electrodes and real life sample analysis for the determination of Fe(II), Cu(II) and Fe(III) ions.

Redox behaviour of three ionophores IFE, ICU and IFE(III) based on the Schiff Base was studied with cyclic voltammetry and differential pulse voltammetry and without substantial interference from the other metal ions and their binding capacity was determined with Fe(II), Cu(II) and Fe(III) ions. From the voltammetric titration experiments, the limit of detections were observed as 6.13×10^{-8} mol/L for Fe(II), 9.32×10^{-9} mol/L for Cu(II) and 5.2×10^{-8} mol/L for Fe(III) ions. Chemical interactions of ligands towards respective metals ions also confirmed by the theoretical calculations. The study also provided the voltammetric analysis of organic nanoparticles of IFE compound. Dynamic light scattering (DLS) and transmission electron microscopy (TEM) have been used to analyse the size and morphology of prepared organic nanoparticles. The detection limit for the sensor is 8.2×10^{-8} mol L^{-1} and by using this as a voltammetric sensor for determining copper in daily life sample analysis, analytical utility was validated.

A series of imine-based receptor ionophores were chosen to study the effect of remote substituents with extended number of heteroatoms. For example, IFE has only one amine group attached to the imine bond while ICU and IFE(III) have respectively 2 and 3 amine

groups attached to the Schiff base. The study yielded the novel information that changes of remote substituents in a given receptor molecule can be used to shift selectivity from one target species to another. For example, selectivity of the IFE ionophore changed from Fe(II) to Cu(II) and Fe(III), respectively for the ionophores with substituents with increasing number of heteroatoms. Effect of remote substituents attached to the Schiff base greatly influence the electronic environment in the pseudo-cavity formed by the heteroatoms. The three Schiff base ionophores have been studied with three different analytical techniques i.e., potentiometry, voltammetry and spectrophotometry. It has been established that all the three ionophores respond to the target species in the same manner, irrespective of the type of the transducer used. Response of the ionophores was the similar with three different types of techniques, based on the measurement of Emf, current or optical density. Use of MWCNT improved performance of the ISE in terms of better selectivity coefficient and lower detection limits as compared to unmodified membranes.

These findings demonstrate an excellent potential of IFE, ICU and IFE(III) as sensing materials for the development of potentiometric and voltammetric sensors that can be directly used for real life samples analysis.

LIST OF PUBLICATIONS

Papers in SCI/refereed journals

1. **Sanjeev Kumar**, Susheel K. Mittal*, Jasminder Singh and Navneet Kaur, MWCNT incorporated imine–amine ionophore for electrochemical sensing of copper ions, Analytical Method (2016) 8: 7472-7481 **(I.F.: 2.378)**

2. **Sanjeev Kumar**, Susheel K. Mittal*, Navneet Kaur and Ravneet Kaur, Improved Performance of Schiff Based Ionophore Modified with MWCNT For Fe(II) Sensing By Potentiometry and Voltammetry Supported With DFT Studies, RSC Advances (2017) 7: 16474-16483 **(I.F.: 3.049)**

3. Susheel K. Mittal*, **Sanjeev Kumar** and Navneet Kaur, Enhanced performance of CNT-doped imine based receptors as Fe(III) sensor using potentiometry and voltammetry, Electroanalysis (2018) 31: 1229-1237 **(I.F.: 2.691)**

4. **Sanjeev Kumar**, Susheel K. Mittal*, Navneet Kaur, Enhanced performance of organic nanoparticles of a Schiff base as voltammetric sensor of Cu(II) in aqueous samples, Analytical Method (2019) 11: 359-366 **(I.F.: 2.378)**

Papers/ Posters in Conferences

1. **Poster Presentation** in 7th National Seminar entitled "Synergistic Aspects of Chemical and Other Sciences-2015 (SACOS-2015)" held on 19-20 February, 2015 at Punjabi University, Patiala.

2. **Attended Short Term Course** on "Advance materials and Characterization Techniques" from 01-07 June, 2015 at NIT Jalandhar.

3. **Poster presentation** in National Conference on New Frontiers in Chemistry- From Fundamentals to Applications (NFCFA-2015) held on 18-19 December, 2015 at BITS Pilani, KK Birla Campus, Goa.

4. **Poster Presentation** in 18th CRSI National Symposium in Chemistry held on 05-07 February, 2015 at Punjab University, Chandigarh.

5. **Poster presentation** in 10th National Conference on Chemical and Environmental Science: Innovations and Advances-2018 on 15-16 February, 2018 at Punjabi University, Patiala.

6. **Poster presentation** in 7th National Symposium on Advances in Chemical Sciences on 26-27 March, 2018 at Guru Nanak Dev University, Amritsar.

7. **Poster presentation** in National Conference on "Research in Chemical Sciences: Current Scenario" held on 29 March, 2019 at Sri Guru Granth Sahib World University, Fatehgarh Sahib.